Alpine Entomology 9 2025, 113–151 | DOI 10.3897/alpento.9.171490

PENSOFT

Alpine Entomology

Endemism and hidden diversity of *Habrophlebia*, Eaton, 1881 in Algeria's Northeastern Mountains (Ephemeroptera, Leptophlebiidae)

Boudjéma Samraoui[1,2], Laurent Vuataz[3,4], Michel Sartori[3,4]

1 *Biology Department, University Badji Mokhtar, Annaba, Algeria*
2 *Laboratoire de Conservation des Zones Humides, Université 8 mai 1945, Guelma, Algeria*
3 *Department of Zoology, State Museum of Natural Sciences (Naturéum), Palais de Rumine,Place Riponne 6, CH-1005 Lausanne, Switzerland*
4 *Department of Ecology and Evolution, University of Lausanne (UNIL), CH-1015 Lausanne, Switzerland*

https://zoobank.org/866C37ED-D606-406B-953E-062621C7AED7

Corresponding author: Boudjéma Samraoui (bsamraoui@gmail.com)

Academic editor: Jean-Luc Gattolliat ♦ **Received** 8 September 2025 ♦ **Accepted** 10 November 2025 ♦ **Published** 27 November 2025

Abstract

Northeastern Algeria has recently emerged as a hotspot of freshwater biodiversity and a refugium for both mountainous cold stenothermic and Afrotropical relict species. Intensive surveys of mayflies uncovered striking cryptic diversity within the genus *Habrophlebia* Eaton, 1881 (Ephemeroptera, Leptophlebiidae). By integrating molecular and morphological evidence, we describe five new species (*H. callensis* **sp. nov.**, *H. ghora* **sp. nov.**, *H. seybouse* **sp. nov.**, *H. annaba* **sp. nov.**, and *H. edough* **sp. nov.**). Our findings increase the number of recognised *Habrophlebia* species in the Maghreb from nine to fourteen, all of which are endemic to the region. The results further suggest that northeastern Algeria constitutes a major diversification centre for *Habrophlebia* within the Maghreb and, more broadly, across the Mediterranean basin. Furthermore, distributional patterns support an east–west divide within the Maghreb, most likely shaped by distinct Quaternary glacial refugia. Finally, we provide an updated identification key to the nymphs of *Habrophlebia* species in the western Palaearctic.

Key Words

Biogeography, COI, freshwater biodiversity, Maghreb, mayflies, new species, taxonomy

Introduction

Mayflies, belonging to the order Ephemeroptera, comprise approximately 4,000 species, 500 genera, and 40 families (Sartori and Brittain 2015). Among these families, Leptophlebiidae is one of the most diverse, encompassing eight subfamilies and around 810 species, collectively accounting for about 20% of all known mayfly species (Sartori and Gattolliat 2023). However, within the Palaearctic region, Leptophlebiidae exhibits relatively low diversity, with only 60 species recorded across four subfamilies (Peters and Edmunds 1970; Sartori and Gattolliat 2023). The subfamily Habrophlebiinae includes 25 species in this region, nine of which belong to the genus *Habrophlebia* Eaton, 1881.

In the Maghreb, *Habrophlebia* is represented by six species: two (*H. hassainae* and *H. djurdjurensis*) have been described from Algeria, while the remaining four (*H. vaillantorum*, *H. dakki*, *H. abietis*, and *H. linae*) are currently known only from Morocco. Earlier records of *H. fusca* in the region (Thomas 1998) need confirmation, while the presence of *H. consiglioi*, originally described from Sardinia and later reported in Tunisia (Zrelli et al. 2011a), has proven to be unfounded. Of particular interest is the close genetic relationship between the two Algerian species, with a minimum interspecific COI divergence of 2.1% (El Alami et al. 2023), suggesting recent reproductive isolation (Hebert et al. 2003), as well as the occurrence of numerous hybrid populations in the Rif (El Alami et al. 2025).

Copyright *Boudjéma Samraoui et al.* This is an open access article distributed under the terms of the Creative Commons Attribution License (CC BY 4.0), which permits unrestricted use, distribution, and reproduction in any medium, provided the original author and source are credited.

The Maghreb, forming part of the Mediterranean Basin, is one of the world's biodiversity hotspots (Myers et al. 2000). Freshwater biodiversity in the region is unevenly distributed and primarily concentrated in coastal areas. In northeast Algeria and northwest Tunisia, the Numidia region harbours a wide range of wetlands, including mountainous streams and rivers that support a rich diversity of waterbirds, fish, and amphibians, many endemic to the region (Samraoui and Samraoui 2008; Ben Hassine and Escoriza 2017; Dufresnes et al. 2019). These ecosystems also sustain a diverse assemblage of aquatic insects and zooplankton of varied biogeographic origins (Samraoui et al. 1998). Lowland wetlands harbour Afrotropical relict species such as the dragonflies *Urothemis edwardsii* and *Acisoma inflatum* (Samraoui et al. 1993); the montane zones act as refugia for cold-stenothermic taxa, including the aeshnid *Aeshna cyanea* (Samraoui and Alfarhan 2015) and *Pyrrhosoma nymphula* (Korbaa et al. 2014). Following the pioneering studies of Eaton (1899) and Lestage (1925), research on Algerian mayflies stagnated for much of the twentieth century, before resuming in its final decades and culminating in the synthesis by Thomas (1998). Since the early 21st century, there has been renewed interest in the taxonomy and ecology of Algerian mayflies, resulting in a number of new publications (e.g. Soldán et al. 2005). More recently, several additions to the Algerian mayfly checklist have been made (Benhadji et al. 2018, 2019; Kechemir et al. 2020; Samraoui et al. 2021a, 2021b; Kaltenbach et al. 2022), along with reports of numerous yet undescribed species (Labdaoui et al. 2024; Hezil et al. 2025).

The aim of this study is to investigate the diversity of the genus *Habrophlebia* in northeastern Algeria by integrating molecular (COI) and morphological data, with the objectives of providing preliminary ecological information on species distribution, habitats, and phenology, and offering biogeographical insights into the region's role in the diversification of the genus.

Material and methods

Material for this study was collected from rivers and streams across northeastern Algeria between 2018 and 2022 (Fig. 1). The study area, as well as the sampling protocol for nymphs, are described in detail by Samraoui et al. (2021a, 2021b). Adult specimens were captured along stream margins using a hand net.

Morphological analyses

Specimens were observed under a Leica MZ12 and M205C stereomicroscope. Nymphs were dissected in Cellosolve (2-ethoxyethanol); mouthparts, legs and the abdomen were mounted on microscopic slides with Euparal® as the medium. Microscopic pictures were taken using an Olympus BX51 microscope coupled with an Olympus SC50 camera; pictures were enhanced with the stacking software Olympus Stream Basic ver. 2.3.2. and Adobe Photoshop ver. 21.2.2. Pictures of habitus were made using a Canon EOS 6D camera and the Visionary Digital Passport imaging system (formerly available and distributed by Dun Inc., Virginia), and processed with Adobe Photoshop Lightroom and Helicon Focus ver. 5.3. For scanning electron microscopy (SEM) imaging, eggs were dehydrated in pure ethanol, coated with 12 nm platinum and SEM pictures were performed at Lausanne University with a FEI Quanta FEG 250 at 10 kV with a WD ranging between 10.1 and 12.1 mm. Final figure plates were assembled in Adobe Photoshop Elements 2022 ver. 20.0.

Molecular analyses

To complement our morphological investigations, we analyzed a 658 bp fragment of the mitochondrial cytochrome oxidase subunit 1 gene (COI). The dataset comprises the 91 West Palearctic *Habrophlebia* COI sequences from El Alami et al. (2025) and 27 newly generated sequences from Algerian specimens (Table 1), for a total of 118 sequences. DNA from the new specimens was extracted using the non-destructive method outlined in Vuataz et al. (2011). PCR amplification, purification, and sequencing followed the protocol of El Alami et al. (2022a). Forward and reverse reads were assembled and edited in CodonCode Aligner ver. 12.0.1 (CodonCode Corporation, Dedham, MA). Two sequences from *Habroleptoides* Schönemund, 1929 were retrieved from GenBank and used as outgroups. All sequences were aligned in MAFFT (Katoh et al. 2019) via Jalview ver. 2.11.4.1 (Waterhouse et al. 2009) with default settings. The number of parsimony-informative sites was calculated in MEGA ver. 10.2.4 (Kumar et al. 2018; Stecher et al. 2020).

To examine and visualize COI evolutionary divergence, we used pairwise genetic distances and gene tree approaches. Pairwise distances were calculated in R ver. 4.5.1 (R Core Team 2025) using the dist.dna function from the ape ver. 5.8.1 package (Paradis and Schliep 2019), with the raw model and the pairwise.deletion option to obtain uncorrected p-distances (see Srivathsan and Meier 2012), excluding missing data pairwise. Mean, minimum, and maximum distances within and between putative COI species (hereafter Molecular Operational Taxonomic Units, MOTUs), were calculated using the ddply function from the plyr ver. 1.8.9 package (Wickham 2011). The 97 previously published COI sequences were assigned to MOTUs following the 12 clades defined in Fig. 13 of El Alami et al. (2025), while the 27 sequences generated in this study were assigned based on the species delimitation analyses described below.

Before reconstructing the COI gene tree, the best evolutionary model (GTR + Γ + I) was selected using the second-order Akaike information criterion (AICc; Hurvich and Tsai 1989) in JmodelTest ver. 2.1.10 (Darriba et al. 2012) with three substitution schemes, six gamma categories, and default settings for other parameters.

Table 1. Details of newly sequenced specimens used in this study, including species name, specimen catalogue number, developmental stage, collection locality with GPS coordinates and date, and GenBank accession numbers. All specimens are paratypes (GenSeq Nomenclature: genseq-2 COI).

Species	Specimen catalogue nb	Stage	Locality	GPS coordinates	Date	GenBank ID
Habrophlebia annaba sp. nov.	GBIFCH00658258	nymph	Edough, O. Agab	36°54'44"N, 7°39'35"E	1.VI.2022	PX283157
Habrophlebia annaba sp. nov.	GBIFCH01118439	nymph	Edough, O. Zouz	36°55'54"N, 7°40'03"E	20.III.2022	PX283166
Habrophlebia annaba sp. nov.	GBIFCH01118440	male imago	Edough, O. Agab	36°54'44"N, 7°39'35"E	1.V.2021	PX283167
Habrophlebia annaba sp. nov.	GBIFCH01314437	nymph	Edough, O. Agab	36°54'44"N, 7°39'35"E	10.II.2022	PX283177
Habrophlebia annaba sp. nov.	GBIFCH01314677	nymph	Edough, O. Agab	36°54'44"N, 7°39'35"E	1.V.2021	PX283178
Habrophlebia annaba sp. nov.	GBIFCH01314689	nymph	Edough, O. Agab	36°54'44"N, 7°39'35"E	26.IV.2021	PX283179
Habrophlebia callensis sp. nov.	GBIFCH00763554	nymph	Hadada, Dar Essalem	36°53'10"N, 8°37'2"E	1.VIII.2019	PX283160
Habrophlebia callensis sp. nov.	GBIFCH00763555	nymph	Hadada, O. Ftitich	36°54'01"N, 8°37'05"E	11.VII.2019	PX283161
Habrophlebia callensis sp. nov.	GBIFCH01118444	nymph	Hadada, O. Ftitich	36°54'01"N, 8°37'05"E	12.III.2020	PX283171
Habrophlebia edough sp. nov.	GBIFCH00654947	nymph	Edough, O. Agab	36°54'44"N, 7°39'35"E	9.IX.2021	PX283153
Habrophlebia edough sp. nov.	GBIFCH00654948	nymph	Edough, O. Agab	36°54'44"N, 7°39'35"E	18.VIII.2021	PX283154
Habrophlebia edough sp. nov.	GBIFCH01118441	nymph	Edough, O. Agab	36°54'44"N, 7°39'35"E	18.VIII.2021	PX283168
Habrophlebia ghora sp. nov.	GBIFCH00673045	nymph	Ghora, O. Guitna inférieur	36°37'5"N, 8°20'46"E	1.V.2019	PX283158
Habrophlebia ghora sp. nov.	GBIFCH00673115	nymph	Ghora, O. Louar supérieur	36°37'1"N, 8°22'47"E	1.V.2019	PX283159
Habrophlebia ghora sp. nov.	GBIFCH00763556	nymph	Ghora, O. Louar supérieur	36°37'1"N, 8°22'47"E	6.VI.2019	PX283162
Habrophlebia ghora sp. nov.	GBIFCH01118437	nymph	Menzel Beldi	36°36'59"N, 8°21'51"E	15.V.2021	PX283164
Habrophlebia ghora sp. nov.	GBIFCH01118438	male imago	Menzel Beldi	36°36'59"N, 8°21'51"E	15.V.2021	PX283165
Habrophlebia ghora sp. nov.	GBIFCH01118442	nymph	El Ayoun	36°50'14"N, 8°36'4"E	15.V.2021	PX283169
Habrophlebia ghora sp. nov.	GBIFCH01118443	male imago	El Ayoun	36°50'14"N, 8°36'4"E	9.V.2021	PX283170
Habrophlebia ghora sp. nov.	GBIFCH01118445	male imago	Ghora, O. Louar supérieur	36°37'1"N, 8°22'47"E	15.V.2021	PX283172
Habrophlebia ghora sp. nov.	GBIFCH01118446	male imago	Ghora, O. Guitna inférieur	36°37'5"N, 8°20'46"E	7.VI.2020	PX283173
Habrophlebia ghora sp. nov.	GBIFCH01118447	nymph	Ghora, O. Louar supérieur	36°37'1"N, 8°22'47"E	10.V.2021	PX283174
Habrophlebia ghora sp. nov.	GBIFCH01118448	male imago	Ghora, O. Louar inférieur	36°37'2"N, 8°22'49"E	15.V.2021	PX283175
Habrophlebia ghora sp. nov.	GBIFCH01118449	nymph	Ghora, O. Guitna supérieur	36°37'0"N, 8°21'19"E	26.IV.2022	PX283176
Habrophlebia seybouse sp. nov.	GBIFCH00658256	nymph	Collo, O. Tizagban	37°00'39"N, 6°22'31"E	21.I.2022	PX283155
Habrophlebia seybouse sp. nov.	GBIFCH00658257	nymph	Collo, O. Tizagban	37°00'39"N, 6°22'31"E	21.I.2022	PX283156
Habrophlebia seybouse sp. nov.	GBIFCH01118436	male imago	Selaoua, O. Cherf	36°20'54"N 7°16'2"E	6.VI.2020	PX283163

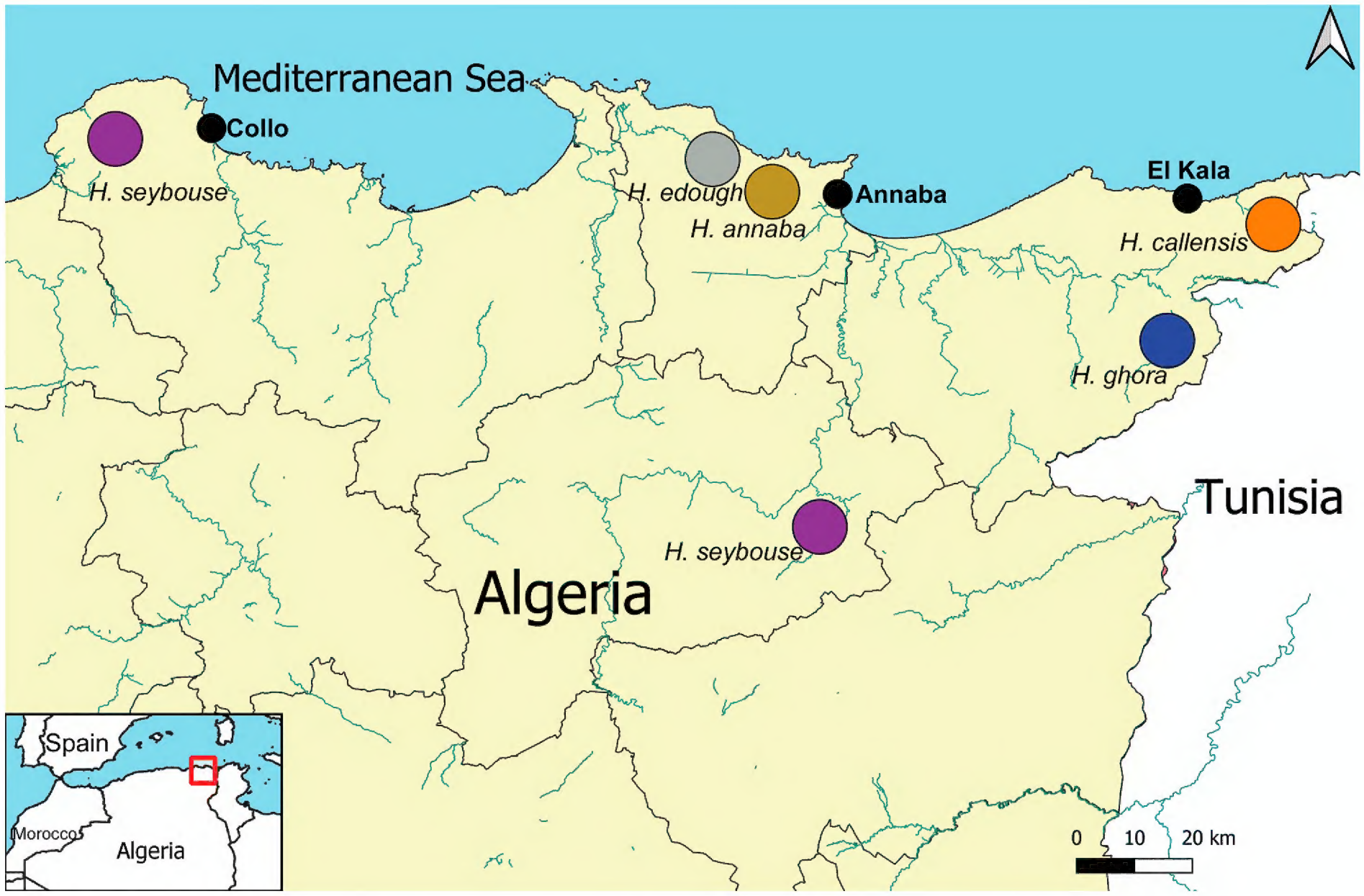

Figure 1. Location map of northeastern Algeria showing the distribution of the newly described *Habrophlebia* species.

To account for different substitution rates among COI codon positions, the dataset was partitioned into positions 1 + 2 and position 3. Bayesian inference was performed in BEAST ver. 1.10.4 (Suchard et al. 2018) on the CIPRES Science Gateway (Miller et al. 2010). The input file was generated in BEAUTi ver. 1.10.4 (Suchard et al. 2018), incorporating the selected model and partition scheme. A relaxed molecular clock (uncorrelated lognormal) and a UPGMA starting tree were used, with default values for other parameters. Two independent Markov chain Monte Carlo (MCMC) runs of 100 million generations each were performed, sampling every 1000 generations. Convergence was assessed visually in Tracer ver. 1.7.2 (Rambaut et al. 2018). Log and tree files from the two runs were combined in LogCombiner ver. 1.10.4 (Suchard et al. 2018) after discarding the first 10% of trees as burn-in, ensuring all parameters had effective sample sizes (ESS) > 200. The maximum clade credibility tree was produced in TreeAnnotator ver. 1.10.4 (Suchard et al. 2018), with node heights set to common ancestor heights and default settings for other parameters. The tree was visualized and edited in iTOL ver. 7.2.1 (Letunic and Bork 2024).

Finally, we applied three contrasting single-locus species delimitation methods to the COI dataset: the distance-based ASAP (Assemble Species by Automatic Partitioning; Puillandre et al. 2020) and the tree-based mPTP (multi-rate Poisson Tree Processes; Kapli et al. 2017) and GMYC (General Mixed Yule-Coalescent; Pons et al. 2006; Fujisawa and Barraclough 2013) approaches. The ASAP analysis was performed in ASAPy ver. 1.0, downloaded from the iTaxoTools platform (Vences et al. 2021; https://itaxotools.org). Genetic distances were calculated from the COI alignment using simple p-distances, with all other settings left at default. The best partition was selected based on the lowest asap-score. Since two partitions had the same lowest scores, we chose the one with a threshold distance closest to 3% divergence, which aligns with previously reported intra- to inter-species thresholds in Ephemeroptera (Gattolliat et al. 2015). The mPTP analysis was conducted using the webserver https://mptp.h-its.org/#/tree with the BEAST tree generated earlier as input, and the command line execution "mptp --ml --multi". For the GMYC approach, the ultrametric tree was generated in BEAST following the same procedure as above, but using a reduced dataset that excluded outgroups and pruned haplotypes (see Talavera et al. 2013) with Collapsetypes ver. 4.6 (Chesters 2013). The best-fit evolutionary model (GTR + Γ + I) was re-estimated for this reduced dataset using the same method as before. GMYC was then implemented in R with the SPLITS package ver. 1.0.20 (Ezard et al. 2009), using the single-threshold model, which has been shown to outperform the multiple-threshold version (Fujisawa and Barraclough 2013).

Abbreviations

MZL Muséum Cantonal des Sciences Naturelles (Naturéum), Lausanne (Switzerland).

Results

Systematics

Descriptions

Habrophlebia ghora Sartori, Vuataz & Samraoui, sp. nov.

https://zoobank.org/213C2984-EAF5-4BF4-B2D1-20D7A809E083

Figs 2–6

Habrophlebia consiglioi sensu Zrelli et al. (2011a), nec Biancheri 1959.
Habrophlebia spK, Samraoui et al. 2021b; *Habrophlebia* sp. 11, Hezil et al. 2025.

Material examined. ***Holotype*:** one nymph in ethanol (GBIFCH00654989), Algeria, Wilaya of El Tarf, Ghora, Oued Louar supérieur, 36°37'1"N, 8°22'47"E, 594 m, 1.V.2019, B. Samraoui leg., MZL.

Paratypes. Algeria, Wilaya of El Tarf, Ghora, Oued Louar supérieur, same data as holotype, 135 nymphs in ethanol (GBIFCH00672312), 1 nymph on slide (GBIFCH00673115); same locality as holotype, 6.VI.2019, 1 nymph on slide (GBIFCH00763556); same locality as holotype, 10.V.2021, 20 nymphs in ethanol (GBIFCH00892922), 1 nymph on slide (GBIFCH01118447); same locality as holotype, 15.V.2021, 9 nymphs in ethanol (GBIFCH00892917), 21 male imagos in ethanol (GBIFCH00892924), 1 male imago in ethanol (GBIFCH01118445) • Wilaya of El Tarf, Ghora, Oued Louar inférieur, 36°37'2"N, 8°22'49"E, 589 m, 15.V.2021, 7 male imagos in ethanol (GBIFCH01118448, GBIFCH01123083) • Wilaya of El Tarf, Ghora, Oued Guitna supérieur, 36°37'0"N, 8°21'19"E, 584 m, 26.IV.2022; 1 nymph on slide (GBIFCH01118449), 10 nymphs in ethanol (GBIFCH01123084) • Wilaya of El Tarf, Ghora, Oued Guitna inférieur, 36°37'5"N, 8°20'46"E, 476 m, 1.V.2019, 1 nymph on slide (GBIFCH00673045); same locality, 1.VI.2020, 12 male imagos in ethanol (GBIFCH00892916); same locality, 7.VI.2020, 28 male, 1 female imagos (GBIFCH00892915), 1 male imago (GBIFCH01118446); same locality, 6.VI.2021, 1 nymph in ethanol (GBIFCH01123082); same locality, 26.IV.2022, 1 nymph in ethanol (GBIFCH00892921); same locality, 5.V.2022, 1 male imago in ethanol (GBIFCH00892919); same locality, 12.V.2022, 1 female imago in ethanol (GBIFCH00892918); same locality, 18.V.2022, 3 male, 4 female imagos (GBIFCH00892914); same locality, 21.V.2022, 2 male imagos in ethanol (GBIFCH00892920); same locality, 30.V.2022, 1 male, 3 female imagos in ethanol (GBIFCH00892913). • Wilaya of El Tarf, El Ayoun; 36°50'14"N, 8°36'4"E, 263 m, 9.V.2021, 1 male imago in ethanol (GBIFCH01118443), 4 nymphs, 22 male imagos in ethanol (GBIFCH00654970); same locality, 15.V.2021, 1 nymph on slide (GBIFCH01118442), 7 nymphs in ethanol (GBIFCH00892923, GBIFCH00654971) • Wilaya of El Tarf, Menzel Beldi; 36°36'59"N, 8°21'51"E, 590 m, 15.V.2021, 5 nymphs, 7 male imagos in ethanol (GBIFCH00654986), 1 male imago in ethanol (GBIFCH01118438), 1 nymph on slide (GBIFCH01118437). All B. Samraoui leg., MZL.

Other material. Algeria, Wilaya of El Tarf, Ghora, Oued Louar supérieur, 36°37'1"N, 8°22'47"E, 594 m, 21.I.2019, 3 nymphs (GBIFCH00834912); same locality, 16.IV.2019, 4 nymphs (GBIFCH00834904); same locality, 1.V.2019, 81 nymphs (GBIFCH00672312-GBIFCH00672313); same locality, 6.VI.2019, 50 nymphs (GBIFCH00672308); same locality, 1.VII.2019, 10 nymphs (GBIFCH00835008); same locality, 22.I.2020, 7 nymphs (GBIFCH00835007); same locality, 18.IV.2018, 15 nymphs (GBIFCH00889986). • Wilaya of El Tarf, Ghora, Oued Louar inférieur, 36°37'3"N, 8°22'49"E, 589 m, 18.IV.2018, 1 nymph (GBIFCH00889509); same locality, 6.VI.2019, 45 nymphs (GBIFCH00672306); same locality, 1.VII.2019, 3 imagos (GBIFCH00835071), 10 nymphs (GBIFCH00835082). • Wilaya of El Tarf, Ghora, Oued Guitna supérieur, 36°37'0"N, 8°21'19"E, 584 m, 14.VI.2018, 15 nymphs (GBIFCH00889962); same locality, 6.VI.2019, 15 nymphs (GBIFCH00834830); same locality, 1.VII.2019, 3 imagos (GBIFCH00834537). • Wilaya of El Tarf, Ghora, Oued Guitna inférieur, 36°37'5"N, 8°20'46"E, 476 m, 1.V.2019, 8 nymphs (GBIFCH00672315). • Wilaya of El Tarf, Ghora, Oued Guitoun, 36°37'0"N, 8°19'34"E, 293 m, 14.VI.2018, 2 nymphs (GBIFCH00889505). • Wilaya of El Tarf, Kherrata, Oued Bougous, 36°38'2"N, 8°18'25"E, 262 m, 18.IV.2018, 4 nymphs (GBIFCH00889513). • Wilaya of El Tarf, Zitoun Meftah, Bayadh, 36°38'0"N, 8°21'55"E, 282 m, 28.III.2018, 2 nymphs (GBIFCH00889989); same locality, 1.VII.2019, 3 nymphs (GBIFCH00834516). • Wilaya of El Tarf, Ghora, Oued Houadfia, 36°36'0"N, 8°23'29"E, 455 m, 5.VI.2018, 21 nymphs (GBIFCH00835076-GBIFCH00889532); same locality, 13.III.2019, 1 nymph (GBIFCH00672309); same locality, 19.V.2019, 60 nymphs (GBIFCH00672310), one nymph on slide (GBIFCH01225270); same locality, 6.VI.2019, 25 nymphs (GBIFCH00834910). • Wilaya of El Tarf, Oued Bougous, 36°39'0"N, 8°19'59"E, 610 m, 28.III.2018, 2 nymphs (GBIFCH00889521). • Wilaya of El Tarf, Oued Besbassa, 36°39'0"N, 8°20'1"E, 233 m, 28.III.2018, 14 nymphs (GBIFCH00889982). • Wilaya of El Tarf, Oued Khemissa, 36°39'0"N, 8°21'57"E, 237 m, 28.III.2018, 7 nymphs (GBIFCH00889540). • Wilaya of El Tarf, Oued Oudaï Smid, 36°40'0"N, 8°22'49"E, 202 m, 28.III.2018, 7 nymphs (GBIFCH00889987). All in ethanol, B. Samraoui leg., MZL.

Tunisia, Jendouba Governorate, Aïn Draham, Oued Ennour, 36°48'0"N, 8°39'31"E, 418 m, 28.IV.2010, 1 nymph in ethanol (GBIFCH00281533); same locality, 25.IV.2009, 1 nymph on slide (GBIFCH01225269); S. Zrelli leg., MZL.

Etymology. The name "Ghora" is derived from the Coot (*Fulica atra*), known locally as "Ghor", whose conspicuous white frontal shield evokes the image of a snow-capped peak. Mount Ghora (Djebel Ghora), situated on the Algerian–Tunisian border, takes its name from this association and forms part of the Kroumiria massif.

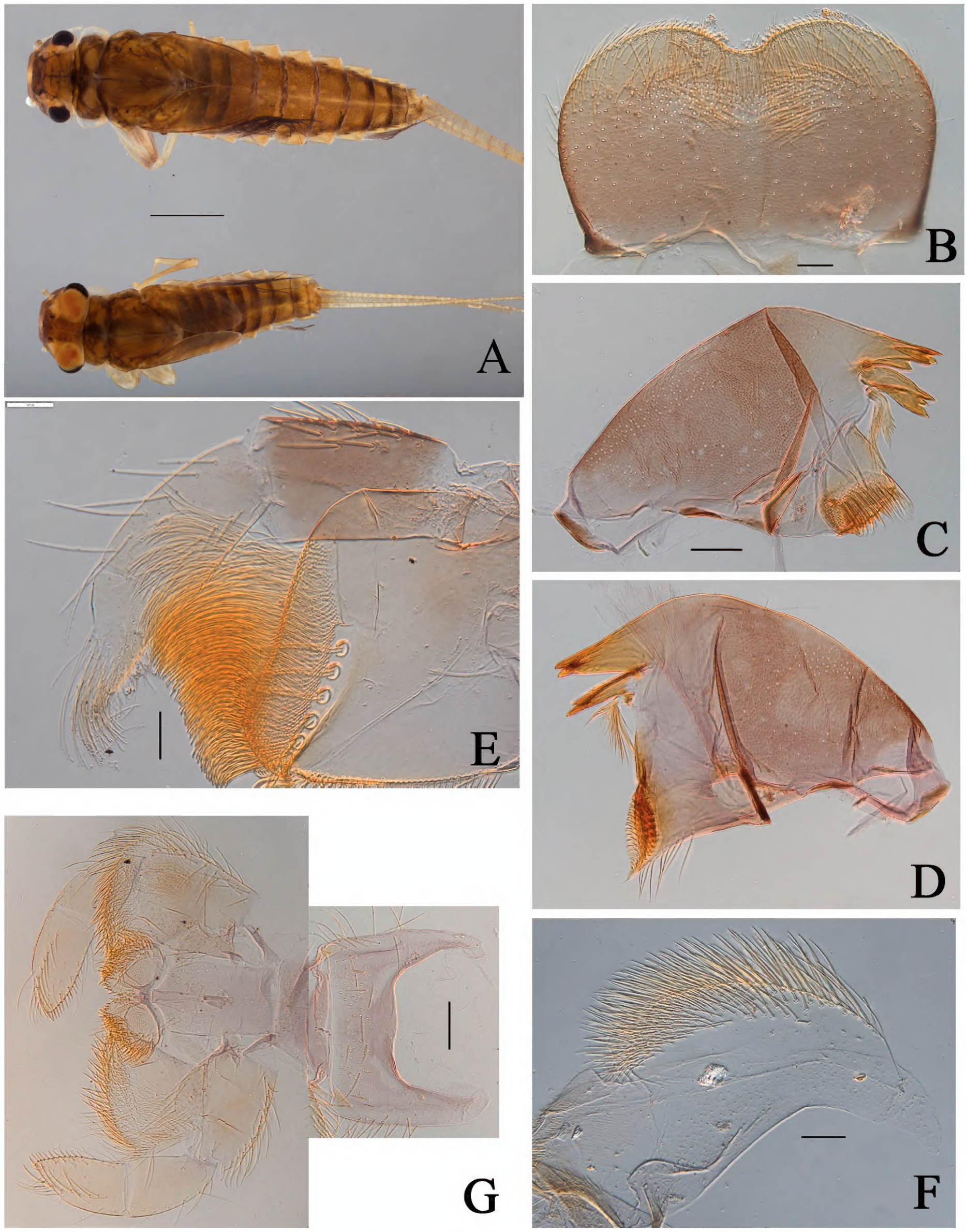

Figure 2. *H. ghora* sp. nov., habitus of female (above) and male (below) nymphs (**A**); labrum (**B**); left mandible (**C**); right mandible (**D**); maxilla (**E**); hypopharynx, left half (**F**); labium and submentum (**G**). Scale bars: 1 mm (**A**); 50 µm (**B, E, F**); 100 µm (**C, D, G**).

Descriptions. Nymph. Body length of final instar, excluding caudal filaments, up to 5 mm for male and up to 6 mm for female. Cerci as long as body length.

Coloration. General coloration medium brown; light brown between compound eyes and antennae. Upper portion of male eyes light brown to orange (Fig. 2A). Antenna with scape and pedicel greyish brown, filament yellowish. Pro- and mesonotum medium brown, with light brown maculae, on medium; lateroparapsidal sutures dark brown. Legs light to medium brown; dorsal surface

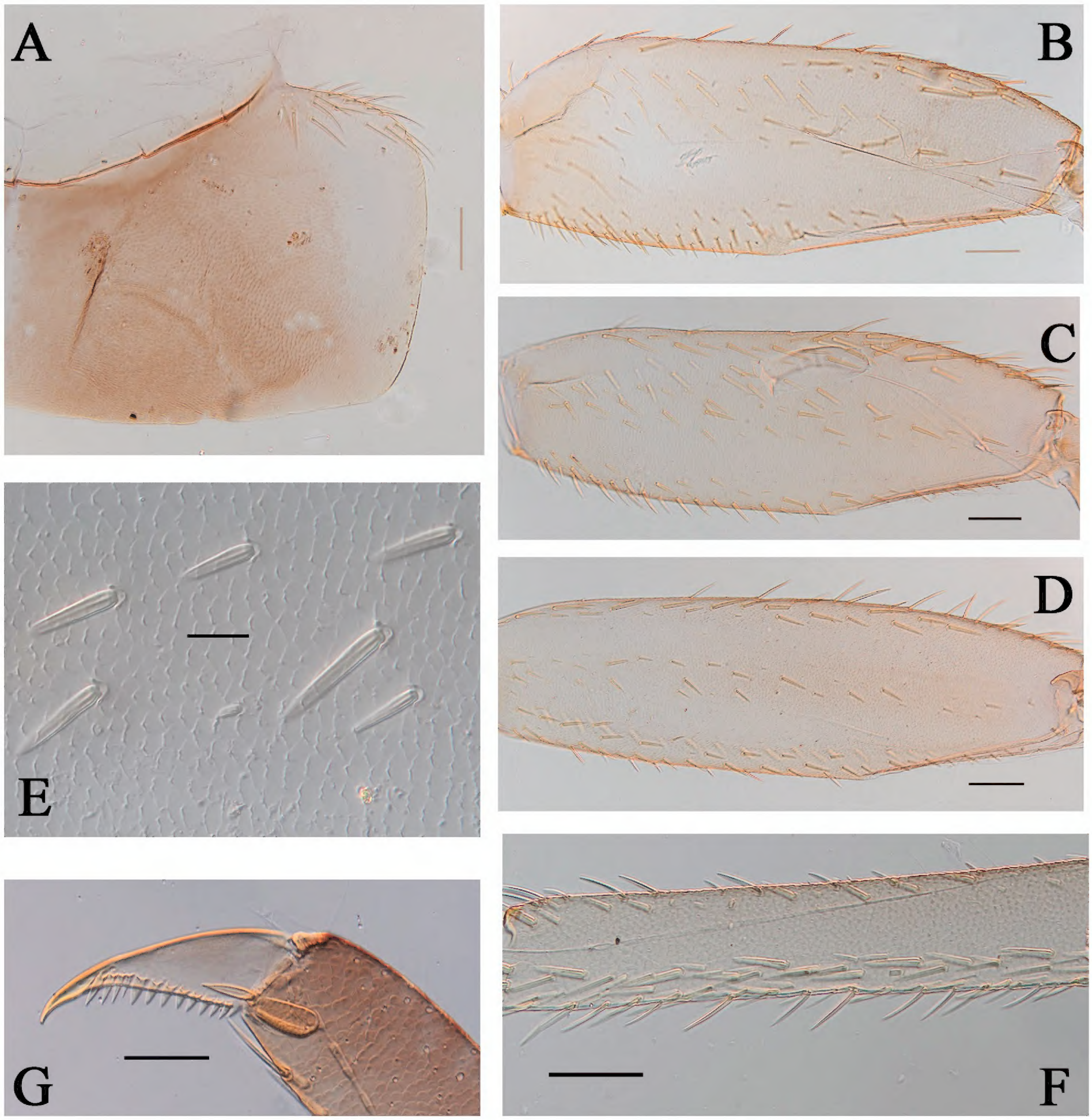

Figure 3. *H. ghora* sp. nov., thoracic structures, pronotum, right half (**A**); fore femur (**B**); mid femur (**C**); hind femur (**D**); setae on upper face of hind femur (**E**); hind tibia (**F**); claw (**G**). Scale bars: 100 µm (**A–D, F**); 20 µm (**E**); 50 µm (**G**).

of femora darker; tibiae and tarsi light brown to yellowish. Abdominal tergites medium brown with a sagittal line paler; distal half of each tergite darker, sometimes with two elongated light maculae medio-anteriorly, on segments I–VI, especially in younger nymphs. Sternites light to medium brown, nervous ganglia well visible. Cerci and paracercus medium brown at base, lighter distally, rather uniform in color, without apparent banding.

Head. Labrum rectangular, ca. 1.6× wider than long (Fig. 2B); dorsal surface covered distally with scattered stout setae; anterior margin with a row of stout, long and spatulate setae medially; emargination smooth, U-shaped, flared, with indistinct flat denticles; ventral surface with two bunches of stout setae medially. Mandibles similar to other *Habrophlebia* species, incisor with three teeth, the lowest on left mandible characterised by distinct basal indentation (Fig. 2C), kinetodontium with 3 teeth, 11–15 long and thin setae below mola of right mandible (Fig. 2D). Maxilla stocky, subapical row of 6–7 pectinate setae (Fig. 2E); maxillary palp with three segments, segment 1 and 2 subequal in length, and longer than segment 3; segment 3 triangular 1.11–1.15× longer than wide at base; all setae on palp segments stout and entire. Hypopharynx with highly developed superlinguae terminated by a membranous digitation (Fig. 2F). Labium with rhomboid glossae, outer margin and apex covered by short, broad setae; paraglossae enlarged laterally, covered with fine and long setae on the dorsal surface; with long, thick setae

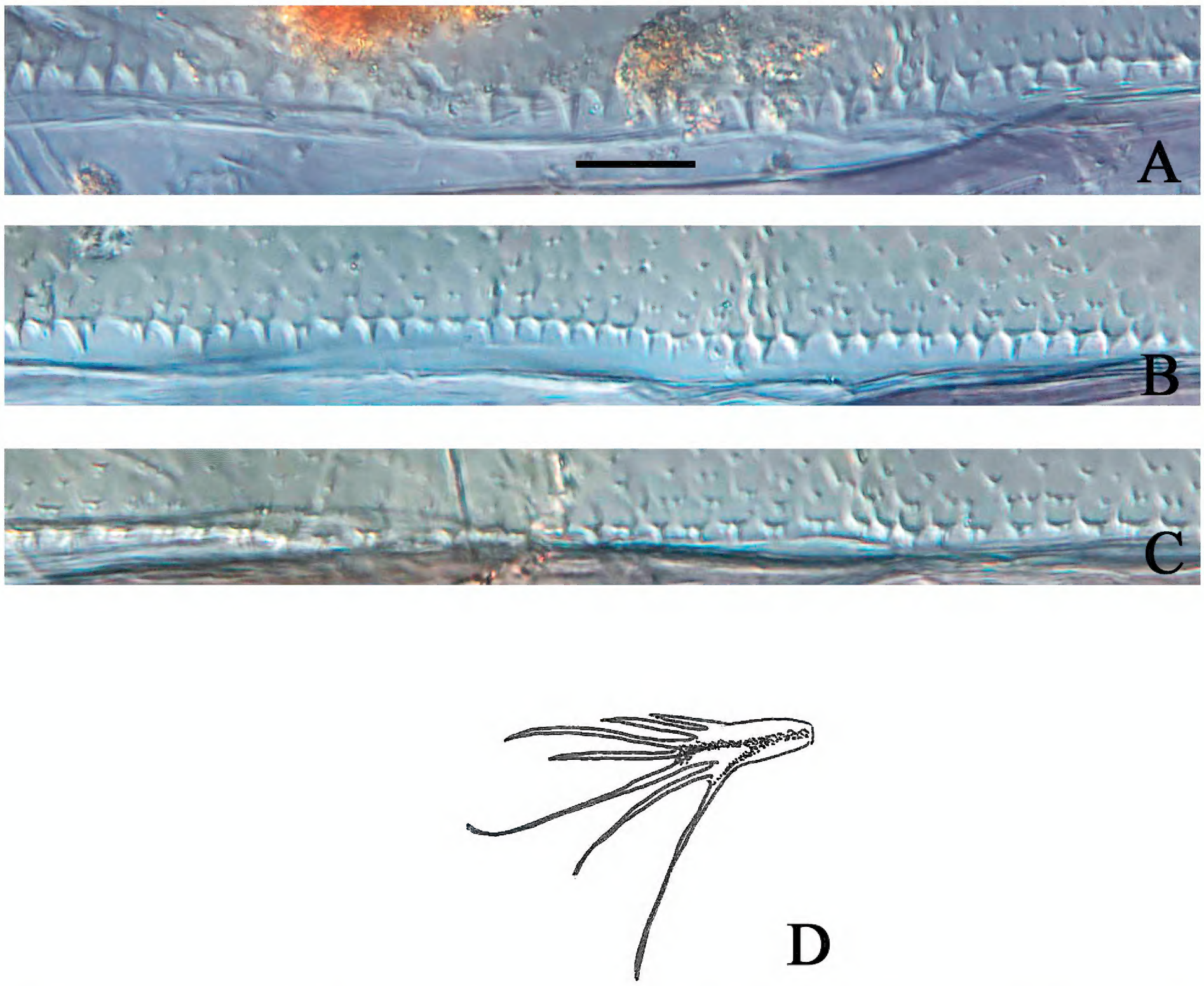

Figure 4. *H. ghora* sp. nov., abdominal structures, posterior margin of tergite IX (**A**); tergite VIII (**B**); tergite VII (**C**); gill (**D**). Scale bar: 20 μm.

on outer margin; labial palp with three segments, inner margin of segment 1 highly dilated near the middle, about 1.20× longer than the maximum width, segment 2 as long as segment 3, ca. 0.8× length of segment 1; segment 3 ca. 1.75–1.80× longer than wide at base, conical shape and with 7–8 stout and long, simple setae on dorsal surface. Submentum with numerous long, stout and pointed setae laterally; ventral surface with few long, stout and pointed setae (Fig. 2G).

Thorax. Pronotum with anterior corners bearing few long and pointed setae laterally, and 6–8 stout and strong setae dorsally. Anterior margin of pronotum with 3–5 stout setae laterally (Fig. 3A). Fore legs femora elongated, ca. 2.65× longer than wide, outer margin and upper surface covered with long, entire and pointed setae (Fig. 3B); tibiae slightly shorter than femora, outer margin with sparse thin and long setae, inner margin with long stout and feathered or entire setae more numerous near apex; tarsi 0.55× length of tibiae, outer margin with sparse long and thin setae, inner margin with long and pointed entire setae. Middle legs similar to fore legs, femora ca. 2.9× longer than wide, dorsal surface of femora with more numerous and slightly longer stout and pointed setae (Fig. 3C); tibiae slightly shorter than femora; tarsi 0.5× length of tibiae. Hind legs with femora 3.4× longer than wide (Fig. 3D), dorsal surface covered with stout, long and short, pointed or rounded and entire (non-feathered) setae more or less in rows (Fig. 3E); hind tibiae as long as hind femora, outer margin with scattered stout, pointed setae; inner margin with stout, pointed and entire setae (Fig. 3F); tarsi 0.45× length of tibiae, outer margin with few long and thin setae, inner margin with long, stout, pointed and entire setae. Claws of all legs slightly hooked, with 12–14 denticles that decrease in size from the apex to the tarsus (Fig. 3G).

Abdomen. Posterolateral expansions only on segments VIII and IX. Posterior margin of tergite IX with triangular, broad and narrow, pointed spines, ca. 1.5–2.5× longer than wide at base (Fig. 4A); tergite VIII with small triangular, narrow spines 1.5–2× longer than wide (Fig. 4B); tergite VII with tiny needle-shaped spines (Fig. 4C); tergites VI and above with barely visible spines. Gills present on segments I–VII; all gills elongated with long filaments; dorsal lamella bearing 4–5 filaments, ventral lamella with 2–3 filaments (Fig. 4D).

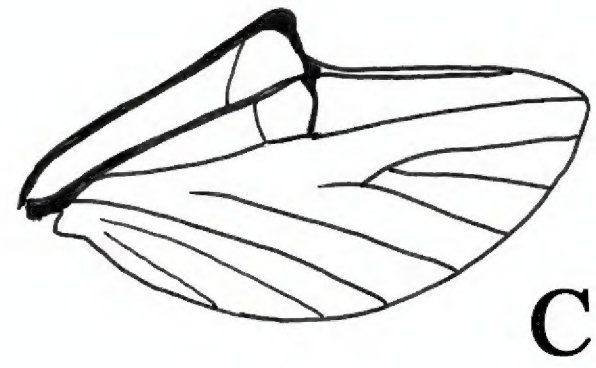

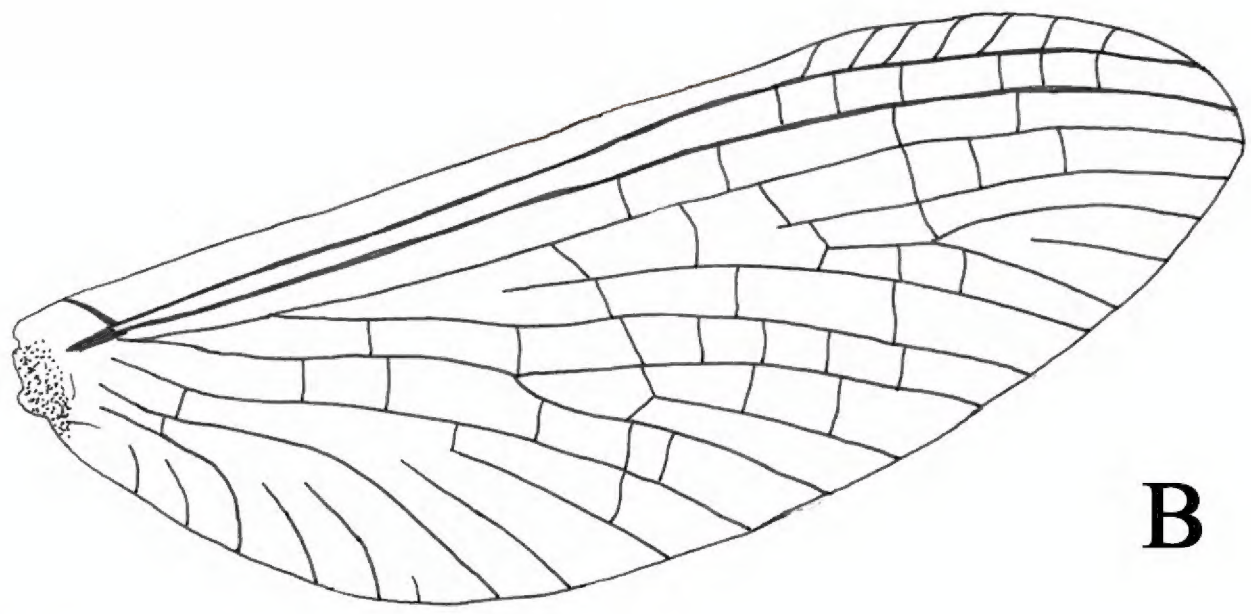

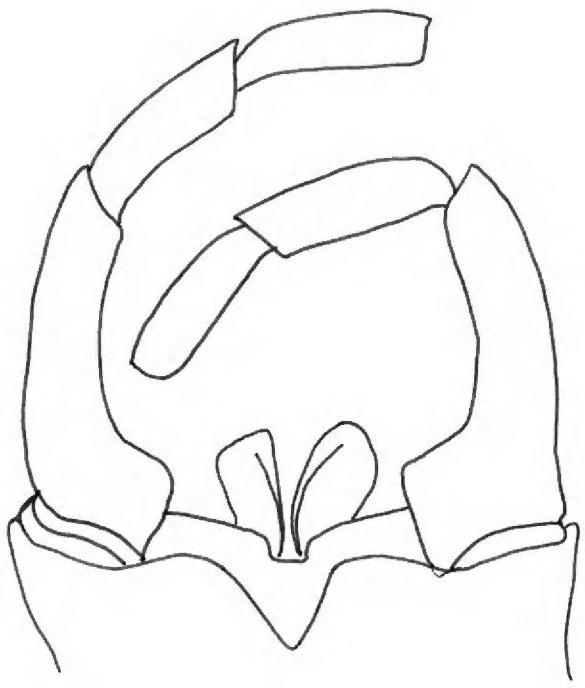

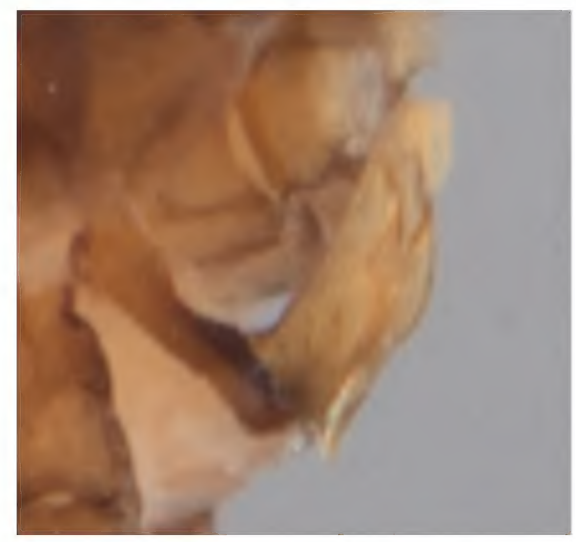

Figure 5. *H. ghora* sp. nov., male imago in lateral view (**A**); forewing (**B**); hindwing (**C**); genitalia in ventral view (**D**); penis in lateral view (**E**). Scale bar: 1 mm.

Imago. ***Male imago.*** Size: body length: ca. 5.5 mm; forewing length: 5.0–5.5 mm; cerci and terminal filament broken.

Head dark brown; basal portion of compound eyes greyish, upper portion light brown, scape dark brown, pedicel medium brown, flagellum light brown (Fig. 5A).

Thorax. Pronotum dark brown; meso- and metanotum uniformly dark brown, pleurae, coxae, and trochanters medium brown, washed with dark brown; fore femora dark brown, fore tibiae medium brown, tarsi light brown; mid- and hind legs with femora medium brown, dark brown distally, tibiae and tarsi medium brown. Femur/tib-

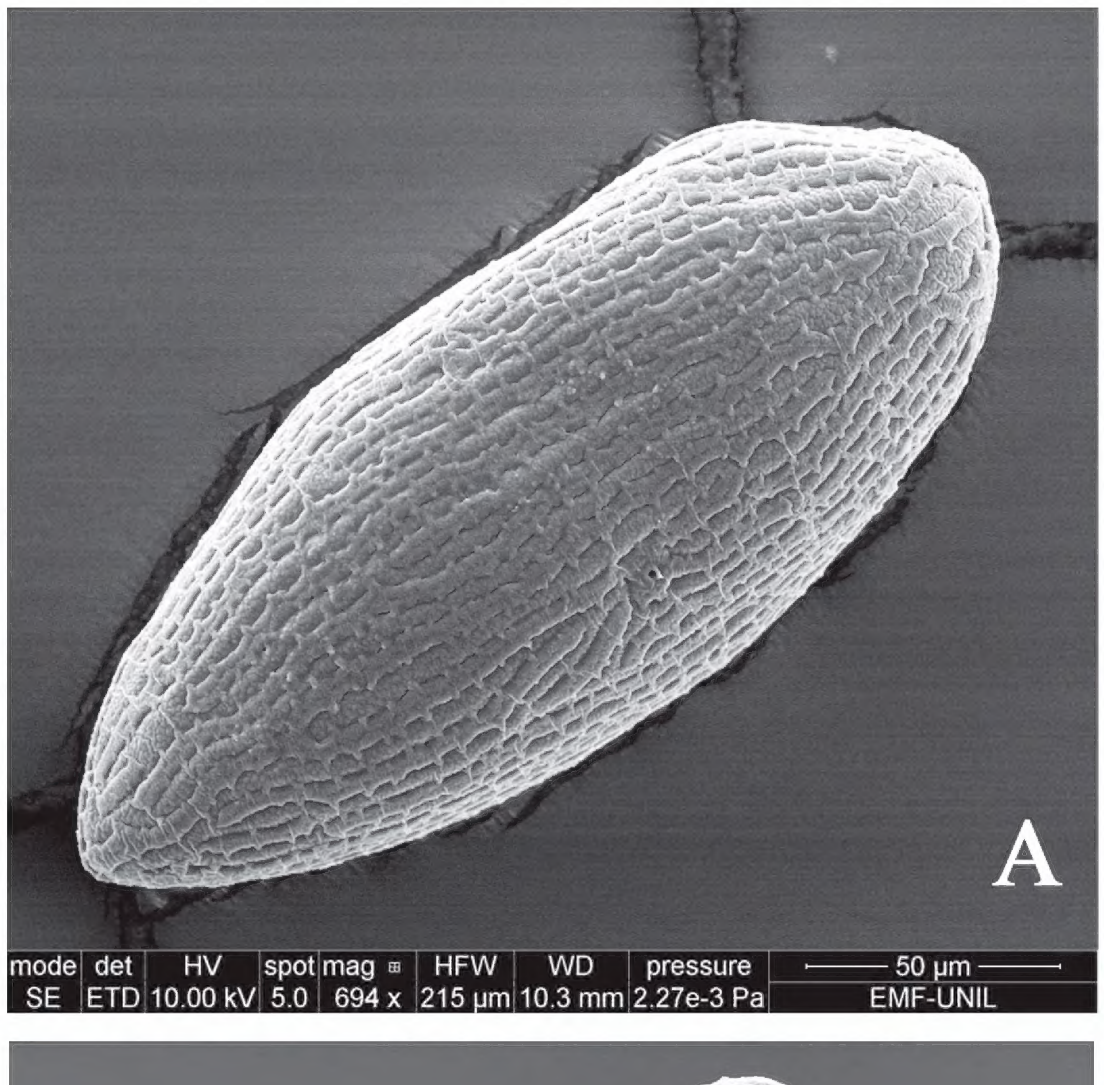
A
mode det HV spot mag HFW WD pressure 50 µm
SE ETD 10.00 kV 5.0 694 x 215 µm 10.3 mm 2.27e-3 Pa EMF-UNIL
B
mode det mag HV HFW WD 100 µm
SE ETD 1 146 x 10.00 kV 260 µm 12.1 mm EMF-UNIL

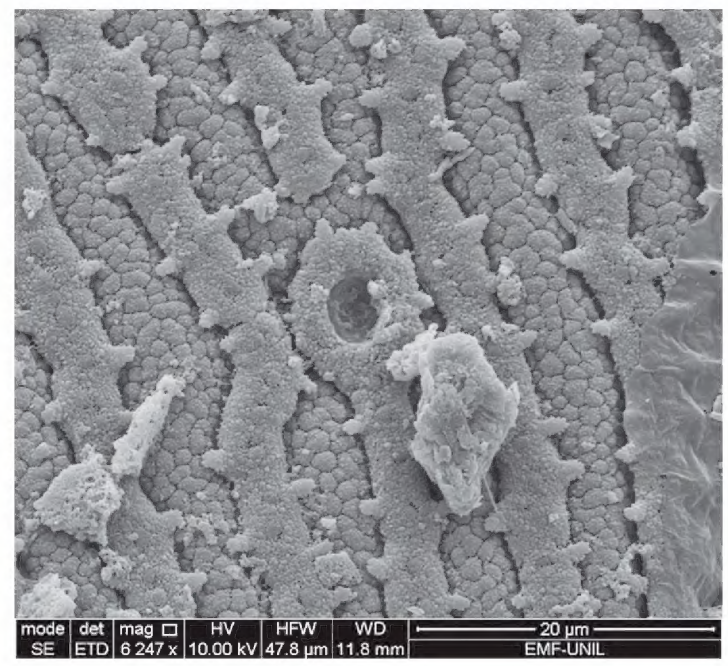

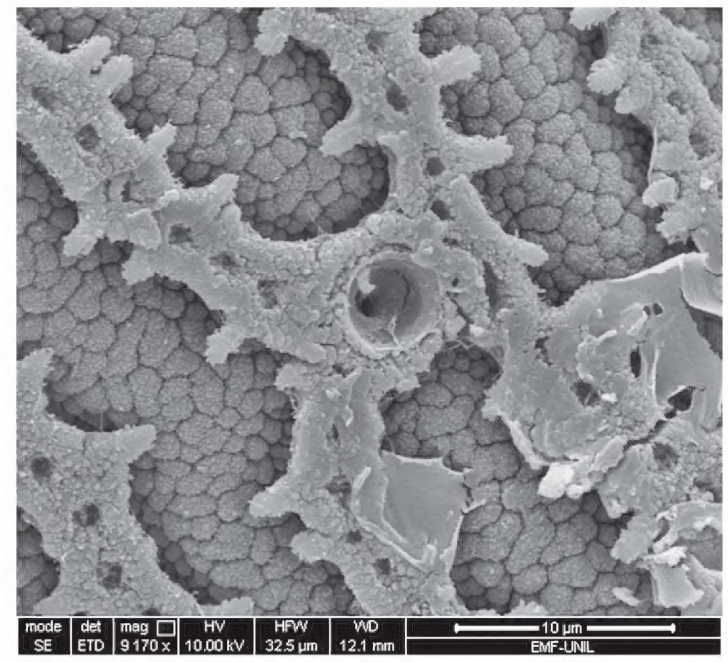

Figure 6. *H. ghora* sp. nov., egg in toto (**A, B**); micropyle and details of the chorion (**C, D**); specimen from Oued Houdfia (**A–C**); specimen from Oued Louar (**B–D**).

ia/tarsi ratio in fore leg: 1/1.15/0.6/0.4/0.3/0.15; mid leg: 1/1.15/0.05/0.08/0.08/0.2; hind leg: 1/1.25/0.1/0.1/0.1/0.15. Fore claws similar, paddle-shaped, mid- and hind claws dissimilar, one paddle-like and one hooked. Forewing transparent, pterostigmatic area milky with 6–7 oblique and simple transversal veins, longitudinal veins medium brown, transversal veins light brown. MA and MP forks asymmetrical, cubital field with two long and sometimes one short intercalary veins (Fig. 5B). Hindwing with rounded costal process approximately in the middle of the wing; vein Sc long, very close to the costal one and reaching it almost at the tip of the wing (Fig. 5C).

Abdomen. Tergites greyish brown, posterior margin of each segment dark brown; sternites light brown, nervous ganglia tinted with medium brown. Styliger plate medium brown, dark brown along the margins, first segment of the gonopods medium brown at base, lighter at apex, segments 2 and 3 yellowish brown. Posterior margin of the styliger plate almost straight in the middle, median incision V-shaped (Fig. 5D); segment 1 subequal in length to segments 2 and 3 combined; inner margin of segment 1 with a broad base, and without bulge on outer margin. Penis lobes rounded and tight together, ventral spine long, thick and curved outwards, almost reaching

the base of the styliger plate (Fig. 5E). Cerci and terminal filament broken.

Female imago. Size: body length: 4.5–5.0 mm; forewing length: 5.0–5.5 mm.

Forewing transparent, longitudinal and transversal veins dark brown; pterostigmatic area with 7–9 oblique and simple transversal veins. MA and MP forks asymmetrical, cubital field with two long intercalary veins. Hindwing with rounded costal process approximately in the middle of the wing; vein Sc reaching the costal margin at mid length to the tip of the wing.

Eggs ovoid, ca. 225 µm × 95 µm, with longitudinal ribs punctuated or not punctuated, bearing transversal small outgrowths, making the whole structure resemble barbed wire (Figs 6A, B). Micropyle in equatorial area (Figs 6C, D).

Habrophlebia seybouse Sartori, Vuataz & Samraoui, sp. nov.

https://zoobank.org/64A69EDE-4EDA-41EA-A610-32F3FBFC33E7

Figs 7–11

Habrophlebia sp., Samraoui et al. 2021a; *Habrophlebia* sp. 12, Hezil et al. 2025.

Material examined. ***Holotype*:** one nymph in ethanol (GBIFCH00902493), Algeria, Wilaya of Guelma, Selaoua, Oued Cherf; 36°20'54"N 7°16'2"E, 589 m, 24.V.2018, B. Samraoui leg., MZL.

Paratypes. Algeria, Wilaya of Guelma, Selaoua, Oued Cherf, same data as holotype, 48 nymphs in ethanol (GBIFCH00889515), 3 nymph on slide (GBIFCH00672305, GBIFCH00673039, GBIFCH01224096); same locality as holotype, 27.V.2020, 1 male, 1 female in ethanol (GBIFCH00654985), B. Samraoui leg.; same locality as holotype, 6.VI.2020, 6 males, 4 females in ethanol (GBIFCH01118436, GBIFCH00654984), B. Samraoui leg., MZL • Wilaya of Guelma, Ayoun, Oued Aar, 7 36°12'50"N, 7°27'48"E, 892 m, 24.V.2018, 1 nymph in ethanol (GBIFCH00763557), B. Samraoui leg., MZL • Wilaya of Skikda, Collo, Oued Tizagban; 37°00'39"N, 6°22'31"E, 492 m, 21.I.2022; 2 nymphs on slide (GBIFCH00658256, GBIFCH00658257), B. Samraoui leg., MZL.

Etymology. The name *Ubus* derives from pre-Roman, possibly Punic or Amazigh (Berber), roots. In ancient sources, *Ubus* referred to the river now known as Oued Seybouse, one of Algeria's major waterways. The river originates in the Hauts Plateaux and flows northwards to the Mediterranean Sea near Annaba.

Descriptions. Nymph. Body length of final instar, excluding caudal filaments, up to 7 mm for male and up to 8 mm for female. Cerci as long as body length.

Coloration. General coloration medium brown; dark brown between ocelli, light brown in front and on the clypeus. Upper portion of male eyes light brown to orange (Fig. 7A). Antenna with pedicel greyish brown, scape light brown and filament yellowish. Pro- and mesonotum medium brown, with light brown maculae, on medium and lateral margins; lateroparapsidal sutures dark brown. Legs light to medium brown; dorsal surface of fore femora dark brown in mature nymphs; tibiae light brown to yellowish, except at base with the femur grayish brown; tarsi light brown to yellowish. Abdominal tergites dark brown with a sagittal line paler and two elongated light maculae medio-anteriorly, especially well visible on segments I–VI. Sternites light to medium brown, nervous ganglia well visible. Cerci and paracercus medium brown at base, lighter distally, dark banding slightly visible every two segments proximally.

Head. Labrum rectangular, ca. 1.75× wider than long (Fig. 7B); dorsal surface covered distally with scattered stout setae; anterior margin with a row of stout, long and spatulate setae medially; emargination narrow, U–shaped without flat denticles; ventral surface with two bunches of stout setae medially. Mandibles similar to other *Habrophlebia* species, incisor with 3 teeth, kinetodontium with 3 teeth (Fig. 7C), 13–14 long and thin setae below mola of right mandible (Fig. 7D). Maxilla stocky, subapical row of 6–7 pectinate setae (Fig. 7E); maxillary palp with three segments, segment 1 and 2 subequal in length, and longer than segment 3; segment 3 triangular 1.21–1.45× longer than wide at base; all setae on palp segments stout and entire. Hypopharynx with highly developed superlinguae terminated by a membranous digitation (Fig. 7F). Labium with rhomboid glossae, outer margin and apex covered by short, broad setae; paraglossae enlarged laterally, covered with fine and long setae on dorsal surface; with long, thick setae on outer margin; labial palp with three segments, inner margin of segment 1 highly dilated near the middle, about 1.25–1.30× longer than maximum width, segment 2 as long as segment 3, ca. 0.7–0.8× length of segment 1; segment 3 ca. 1.8–2.0× longer than wide at base, conical shape and with 6–7 stout and long, simple setae on dorsal surface. Submentum with numerous long, stout and pointed setae laterally; ventral surface with few long, stout and pointed setae (Fig. 7G).

Thorax. Pronotum with anterior corners bearing few long and pointed setae laterally, and 1–3 stout and strong setae dorsally. Anterior margin of pronotum without or with rarely 1–2 stout setae (Fig. 8A). Fore legs femora elongated, ca. 2.5× longer than wide, outer margin and upper surface covered with long, entire and pointed setae (Fig. 8B); fore tibiae subequal in length to femora, outer margin with thin and long setae, inner margin with long stout and feathered or entire setae especially near apex; tarsi 0.5× length of tibiae, outer margin with long and thin setae, inner margin with long and pointed entire setae. Middle legs similar to fore legs, femora ca. 3× longer than wide, dorsal surface of femora with more numerous and slightly longer stout and pointed setae (Fig. 8C); tibiae and femora of subequal length; tarsi 0.5× length of tibiae. Hind legs with femora 3.5× longer than wide (Fig. 8D), dorsal surface covered with stout, long, pointed and entire (non-feathered) setae (Fig. 8E); hind tibiae as long as hind femora, outer margin with scattered stout, pointed setae; inner margin with stout,

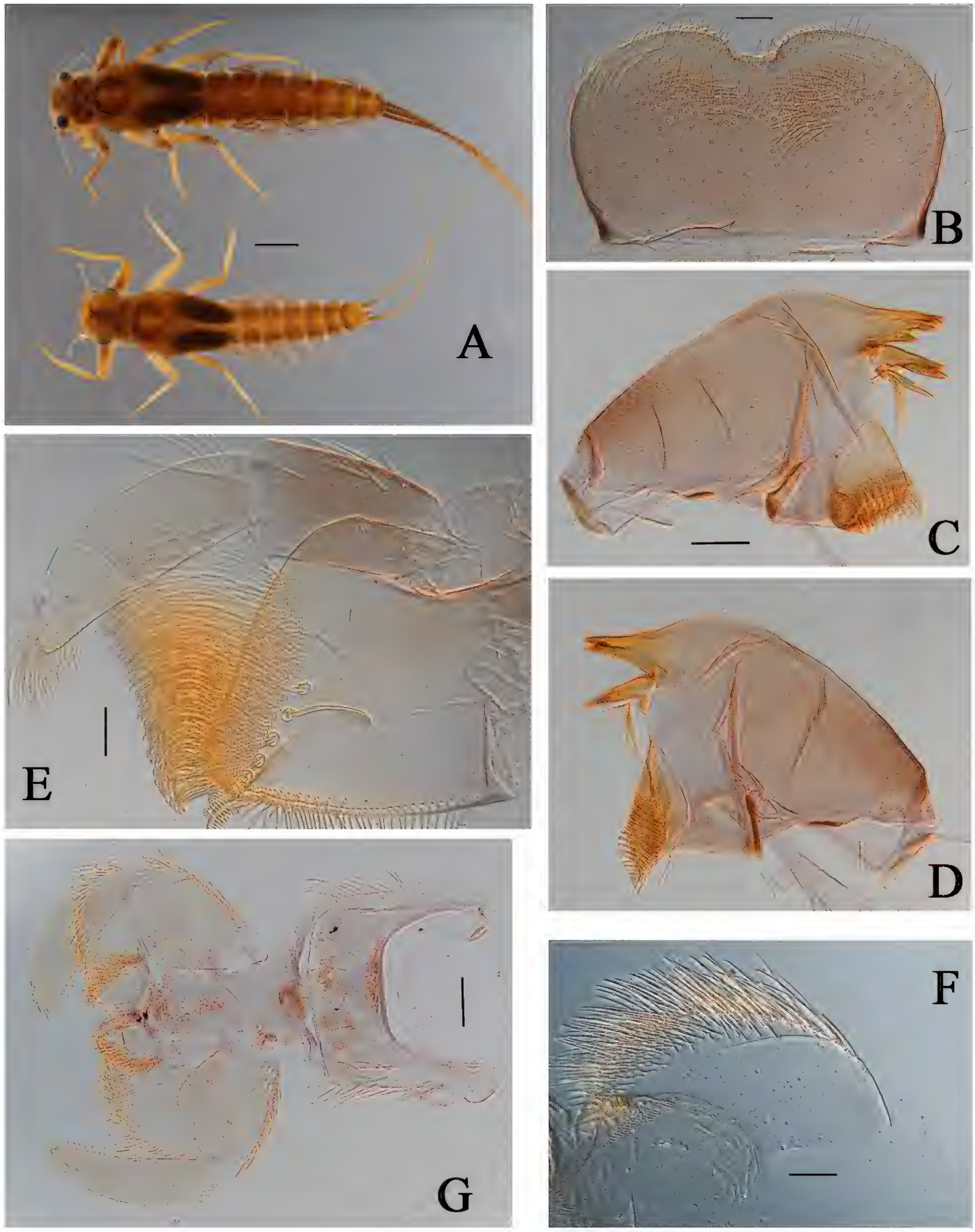

Figure 7. *H. seybouse* sp. nov., habitus of female (above) and male (below) nymphs (**A**); labrum (**B**); left mandible (**C**); right mandible (**D**); maxilla (**E**); hypopharynx, left half (**F**); labium and submentum (**G**). Scale bars: 1 mm (**A**); 50 µm (**B, E, F**); 100 µm (**C, D, G**).

pointed and entire setae (Fig. 8F); tarsi 0.5× length of tibiae, outer margin with long and thin setae, inner margin with long, stout, pointed and entire setae. Claws of all legs slightly hooked, with 14–16 denticles that decrease in size from the apex to the tarsus (Fig. 8G).

Abdomen. Posterolateral expansions only on segments VIII and IX. Posterior margin of tergite IX with triangular, broad, pointed spines, ca. 1.5–2× longer than wide at base (Fig. 9A); tergite VIII with triangular, narrow spines 2× longer than wide (Fig. 9B); from tergite VII to tergite V, spines

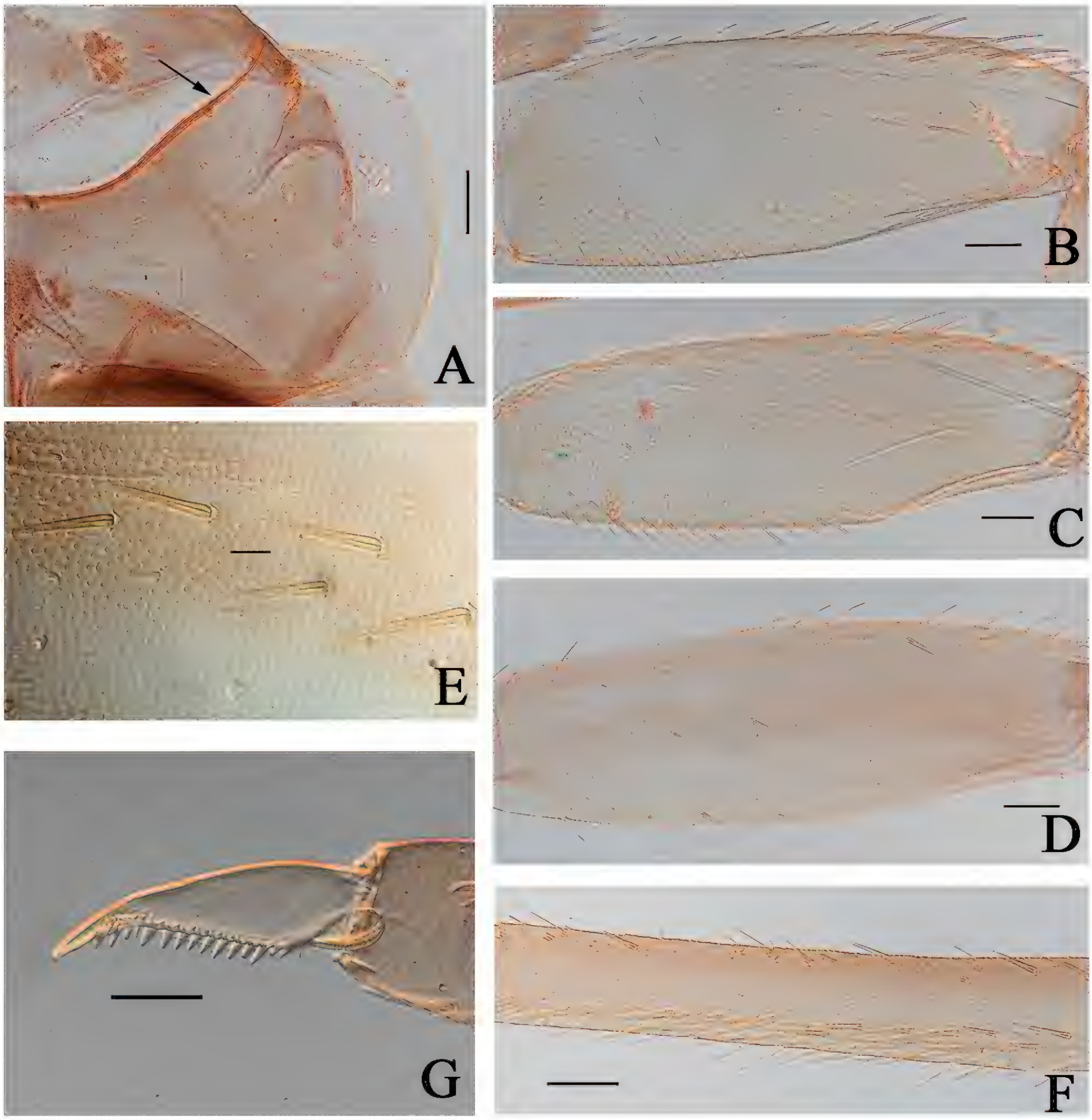

Figure 8. *H. seybouse* sp. nov., thoracic structures, pronotum, right half (**A**); fore femur (**B**); mid femur (**C**); hind femur (**D**); setae on upper face of hind femur (**E**); hind tibia (**F**); claw (**G**). Scale bars: 100 µm (**A–D, F**); 20 µm (**E**); 50 µm (**G**).

becoming smaller, needle-shaped (Figs 9C, D); tergites I–IV with barely visible spines. Gills present on segments I–VII; all gills elongated with long filaments; dorsal lamella bearing 5–6 filaments, ventral lamella with 3–4 filaments (Fig. 9E).

Imagos. ***Male imago.*** Size: body length: 5.5–6.0 mm; forewing length: 5.3–5.6 mm; cerci and terminal filament broken.

Head medium brown, dark brown between ocelli; basal portion of compound eyes greyish, upper portion orange brown, scape medium brown, pedicel dark brown, flagellum light brown.

Thorax. Pronotum greyish brown, washed with dark brown; meso- and metanotum uniformly dark brown, pleurae, coxae, and trochanters greyish brown, washed with dark brown; fore femora dark brown, fore tibiae medium brown, tarsi light brown; mid- and hind legs with femora greyish brown, dark brown distally, tibiae medium brown and tarsi medium brown, except the last segment light brown. Femur/tibia/tarsi ratio in fore leg: 1/1.2/0.4/0.4/0.3/0.1; mid leg: 1/1.2/0.1/0.06/0.06/0.1; hind leg: 1/1.05/0.1/0.05/0.05/0.15. Fore claws similar, paddle-shaped, mid- and hind claws dissimilar, one paddle-like and one hooked. Forewing transparent, pterostigmatic area milky with 6–8 oblique and simple transversal veins, longitudinal veins medium brown, transversal veins light brown. MA and MP forks asymmetrical, cubital field with two long intercalary veins (Fig. 10A). Hindwing with rounded costal process approximately in the middle of the wing; vein

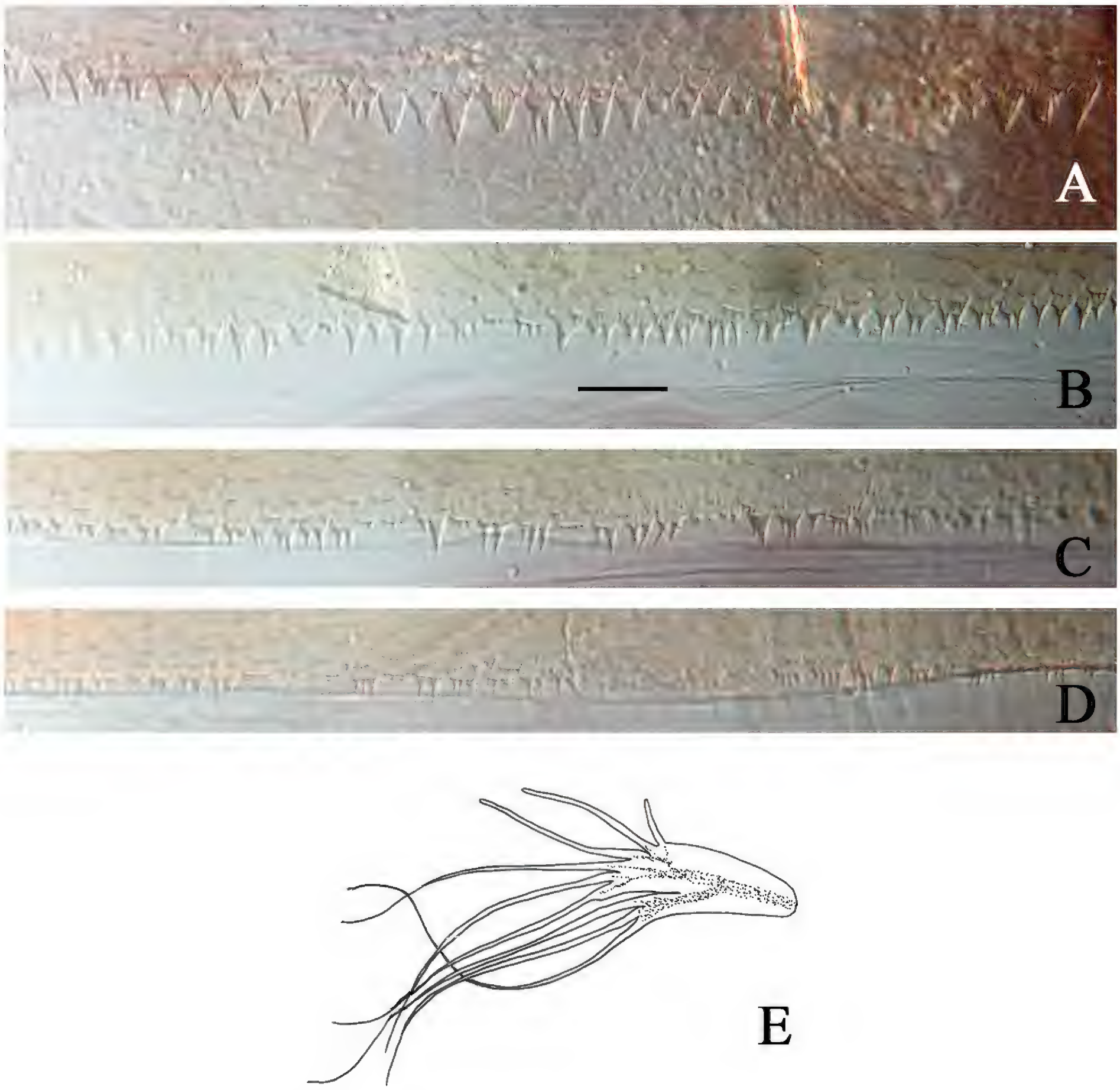

Figure 9. *H. seybouse* sp. nov., abdominal structures, posterior margin of tergite IX (**A**); tergite VIII (**B**); tergite VII (**C**); tergite VI (**D**); gill (**E**). Scale bar: 20 µm.

Sc short, reaching the costal margin at mid-length between costal process and the tip of the wing (Fig. 10C).

Abdomen. Tergites and sternites medium brown, posterior third or half of each segment dark brown. Styliger plate medium brown, dark brown along the margins, first segment of the gonopods medium brown, segments 2 and 3 yellowish brown. Posterior margin of the styliger plate almost straight in the middle, median incision V-shaped (Fig. 10D); segment 1 subequal in length to segments 2 and 3 combined; inner margin of segment 1 with a broad base, and without bulge on the outer margin. Penis lobes rounded and tight together, ventral spine long, thin and curved outwards, almost reaching the base of the styliger plate (Fig. 10E). Cerci and terminal filament broken.

Female imago. Size: body length: 7.0–7.5 mm; forewing length: 7.5–8.0 mm.

Forewing transparent, slightly tinted in brown in subcostal field; longitudinal and transversal veins dark brown; pterostigmatic area with ca. 7–8 oblique and simple transversal veins. MA and MP forks asymmetrical, cubital field with two long intercalary veins. Hindwing with rounded costal process approximately in the middle of the wing; vein Sc long, reaching the costal margin almost at the tip of the wing (Fig. 10B).

Eggs ovoid, ca. 245 µm × 100 µm, with longitudinal ribs punctuated, bearing transversal small outgrowths, making the whole structure resemble barbed wire (Fig. 11A). Micropyle in equatorial area (Fig. 11B).

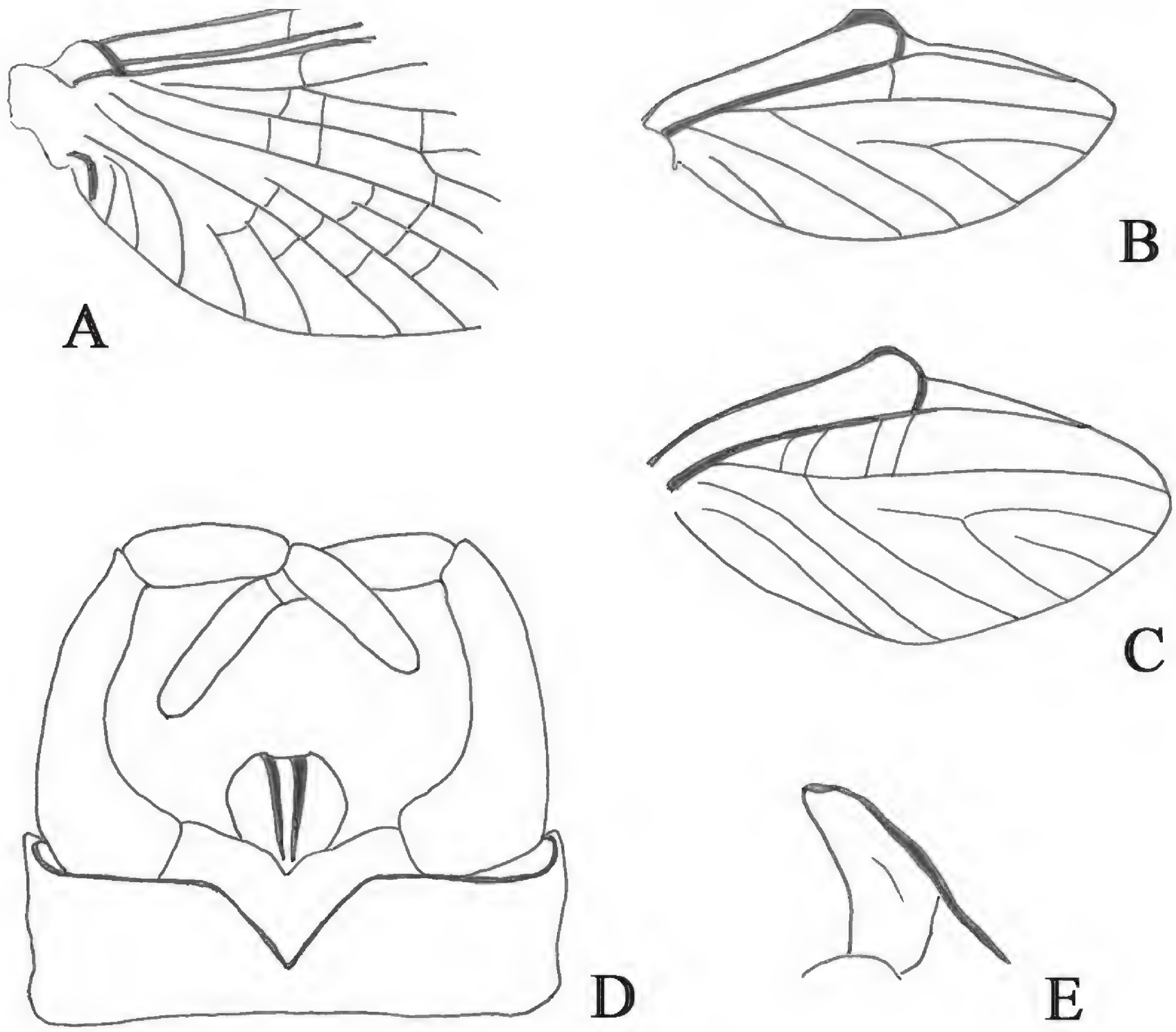

Figure 10. *H. seybouse* sp. nov., cubital field of female imago (**A**); hindwing of female imago (**B**); hindwing of male imago (**C**); genitalia in ventral view (**D**); penis in lateral view (**E**).

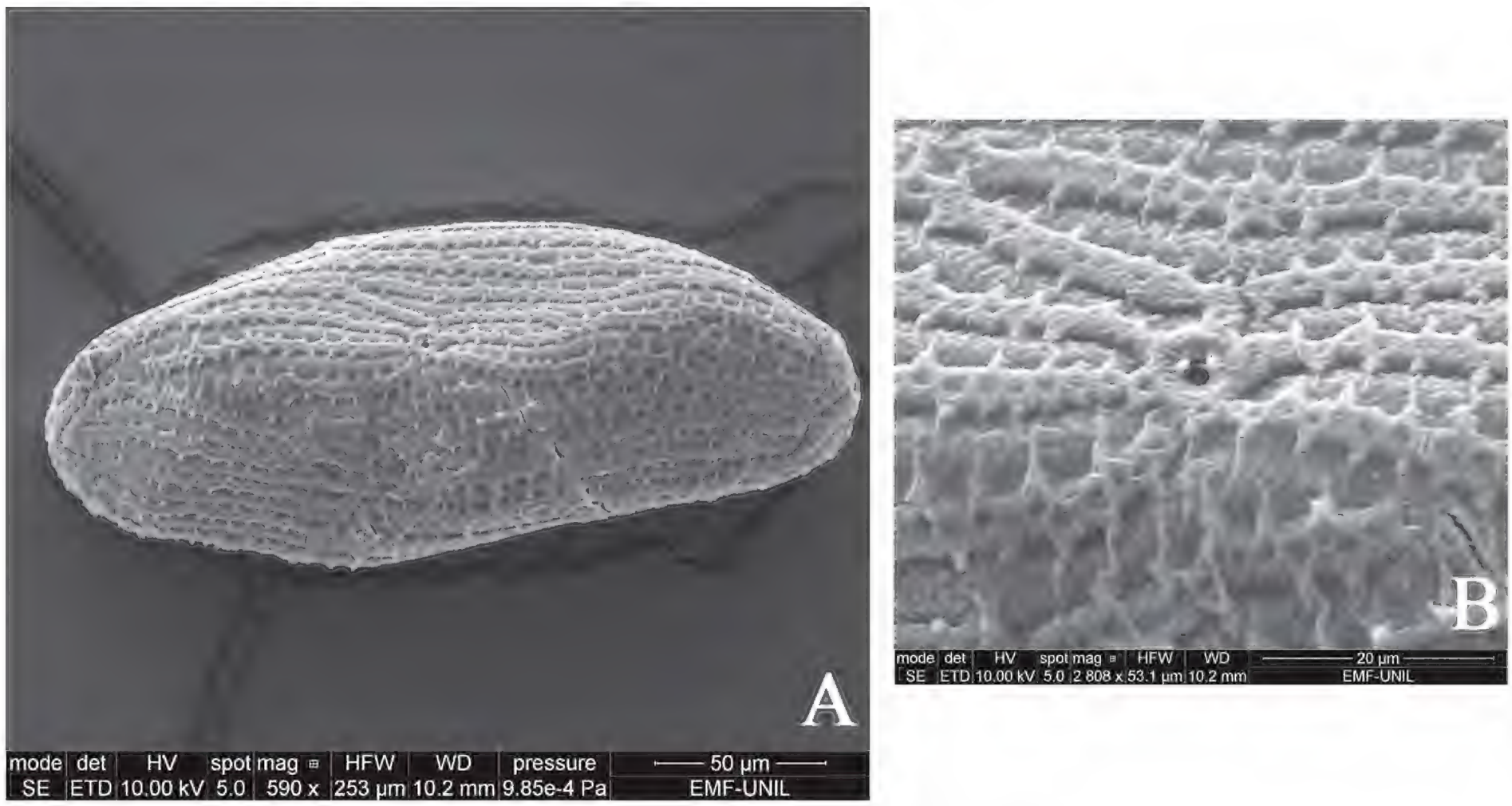
A
mode det HV spot mag HFW WD pressure 50 µm
SE ETD 10.00 kV 5.0 590 x 253 µm 10.2 mm 9.85e-4 Pa EMF-UNIL
B
mode det HV spot mag HFW WD 20 µm
SE ETD 10.00 kV 5.0 2 808 x 53.1 µm 10.2 mm EMF-UNIL

Figure 11. *H. seybouse* sp. nov., egg in toto (**A**); micropyle and details of the chorion (**B**).

Habrophlebia callensis Sartori, Vuataz & Samraoui, sp. nov.

https://zoobank.org/BB3DBAD0-64A9-4E23-B7DC-D00F91A3D31C

Figs 12–16

Habrophlebia spH, Samraoui et al. 2021b; *Habrophlebia* sp. 7, Hezil et al. 2025.

Material examined. ***Holotype*:** one nymph in ethanol (GBIFCH00902495), Algeria, Wilaya of El Tarf, Hadada, Dar Essalem; 36°53'10"N, 8°37'2"E, 201 m, 11.VII.2019, B. Samraoui leg., MZL.

Paratypes. Algeria, Wilaya of El Tarf, Dar Essalem, same data as holotype, 2 nymphs in ethanol (GBIFCH00829846); same locality as holotype, 1.VIII.2019, 1 nymph on slide (GBIFCH00763554), B. Samraoui leg.; same locality as holotype, 18.IV.2019, 12 nymphs in ethanol (GBIFCH00829847), B. Samraoui leg., same locality as holotype, 2.V.2019, 4 nymphs in ethanol (GBIFCH00829845), B. Samraoui leg., same locality as holotype, 25.VI.2019, 1 nymph in ethanol (GBIFCH00829842), B. Samraoui leg.; same locality as holotype, 23.I.2020, 1 nymph in ethanol (GBIFCH00832063), B. Samraoui leg., MZL • Wilaya of El Tarf, Hadada, Chaaba Waera, 36°53'37"N, 8°36'27"E, 113 m, 2.V.2019, 12 nymphs in ethanol (GBIFCH00829837, GBIFCH00829836), B. Samraoui leg., same locality, 9.III.2019, 13 nymphs in ethanol, (GBIFCH00829838), B. Samraoui leg., MZL. • Wilaya of El Tarf, Hadada, Oued Ftitich; 36°54'01"N, 8°37'05"E, 165 m, 18.IV.2019, 6 nymphs in ethanol (GBIFCH00672314), 1 nymph on slide (GBIFCH01231272), B. Samraoui leg.; same locality, 11.VII.2019, 1 nymph on slide (GBIFCH00763555), B. Samraoui leg.; same locality, 23.I.2020, 4 nymphs in ethanol (GBIFCH00832011), B. Samraoui leg.; same locality, 12.III.2020, 2 nymphs in ethanol (GBIFCH00654972), 1 nymph on slide (GBIFCH01118444), B. Samraoui leg.; same locality, 18.V.2022, 2 females (GBIFCH00654974), B. Samraoui leg.; same locality, 25.V.2022, 1 male (GBIFCH01314443), B. Samraoui leg.; same locality, 1.VI.2022, 1 female (GBIFCH00654975), B. Samraoui leg., all MZL.

Etymology. The name of El Kala derives from the Arabic *al-Qal'a* ("the fortress"), a reference to its strategic role through history. During the French period it was known as *La Calle*, while in antiquity it was recorded as *Thinisa in Numidia*.

Descriptions. Nymph. Body length of final instar, excluding caudal filaments, up to 6 mm for male and up to 7 mm for female. Cerci as long as body length.

Coloration. General coloration medium brown; dark brown between ocelli, whitish in front of the eyes, light brown in front and on the clypeus. Upper portion of male eyes light brown to orange. Antenna with pedicel greyish brown, scape light brown and filament yellowish. Pro- and mesonotum dark brown, with light brown maculae, on medium and lateral margins; lateroparapsidal sutures dark brown. Legs light to medium brown; dorsal surface of fore femora dark brown, fore tibiae greyish brown; mid- and hind legs light brown to yellowish, except at apex of femora grayish brown; tarsi light brown to yellowish. Abdominal tergites medium brown with three pairs of lighter maculae, especially well visible on segments I–VI (Fig. 12A); posterolateral angles and posterior margin of tergites I–VIII dark brown. Sternites medium brown to greyish brown, nervous ganglia well visible (Fig. 12B). Cerci and paracercus medium brown at base, lighter distally, dark banding slightly visible every two segments proximally.

Head. Labrum rectangular, ca. 1.85× wider than long (Fig. 12C); dorsal surface covered distally with scattered stout setae; anterior margin with a row of stout, long and spatulate setae medially; emargination narrow, U-shaped with flat denticles; ventral surface with two bunches of stout setae medially. Mandibles similar to other *Habrophlebia* species, incisor with 3 teeth, the lowest of the left mandible with a clear indentation (Fig. 12D), kinetodontium with 3 teeth, 14–15 long and thin setae below mola of right mandible (Fig. 12E). Maxilla stocky, subapical row of 5 or 6 pectinate setae (Fig. 12F); maxillary palp with three segments, segment 1 and 2 subequal in length, and longer than segment 3; segment 3 triangular 1.51–1.71× longer than wide at base; all setae on palp segments stout and entire. Hypopharynx with highly developed superlinguae terminated by a membranous digitation (Fig. 12G). Labium with rhomboid glossae, outer margin and apex covered by short, broad setae; paraglossae enlarged laterally, covered with fine and long setae on the dorsal surface; with long, thick setae on the outer margin; labial palp with three segments, inner margin of segment 1 highly dilated near the middle, about 1.15–1.20× longer than the maximum width, segments 2 0.85× length of segment 1, segment 3, ca. 0.75× length of segment 1; segment 3 ca. 1.7–1.8× longer than wide at base, conical shape and with 5–7 stout and long, simple setae on dorsal surface. Submentum with numerous long, stout and pointed setae laterally and on ventral surface (Fig. 12H).

Thorax. Pronotum with anterior corners bearing numerous long and pointed setae laterally, and dorsally. Anterior margin of pronotum with a row of stout setae (Fig. 13A). Fore legs femora stocky, ca. 2.1× longer than wide, outer margin and upper surface covered with long, entire and pointed setae (Fig. 13B); fore tibiae slightly shorter than femora, outer margin with thin and long setae, inner margin with long stout and feathered or entire setae especially near apex; tarsi 0.55× length of tibiae, outer margin with long and thin setae, inner margin with long and pointed entire setae. Middle legs similar to fore legs, femora ca. 2.5× longer than wide, dorsal surface of femora with numerous and long, stout and pointed setae; tibiae and femora of subequal length; tarsi 0.5× length of tibiae. Hind legs with femora 2.8–3.0× longer than wide (Fig. 13C), dorsal surface covered with stout, long, pointed and entire setae (Fig. 13D); hind tibiae as long as hind femora, outer margin with a row of stout, pointed setae and few thin and long setae; inner margin with stout, pointed and entire

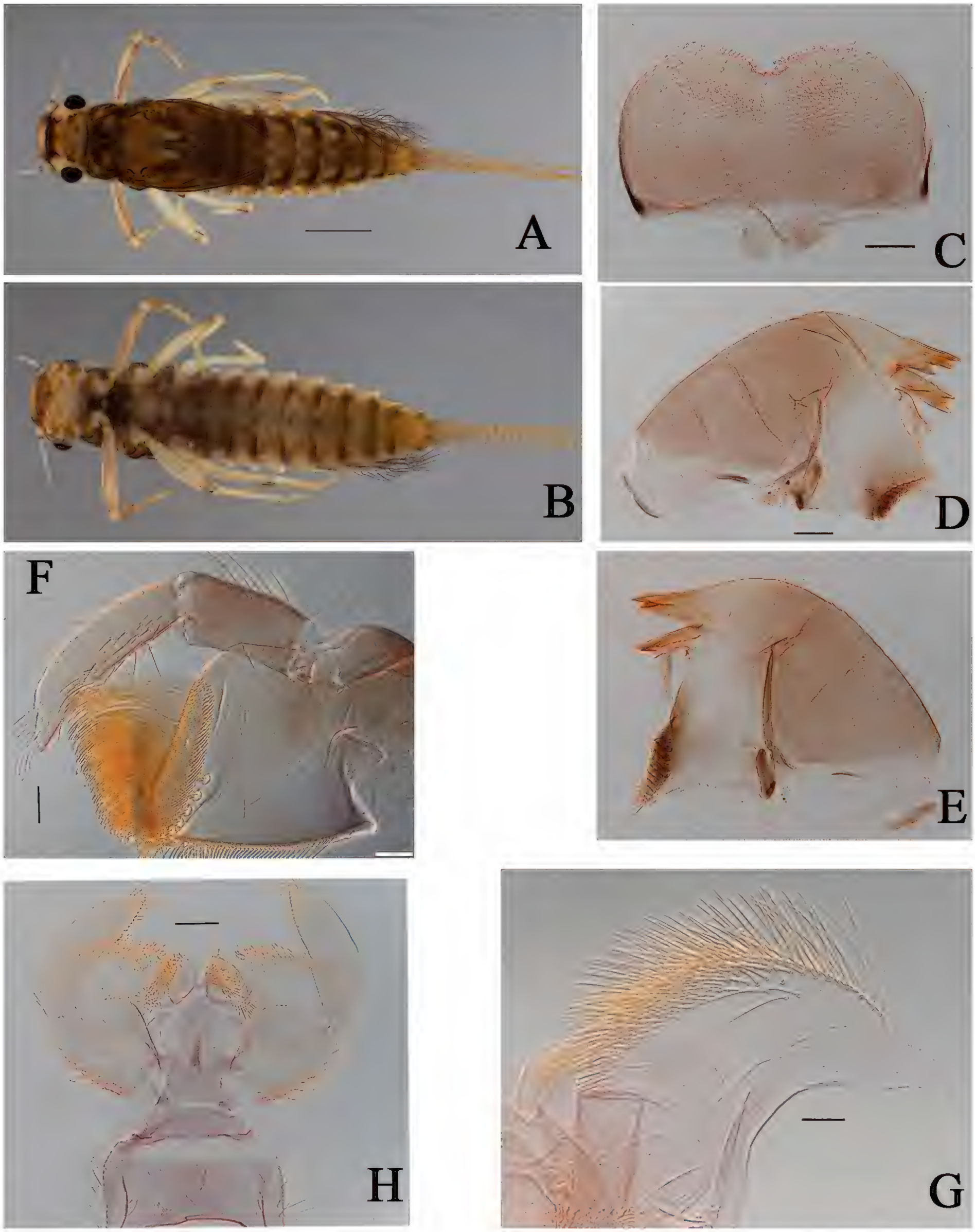

Figure 12. *H. callensis* sp. nov., habitus of female nymph in dorsal (**A**) and ventral position (**B**); labrum (**C**); left mandible (**D**); right mandible (**E**); maxilla (**F**); hypopharynx, left half (**G**); labium and submentum (**H**). Scale bars: 1 mm (**A**); 50 µm (**B, E, F**); 100 µm (**C, D, G**).

setae (Fig. 13E); tarsi 0.4× length of tibiae, outer margin with few long and thin setae, inner margin with long, stout, pointed and entire setae. Claws of all legs slightly hooked, with 17–21 denticles subequal in size (Fig. 13F).

Abdomen. Posterolateral expansions only on segments VIII and IX. Posterior margin of tergite IX with triangular, broad, pointed spines, ca. 1.5–2× longer than wide at base (Fig. 14A); tergite VIII with triangular, narrow

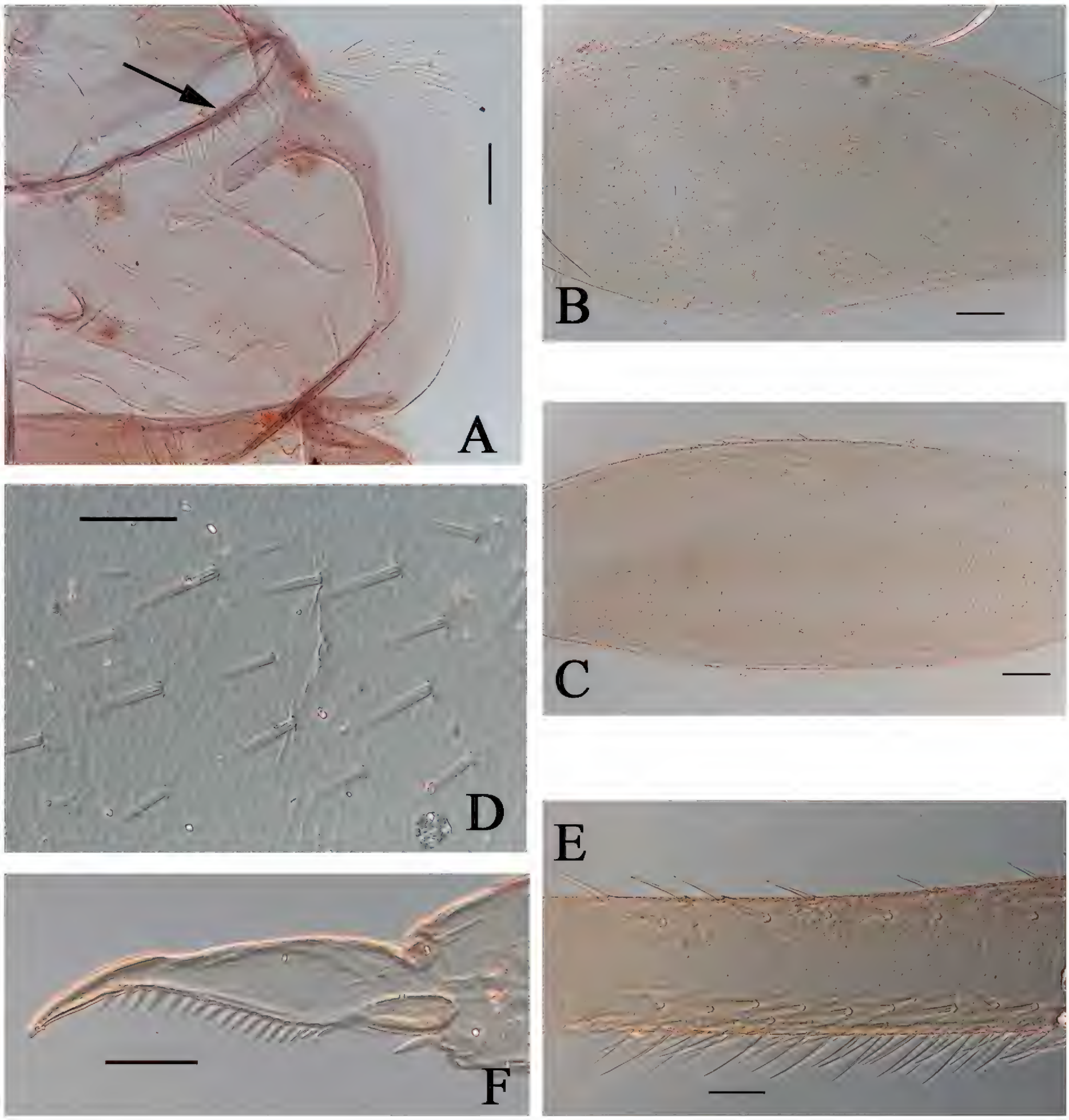

Figure 13. *H. callensis* sp. nov., thoracic structures, pronotum, right half (**A**); fore femur (**B**); hind femur (**C**); setae on upper face of hind femur (**D**); hind tibia (**E**); claw (**F**). Scale bars: 100 µm (**A–C, E**); 20 µm (**D**); 50 µm (**F**).

spines 2× longer than wide (Fig. 14B); from tergite VII to tergite V, spines becoming smaller, needle-shaped (Fig. 14C–E); tergites I–IV with barely visible spines. Gills present on segments I–VII; all gills elongated with long filaments; dorsal lamella bearing 7–8 filaments, ventral lamella with 4–5 filaments (Fig. 14F).

Imagos. ***Male imago*** in poor condition, only mid- and hind legs and abdomen preserved. Mid and hind legs coloration as in nymphs, whitish with apex of femur brownish. Femur/tibia/tarsi ratio in mid leg: 1/1.3/0.06/0.05/0.05/0.1; hind leg: 1/1.3/0.1/0.08/0.06/0.1. Mid- and hind claws dissimilar, one paddle-like and one hooked. Abdomen. Coloration similar to male nymphs. Styliger plate medium brown, dark brown along the margins, first segment of the gonopods medium brown, segments 2 and 3 yellowish brown. Posterior margin of the styliger plate concave, median incision U-shaped (Fig. 15C); segment 1 slightly longer than segments 2 and 3 combined; inner margin of segment 1 with a broad base, and with bulge on the outer margin. Penis lobes rounded and tight together, ventral spine long, thin and slightly curved outwards, reaching the base of the styliger plate (Fig. 15D). Cerci and terminal filament broken.

Female imago: body length: 4.0–4.5 mm; forewing length: 4.5–5.0 mm. Forewing transparent, slightly tinted in brown in subcostal field; longitudinal and transversal veins dark brown; pterostigmatic area with ca. 10 oblique and simple transversal veins. MA and MP forks asymmetrical, cubital field with two long and three short intercalary veins (Fig. 15A). Hindwing with rounded costal process approx-

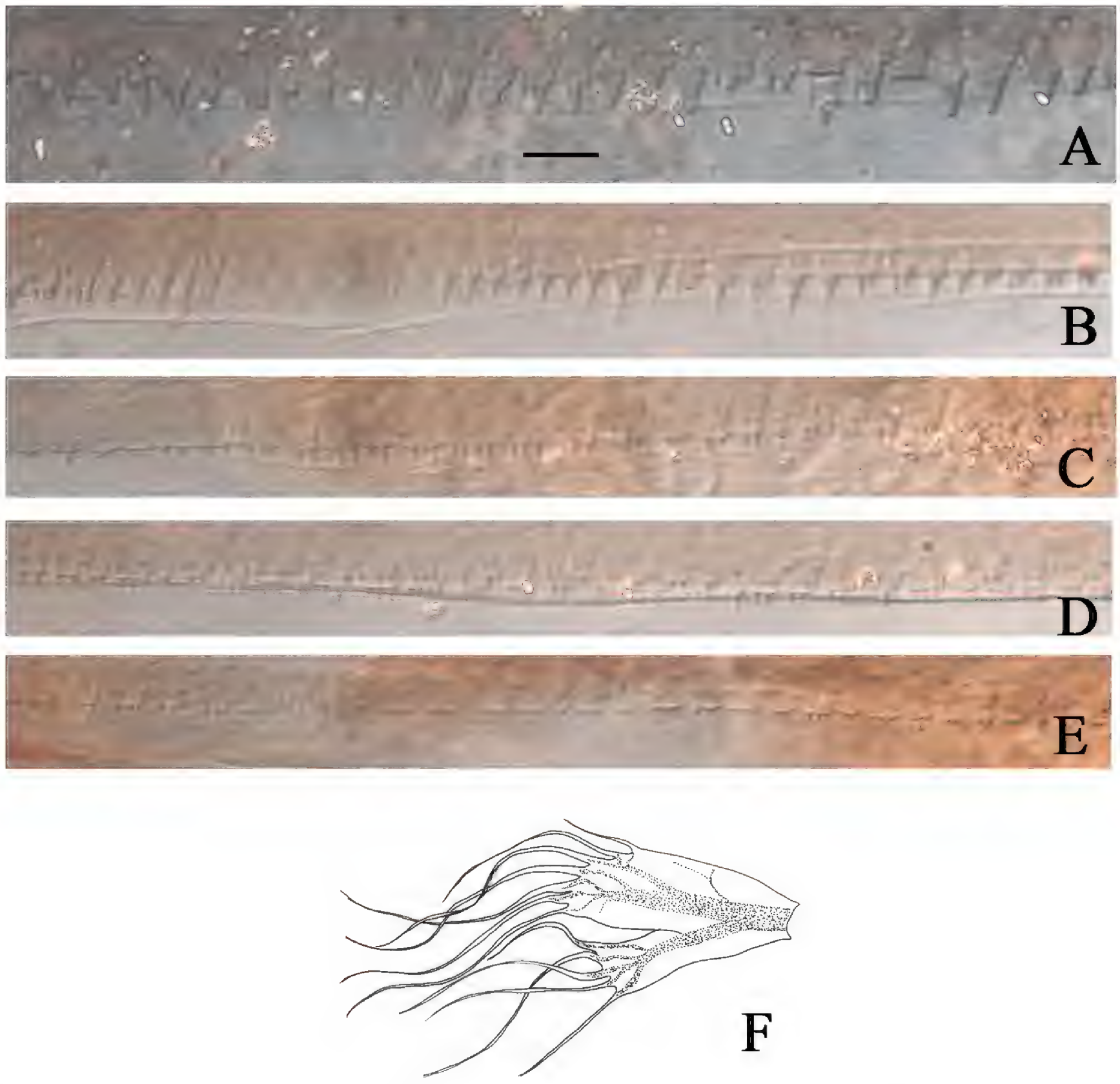

Figure 14. *H. callensis* sp. nov., abdominal structures, posterior margin of tergite IX (**A**); tergite VIII (**B**); tergite VII (**C**); tergite VI (**D**); tergite V (**E**); gill (**F**). Scale bar: 20 µm.

imately in the middle of the wing; vein Sc long, reaching the costal margin almost at the tip of the wing (Fig. 15B).

Eggs ovoid, ca. 200 µm × 90 µm, with longitudinal ribs non-punctuated, the majority running from one pole to the other (Fig. 16A); chorion covered with thin membranous filaments perpendicular to pole axis, sometimes longitudinal. Micropyle in equatorial area (Fig. 16B).

Habrophlebia annaba Sartori, Vuataz & Samraoui, sp. nov.

https://zoobank.org/FF8685EE-013E-450A-AA5A-83B2D2C470B1

Figs 17–21

Habrophlebia sp. 9, Hezil et al. 2025.

Material examined. ***Holotype*:** one nymph in ethanol (GBIFCH00654946), Algeria, Wilaya of Annaba, Edough, Oued Agab, 36°54'44"N, 7°39'35"E, 750 m, 5.VI.2021, B. Samraoui leg., MZL.

Paratypes. Algeria, Wilaya of Annaba, Edough, Oued Agab, same data as holotype, 1 nymph in ethanol (GBIFCH00654980); same locality as holotype, 26.IV.2021, 1 nymph on slide (GBIFCH01314689); 4.V.2022, 1 female imago in ethanol (GBIFCH00654978); 16.V.2021, 1 nymph, 1 female imago in ethanol (GBIFCH00654977); 1.V.2021, 1 male imago in ethanol (GBIFCH01118440); 5.VI.2021, 1 nymph on slide (GBIFCH01314677); 10.II.2022, 1 nymph in ethanol (GBIFCH00654976), 1 nymph on slide (GBIFCH01314437); 1.VI.2022, 1 nymph on slide (GBIFCH00658258) • Wilaya of Annaba, Edough, Oued Zouz, 36°55'54"N, 7°40'03"E, 550 m, 20.III.2022, 15 nymphs in ethanol (GBIFCH00654982), 1 nymph on slide (GBIFCH01118439); same locality, 25.IV.2022, 1 female imago in ethanol (GBIFCH00654983); all B. Samraoui leg., MZL.

Etymology. The name Annaba derives from the Arabic *ʿannāb* (jujube), in reference to the jujube tree (*Ziziphus jujuba*), once abundant in the region. In antiquity, the city was known as *Hippo Regius*, a major centre of Roman

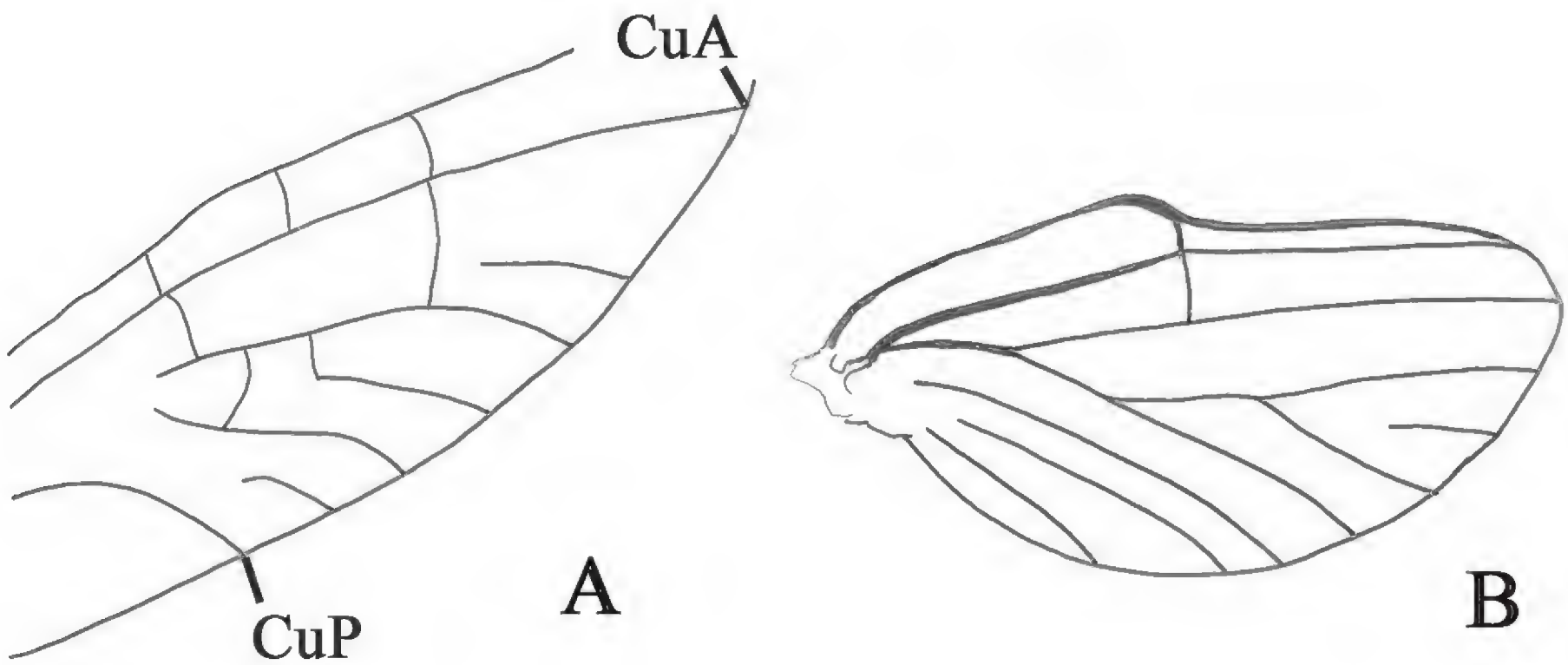

Figure 15. *H. callensis* sp. nov., cubital field of male imago (**A**); hindwing of male imago (**B**); genitalia in ventral view (**C**); penis in lateral view (**D**). Abbreviations: CuA, cubital anterior vein; CuP, cubital posterior vein.

North Africa and the episcopal See of Saint Augustine (354–430 CE). Later, it was renamed *Bouna* in Arabic and was known as *Bône* during the French period.

Descriptions. Nymph. Body length of final instar, excluding caudal filaments, up to 6 mm for male and up to 7 mm for female. Cerci as long as body length.

Coloration. General coloration medium brown; dark brown between ocelli, light brown in front and on the clypeus, especially in young nymphs. Upper portion of male eyes red-brick to reddish brown (Fig. 17B). Antenna with pedicel dark brown, scape greyish brown and filament light brown, more or less entirely whitish in young nymphs. Pronotum medium brown, washed with dark brown in middle and anteriorly, lateral margins whitish; mesonotum medium brown, with dark brown maculae; lateroparapsidal sutures dark brown. Legs light to medium brown; femora dark brown in mature nymphs; tibiae medium brown; tarsi light brown to yellowish. Abdominal tergites dark brown to greyish brown, with two lighter maculae medio-anteriorly, especially well visible on segments I–VII (Fig. 17A). Sternites medium brown in the middle, posterior corner underlined with dark brown laterally, thicker in mature nymphs, nervous ganglia well visible. Cerci and paracercus light brown at base, whitish distally, without dark banding.

Head. Labrum rectangular, ca. 1.55× wider than long (Fig. 17C); dorsal surface covered distally with scattered stout setae; anterior margin with a row of stout, long and spatulate setae medially; emargination flared, U-shaped with flat denticles; ventral surface with two bunches of stout setae medially. Mandibles similar to other *Habrophlebia* species, incisor with 3 teeth, the lowest of left mandible with a clear indentation at base (Fig. 17D), kinetodontium with 3 teeth, 10–11 long and thin setae below mola of right mandible (Fig. 17E). Maxilla stocky, subapical row of 7 or 8 pectinate setae (Fig. 17F); maxillary palp with three segments, segment 1 and 2 subequal in length, and longer than segment 3; segment 3 trian-

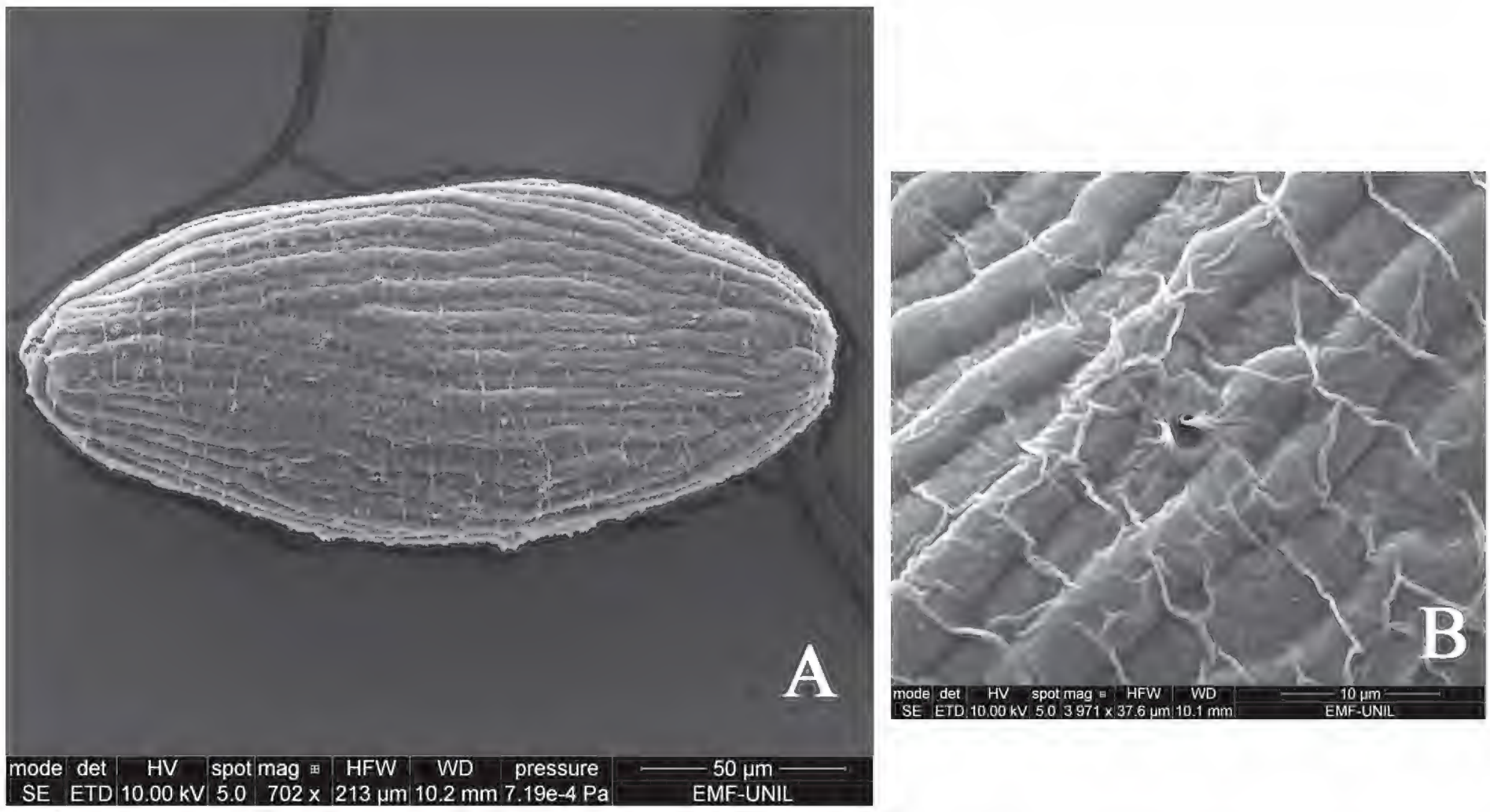
A
mode det HV spot mag HFW WD pressure 50 µm
SE ETD 10.00 kV 5.0 702 x 213 µm 10.2 mm 7.19e-4 Pa EMF-UNIL
B
mode det HV spot mag HFW WD 10 µm
SE ETD 10.00 kV 5.0 3 971 x 37.6 µm 10.1 mm EMF-UNIL

Figure 16. *H. callensis* sp. nov., egg in toto (**A**); micropyle and details of the chorion (**B**).

gular 1.42–1.70× longer than wide at base; all setae on palp segments stout and entire. Hypopharynx with highly developed superlinguae terminated by a membranous digitation. Labium with rhomboid glossae, outer margin and apex covered by short, broad setae; paraglossae enlarged laterally, covered with fine and long setae on the dorsal surface; with long, thick setae on the outer margin; labial palp with three segments, inner margin of segment 1 highly dilated near the middle, about 1.35× longer than the maximum width, segments 2 slightly longer than segment 3, both ca. 0.65–0.70× length of segment 1; segment 3 ca. 1.41–1.54× longer than wide at base, conical shape and with 8–10 stout and long, simple setae on dorsal surface. Submentum with numerous long, stout and pointed setae laterally; ventral surface with numerous long, stout and pointed setae (Fig. 17G).

Thorax. Pronotum with anterior corners bearing few long and pointed setae laterally, and 5–7 stout and strong setae dorsally. Anterior margin of pronotum with numerous stout setae (Fig. 18A). Fore legs femora elongated, ca. 2.45× longer than wide, outer margin and upper surface covered with long, entire and pointed setae (Fig. 18B); fore tibiae subequal in length to femora, outer margin with few thin and long setae, inner margin with several rows of long stout and entire setae; tarsi 0.5× length of tibiae, outer margin with few long and thin setae, inner margin with long and pointed entire setae. Middle legs similar to fore legs, femora ca. 2.6× longer than wide, dorsal surface of femora with more numerous and slightly longer stout and pointed setae; tibiae and femora of subequal length; tarsi 0.5× length of tibiae. Hind legs with femora 2.8× longer than wide (Fig. 18C), dorsal surface covered with stout, long, pointed or blunt and entire (non-feathered) setae (Fig. 18D); hind tibiae as long as hind femora, outer margin with numerous stout, pointed setae; inner margin with stout, pointed and entire setae; tarsi 0.5× length of tibiae, outer margin with long and thin setae, inner margin with long, stout, pointed and entire setae. Claws of all legs slightly hooked, with 15–17 denticles that decrease in size from the apex to the tarsus (Fig. 18E).

Abdomen. Posterolateral expansions only on segments VIII and IX. Posterior margin of tergite IX with triangular, broad, pointed spines, ca. 1.5–2× longer than wide at base (Fig. 19A); tergite VIII with triangular, broad spines 1.5–2× longer than wide (Fig. 19B); tergite VII with slightly shorter spines than tergite VIII (Fig. 19C); tergite VI, with short and broad spines (Fig. 19D), and tergite V with minute but broad spines (Fig. 19E); tergites I–IV with barely visible spines. Gills present on segments I–VII; all gills elongated with long filaments; dorsal lamella bearing 8–10 filaments, ventral lamella with 3–6 filaments (Fig. 19F).

Imagos. ***Male imago.*** Size: body length: 5.5–6.0 mm; forewings missing; cerci and terminal filament broken.

Head dark brown; basal portion of compound eyes blackish, upper portion orange brown, scape and pedicel dark brown, flagellum broken.

Thorax. Pronotum dark brown; meso- and metanotum uniformly dark brown, pleurae, coxae, and trochanters greyish brown, washed with dark brown; fore femora and fore tibiae dark brown, tarsi light brown, apex of each segment dark brown; mid- and hind legs with femora light brown, dark brown distally, tibiae medium brown, dark brown at base, and tarsi medium brown, except the last segment light brown. Femur/tibia/tarsi ratio in fore leg: 1/1.4/0.5/0.5/0.3/0.2; mid leg: 1/1.2/0.1/0.07/0.05/0.1; hind leg: 1/1.2/0.1/0.05/0.05/0.15. Fore claws similar, paddle-shaped, mid- and hind claws dissimilar, one pad-

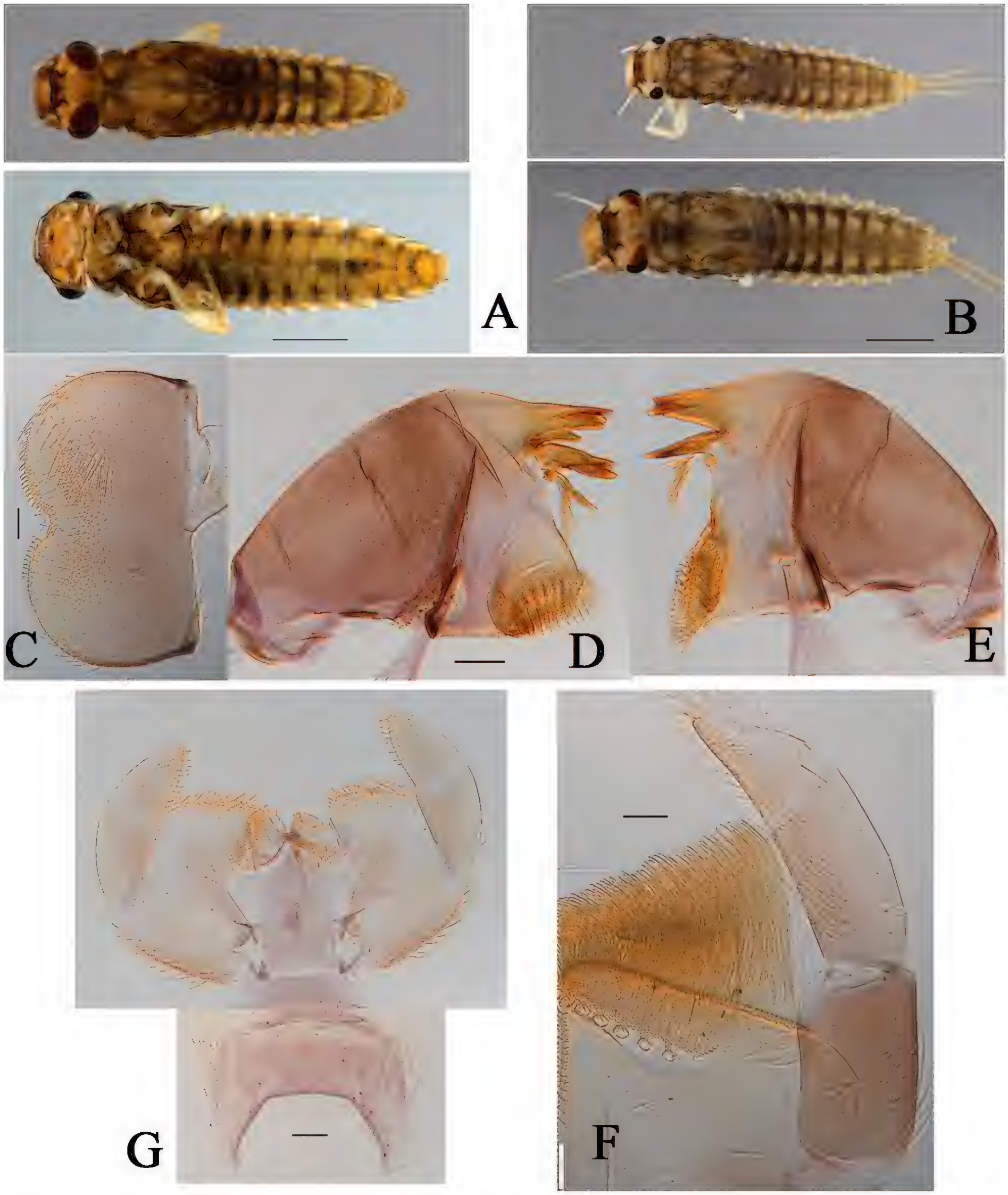

Figure 17. *H. annaba* sp. nov., habitus of mature female nymph (above) and younger nymph (below) (**A**); habitus of mature male nymph (above) and younger nymph (below) (**B**); labrum (**C**); left mandible (**D**); right mandible (**E**); maxilla (**F**); labium and submentum (**G**). Scale bars: 1 mm (**A, B**); 50 µm (**C, G**); 100 µm (**D, E, F**).

dle-like and one hooked. Hindwing with rounded costal process approximately in the middle of the wing; vein Sc long and well separated from the costal vein, reaching the costal margin almost at the tip of the wing (Fig. 20C).

Abdomen. Tergites and sternites medium brown, posterior margin of each segment dark brown. Styliger plate medium brown, dark brown along the margins, gonopods broken. Posterior margin of the styliger plate straight and clearly protruding in the middle, median incision U-shaped (Fig. 20D). Penis lobes rounded and tight together, ventral spine long, thin and straight, almost reaching the base of the styliger plate. Cerci and terminal filament broken.

Female imago. Size: body length: 6.5–7.0 mm; forewing length: 7.0–7.5 mm. Forewing transparent, slightly

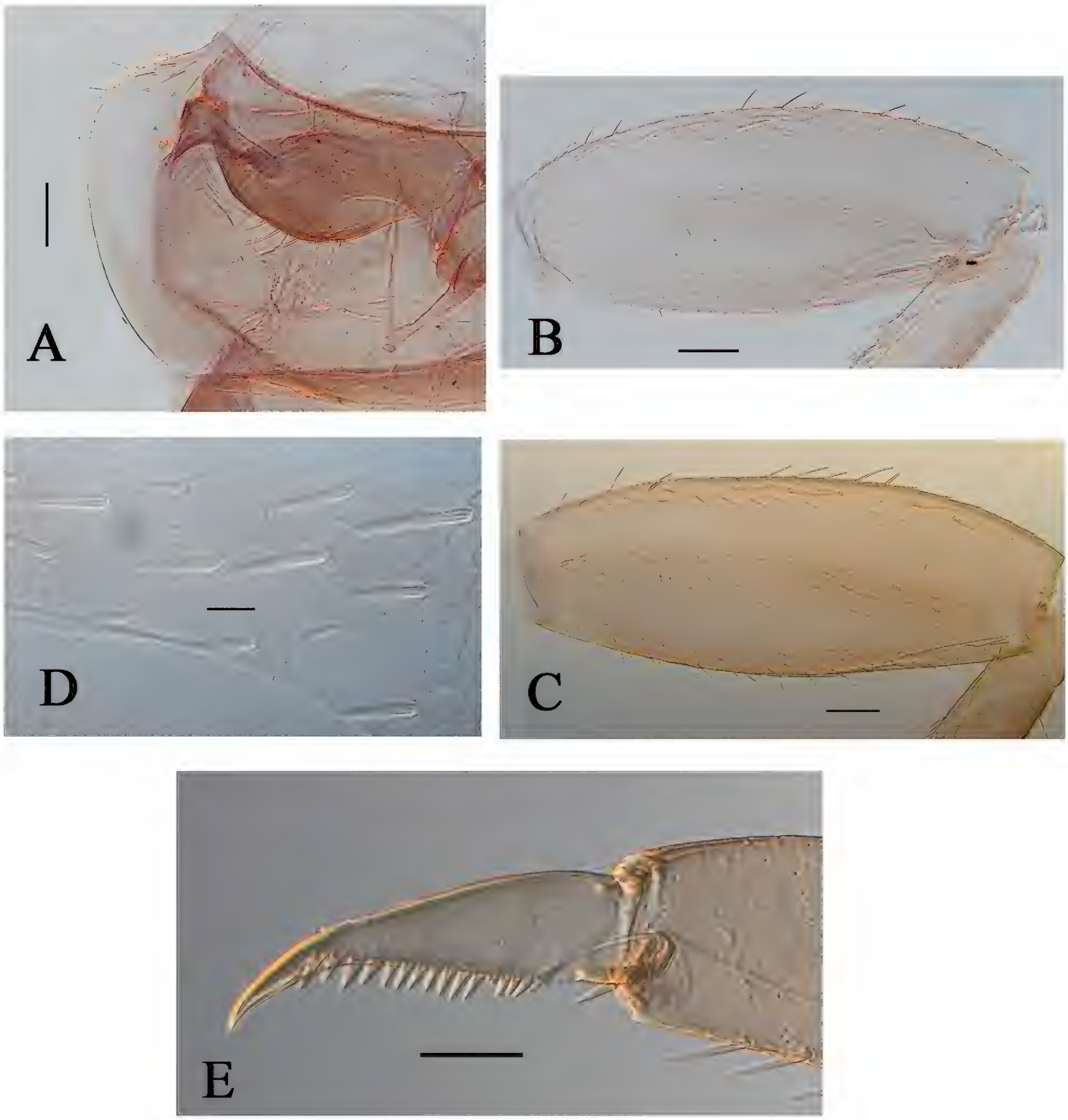

Figure 18. *H. annaba* sp. nov., thoracic structures, pronotum, right half (**A**); fore femur (**B**); hind femur (**C**); setae on upper face of hind femur (**D**); claw (**E**). Scale bars: 100 µm (**A–C**); 20 µm (**D**); 50 µm (**E**).

tinted in brown in subcostal field; longitudinal and transversal veins dark brown; pterostigmatic area with ca. 10 oblique and simple transversal veins. MA and MP forks asymmetrical, cubital field with two long and two short intercalary veins (Fig. 20A). Hindwing with rounded costal process approximately in the middle of the wing; vein Sc long and close to the costal vein, reaching the costal margin before the tip of the wing (Fig. 20B).

Eggs ovoid, ca. 180–195 µm × 80–100 µm, with longitudinal ribs non-punctuated, long and entire, most of them running from one pole to the other (Fig. 21A). Ribs relatively broad, ca. 4.5–5.0 µm in width. In some specimens, chorion folded. Micropyle in equatorial area (Fig. 21B).

Habrophlebia edough Sartori, Vuataz & Samraoui, sp. nov.

https://zoobank.org/9536F790-E5EF-4844-95A1-D3182BBB7434

Figs 22–25

Habrophlebia sp. 17, Hezil et al. 2025.

Material examined. ***Holotype*:** one nymph in ethanol (GBIFCH00654973), Algeria, Wilaya of Annaba, Edough, Oued Agab, 36°54'44"N, 7°39'35"E, 750 m, 9.IX.2021, B. Samraoui leg., MZL.

Paratypes. Algeria, Wilaya of Annaba, Edough, Oued Agab, same data as holotype, 2 nymphs in etha-

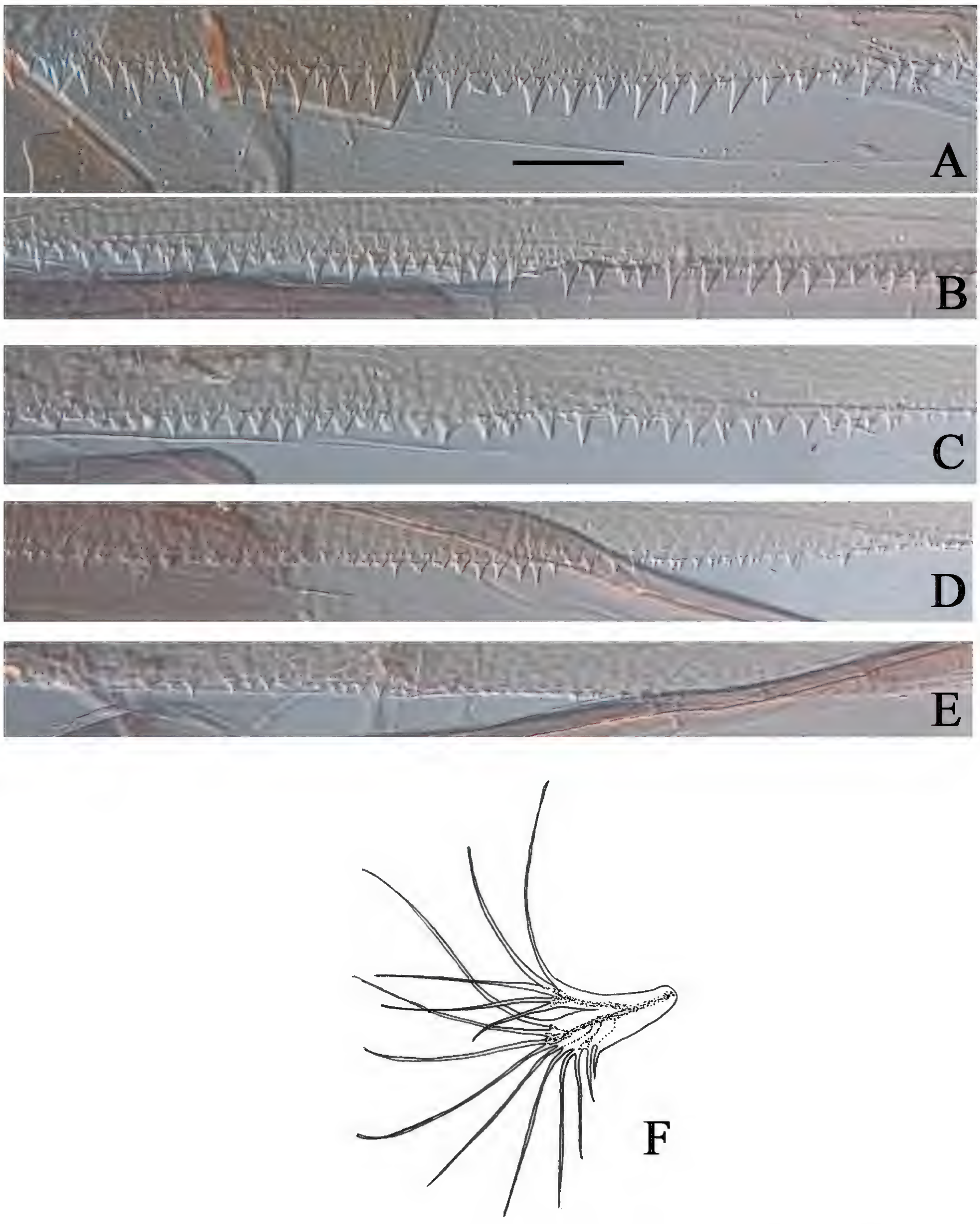

Figure 19. *H. annaba* sp. nov., abdominal structures, posterior margin of tergite IX (**A**); tergite VIII (**B**); tergite VII (**C**); tergite VI (**D**); tergite V (**E**); gill (**F**). Scale bar: 20 µm.

nol (GBIFCH00654981), 1 nymph on slide (GBIFCH00654947); same locality as holotype, 18.VIII.2021, 2 nymphs in ethanol (GBIFCH00654979), 2 nymphs on slide (GBIFCH00654948, GBIFCH01118441).

Etymology. The name Edough (Djebel Edough), designating the prominent mountain massif overlooking the city of Annaba, is thought to derive from undocumented Berber (Amazigh) roots. In antiquity, it was referred to as

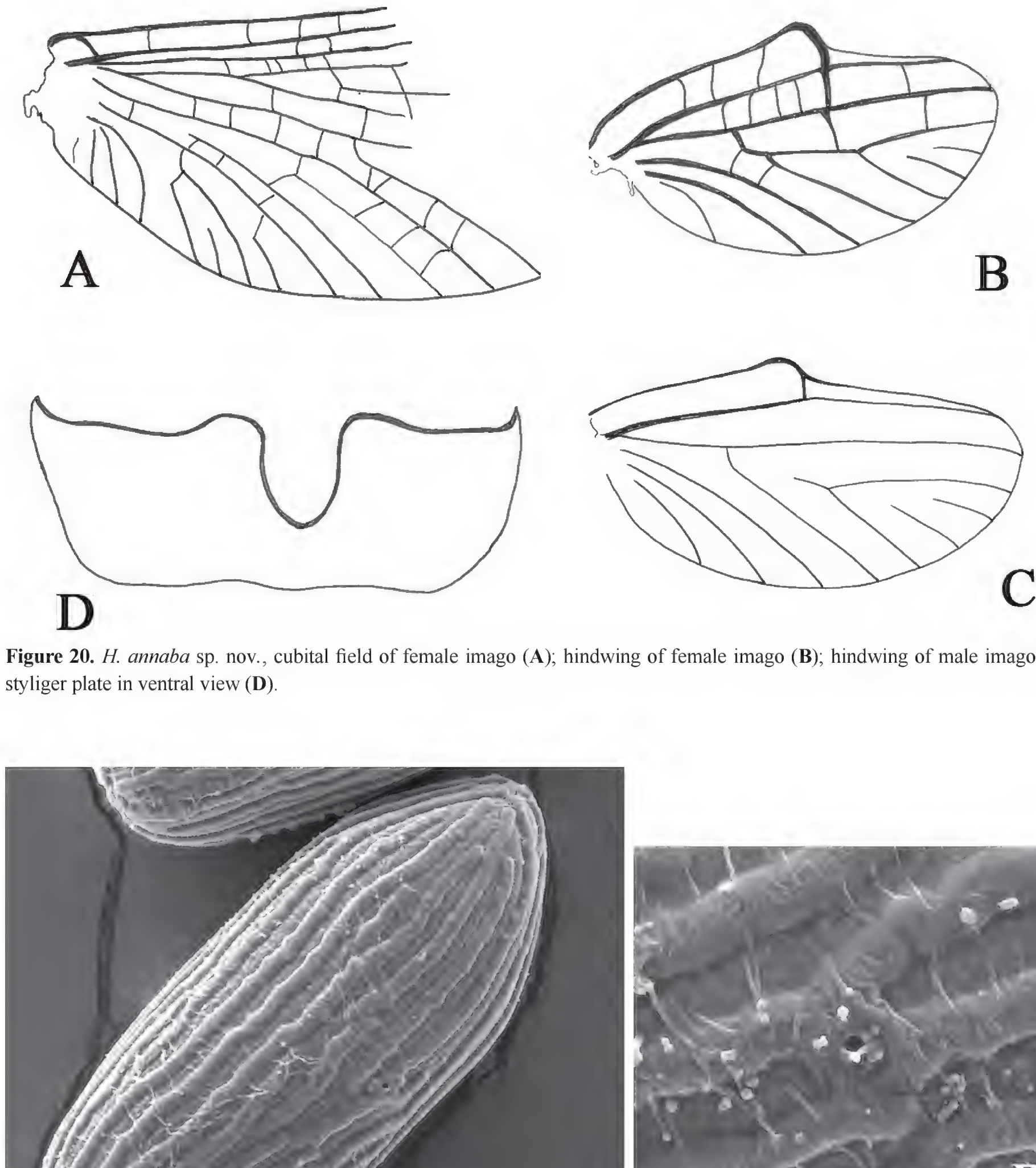

Figure 20. *H. annaba* sp. nov., cubital field of female imago (**A**); hindwing of female imago (**B**); hindwing of male imago (**C**); styliger plate in ventral view (**D**).

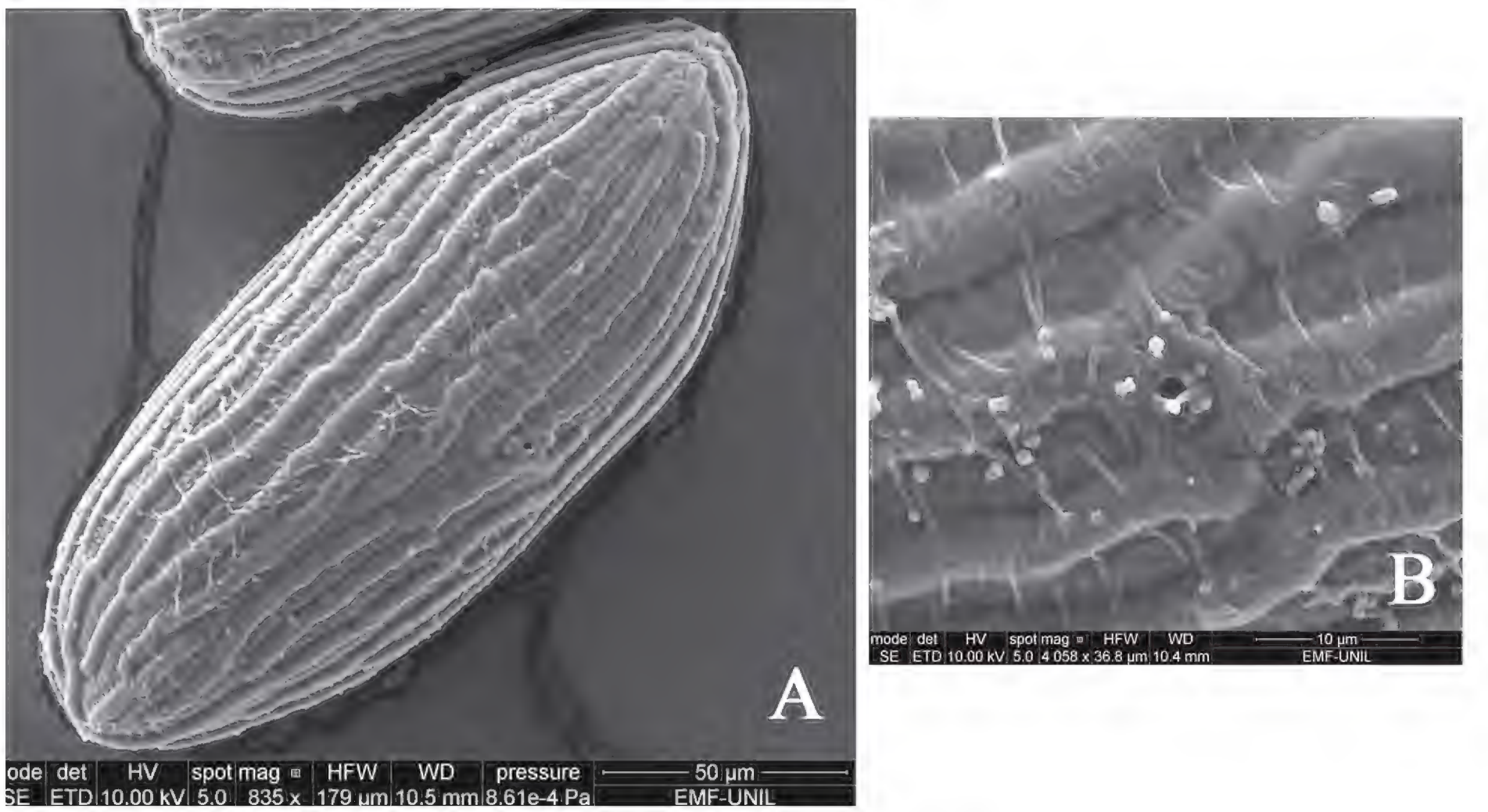
A
ode det HV spot mag HFW WD pressure 50 µm
SE ETD 10.00 kV 5.0 835 x 179 µm 10.5 mm 8.61e-4 Pa EMF-UNIL
B
mode det HV spot mag HFW WD 10 µm
SE ETD 10.00 kV 5.0 4 058 x 36.8 µm 10.4 mm EMF-UNIL

Figure 21. *H. annaba* sp. nov., egg in toto (**A**); micropyle and details of the chorion (**B**).

Mons Pappua by Procopius who describes it as a Numidian stronghold, and as *Mons Giddaba* by Saint Augustine.

Descriptions. Nymph. Body length of final instar, excluding caudal filaments, up to 7 mm for female; male nymphs unknown. Cerci as long as body length.

Coloration. General coloration medium brown; dark brown between ocelli, light brown in front and on the clypeus (Fig. 22A), especially in young nymphs (Fig. 22B). Antenna with pedicel dark brown, scape greyish brown and filament light brown, more or less entirely

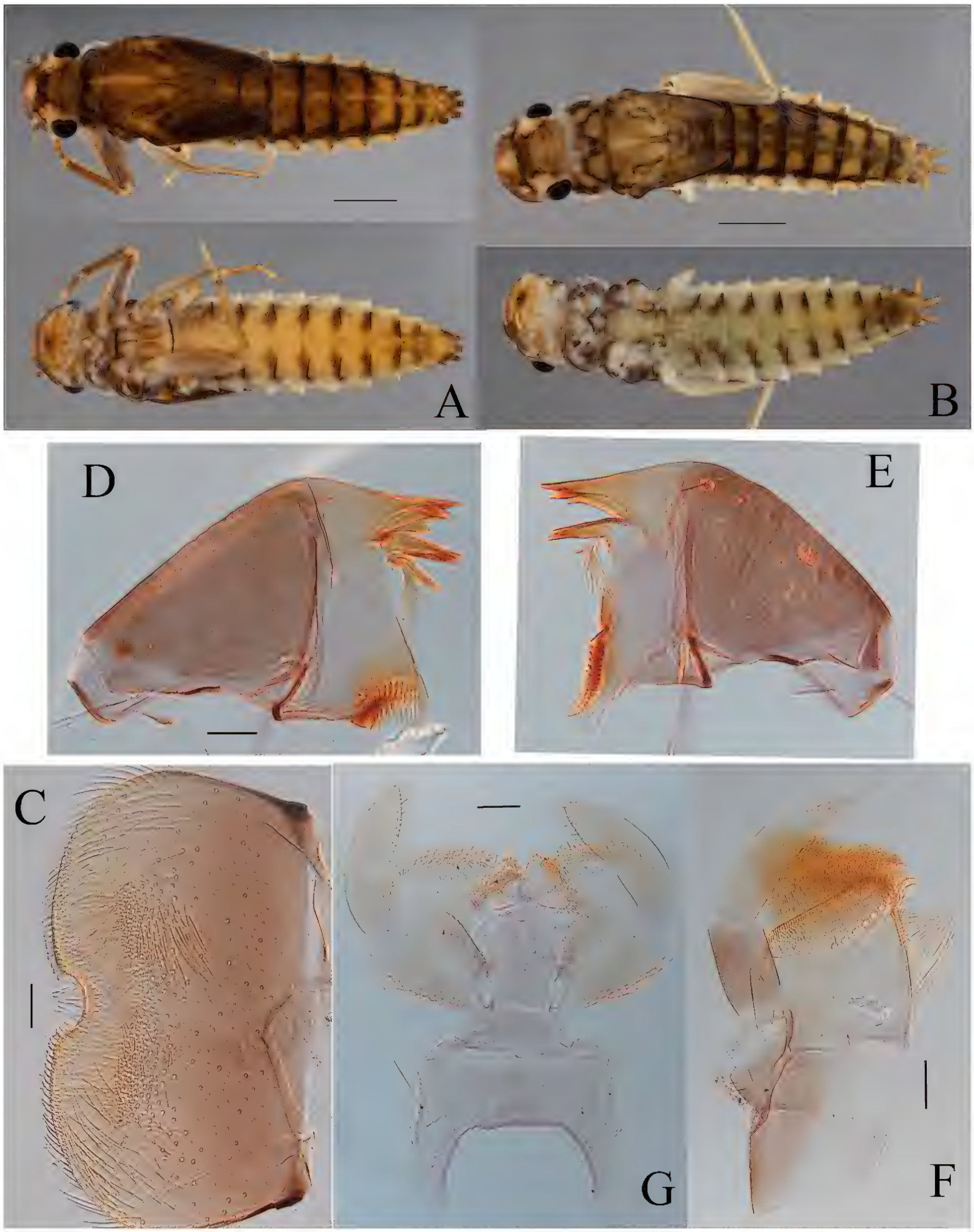

Figure 22. *H. edough* sp. nov., habitus of mature nymph in dorsal (above) and ventral view (below) (**A**); habitus of young nymph in dorsal (above) and ventral view (below) (**B**); labrum (**C**); left mandible (**D**); right mandible (**E**); maxilla (**F**); labium and submentum (**G**). Scale bars: 1 mm (**A, B**); 50 µm (**C, G**); 100 µm (**D, E, F**).

whitish in young nymphs. Pronotum medium brown, washed with dark brown sub-laterally and with a dark brown M-shaped macula in middle, lateral margins whitish; mesonotum medium brown, with dark brown maculae; lateroparapsidal sutures dark brown. Legs light to medium brown; femora dark brown in mature nymphs; tibiae medium brown, with dark brown apex in mature nymphs; tarsi light brown to yellowish. Abdominal terg-

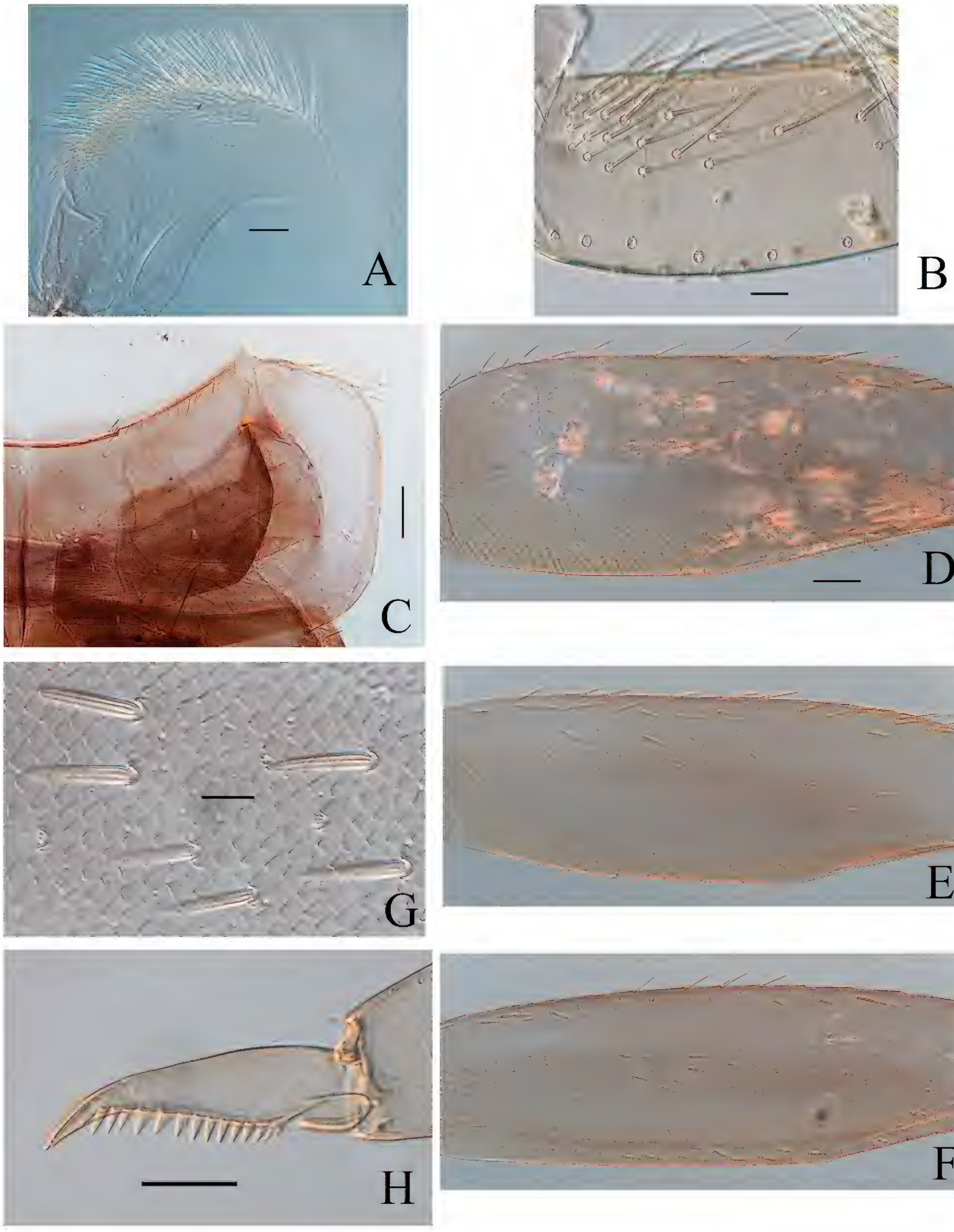

Figure 23. *H. edough* sp. nov., mouthparts and thoracic structures, hypopharynx, left half (**A**); setae on dorsal face of maxillary palp 2 (**B**); pronotum, right half (**C**); fore femur (**D**); mid femur (**E**); hind femur (**F**); setae on upper face of hind femur (**G**); claw (**H**). Scale bars: 100 µm (**A, C–F**); 20 µm (**B, G**); 50 µm (**H**).

ites dark brown to greyish brown, with two lighter maculae medio-anteriorly, especially well visible on segments I–VII in young nymphs (Fig. 22B); maculae less visible in mature nymphs (Fig. 22A). Sternites medium brown in the middle, posterior margin underlined with dark brown laterally, nervous ganglia hardly visible. Cerci and paracercus light brown at base, whitish distally, without dark banding.

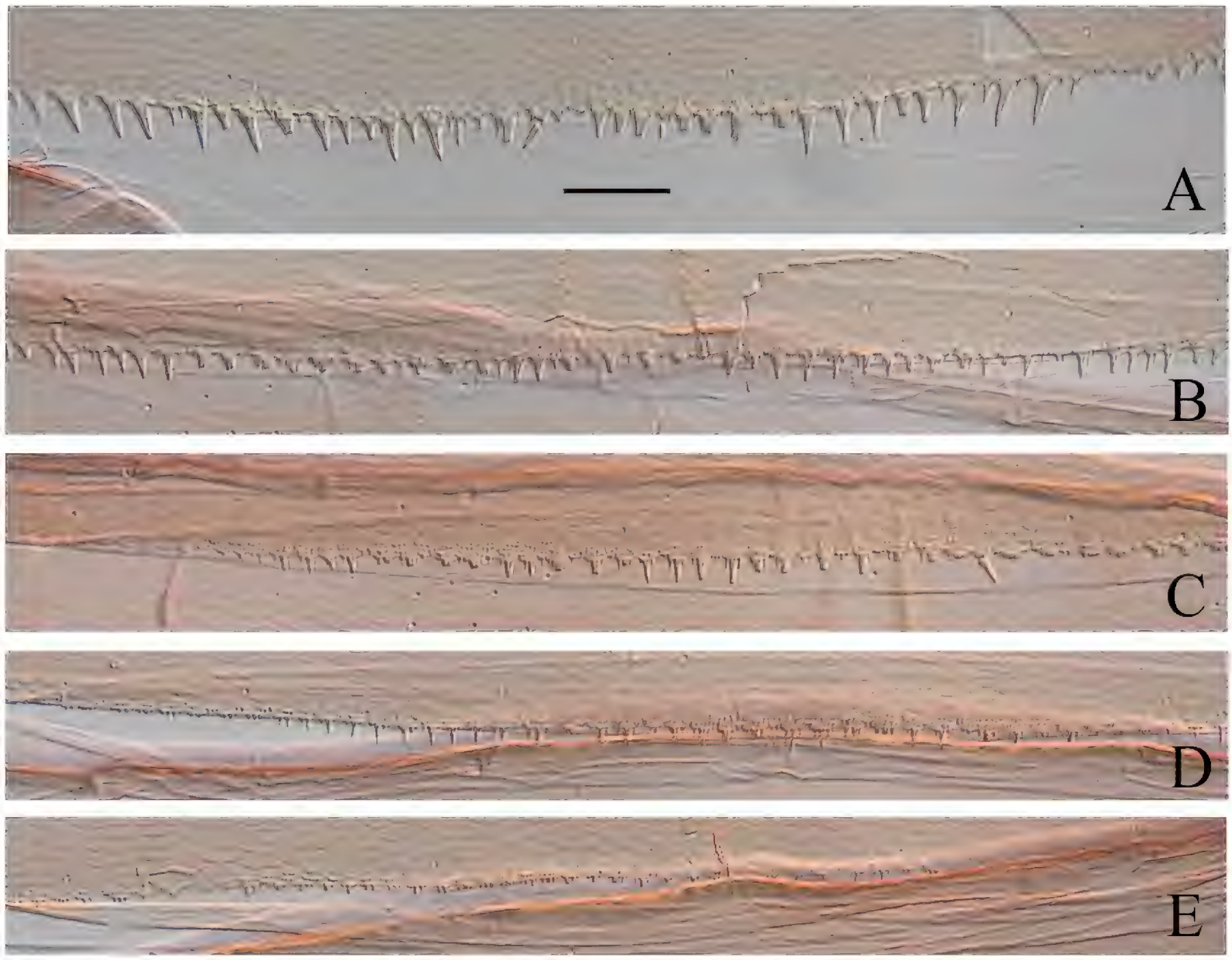

Figure 24. *H. edough* sp. nov., abdominal structures, posterior margin of tergite IX (**A**); tergite VIII (**B**); tergite VII (**C**); tergite VI (**D**); tergite V (**E**); gill (**F**). Scale bar: 20 µm.

Head. Labrum rectangular, 1.75–1.79× wider than long (Fig. 22C); dorsal surface covered distally with scattered stout setae; anterior margin with a row of stout, long and spatulate setae medially; emargination flared, U-shaped with flat denticles; ventral surface with two bunches of stout setae medially. Mandibles similar to other *Habrophlebia* species, incisor with 3 teeth, the lowest of left mandible with a clear indentation at base (Fig. 22D), kinetodontium with 3 teeth, 17–22 long and thin setae below mola of right mandible (Fig. 22E). Maxilla stocky, subapical row of 7 or 8 pectinate setae (Fig. 22F); maxillary palp with three segments, segment 1 and 2 subequal in length, and longer than segment 3; segment 3 triangular 1.41–1.75× longer than wide at base; setae on the dorsal surface of segment 2 feathered (Fig. 23B). Hypopharynx with highly developed superlinguae terminated by a membranous digitation (Fig. 23A). Labium with rhomboid glossae, outer margin and apex covered by short, broad setae; paraglossae enlarged laterally, covered with fine and long setae on dorsal surface; with long, thick setae on the outer margin; labial palp with three segments, inner margin of segment 1 highly dilated near the middle, about 1.35× longer than maximum width, segments 2 slightly shorter than segment 3, segment 2 ca. 0.67× length of segment 1, and segment 3 ca. 0.74×

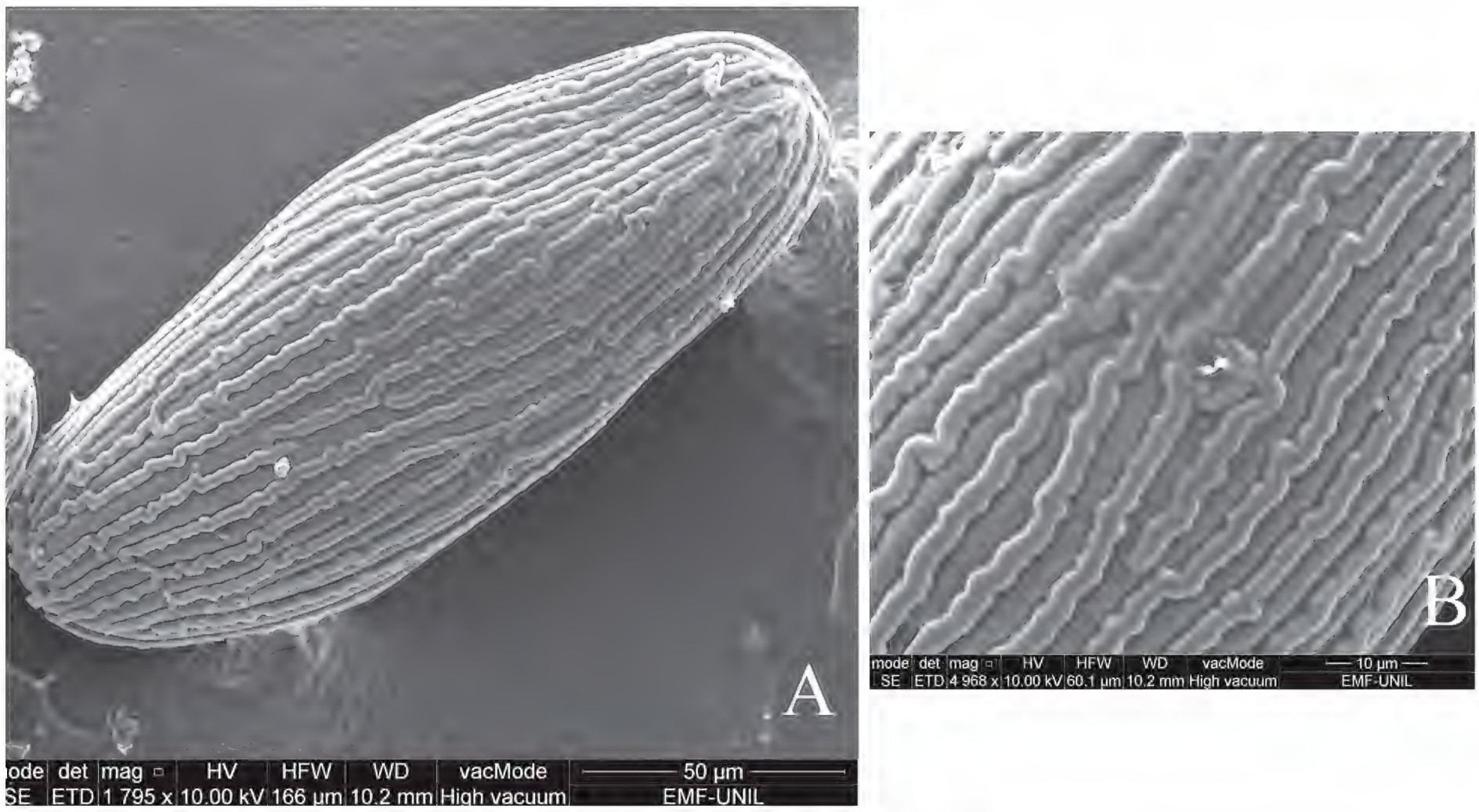
A
mode det mag HV HFW WD vacMode 50 µm
SE ETD 1 795 x 10.00 kV 166 µm 10.2 mm High vacuum EMF-UNIL
B
mode det mag HV HFW WD vacMode 10 µm
SE ETD 4 968 x 10.00 kV 60.1 µm 10.2 mm High vacuum EMF-UNIL

Figure 25. *H. edough* sp. nov., egg in toto (**A**); micropyle and details of the chorion (**B**).

length of segment 1; segment 3 ca. 1.8–2.0× longer than wide at base, conical shape and with 4–7 stout and long, simple setae on dorsal surface (Fig. 22G). Submentum with numerous long, stout and pointed setae laterally; ventral surface with few long, stout and pointed setae (Fig. 22G).

Thorax. Pronotum with anterior corners bearing few long and pointed setae laterally, and 4–6 stout and strong setae dorsally. Anterior margin of pronotum with numerous stout setae (Fig. 23C). Fore legs femora elongated, ca. 2.75× longer than wide, outer margin and upper surface covered with long, entire and pointed setae (Fig. 23D); fore tibiae length 0.95× femora length, outer margin without or with few thin and long setae, inner margin with several rows of long stout, entire or feathered setae; tarsi 0.6× length of tibiae, outer margin with few long and thin setae, inner margin with long, pointed and feathered setae. Middle legs similar to fore legs, femora ca. 3.2× longer than wide (Fig. 23E), dorsal surface of femora with more numerous and slightly longer stout, entire or slightly feathered, pointed setae; tibiae length 0.92× femora length; tarsi 0.45× length of tibiae. Hind legs with femora 3.5× longer than wide (Fig. 23F), dorsal surface covered with stout, long, pointed, feathered setae (Fig. 23G); tibiae length 0.94× femora length, outer margin with numerous stout, pointed and entire setae; inner margin with stout, pointed and feathered setae; tarsi 0.42× length of tibiae, outer margin with long and thin setae, inner margin with long, stout, pointed and entire setae. Claws of all legs slightly hooked, with 15–17 denticles that decrease in size from the apex to the tarsus (Fig. 23H).

Abdomen. Posterolateral expansions only on segments VIII and IX. Posterior margin of tergite IX with triangular, narrow, pointed spines, ca. 2.5–3× longer than wide at base (Fig. 24A); tergite VIII with triangular, narrow spines 1.5–2× longer than wide (Fig. 24B); tergite VII and VI with a mix of short, narrow spines and minute, needle-shaped spines (Fig. 24C, D); tergite V with minute needle-shaped spines (Fig. 24E); tergites I–IV with barely visible spines. Gills present on segments I–VII; all gills elongated with long filaments; dorsal lamella bearing 8–10 filaments, ventral lamella with 4–5 filaments.

Imagos. unknown.

Eggs (extracted from mature female nymphs) ovoid, ca. 175–185 µm × 70–80 µm, with longitudinal ribs non-punctuated, long and entire, most of them not running from one pole to the other (Fig. 25A). Ribs relatively narrow, ca. 2.5–3.0 µm in width. Micropyle in equatorial area (Fig. 25B).

Identification key

A key to distinguish the larvae of all known species from the West Palearctic is provided below. [Nymph of *Habrophlebia antoninoi* Alba-Tercedor, 2000 from southern Spain is still unknown.]

1 Setae on upper face of hind femora entire, not feathered (e.g. Figs 3E, 8E, El Alami et al. 2025, figs 11A, B) 2
– Setae on upper face of hind femora feathered (e.g. Fig. 23G, El Alami et al. 2025, figs 4E, 7E) 7
2 Setae on upper face of hind femora short, truncate or rounded (El Alami et al. 2025, fig. 11A); posterior margin of abdominal tergite IX quadratic (Jacob and Sartori 1984, figs 1, 2)..... *Habrophlebia fusca* (Curtis, 1834) [Europe]
– Setae on upper face of hind femora long and pointed (Fig. 3E, El Alami et al. 2025, fig. 11B); posterior margin of abdominal tergite IX triangular (e.g. Fig. 4A)..... 3

3 Anterior margin of pronotum without row of setae, with at most one or two setae (Figs 3A, 8A); lower lamella of gills generally with less than 4 filaments 4
– Anterior margin of pronotum with row of setae (Figs 13A, 26C, D); lower lamella of gills generally with more than 4 filaments 5
4 Posterior margin of tergite VII-VIII with well-developed triangular spines, two times longer than wide at base; segment 3 of maxillary palp 1.3–1.5× longer than wide at base; gills with 3–4 and 5–6 filaments on lower and upper lamella respectively ..... *Habrophlebia seybouse* sp. nov. [Algeria, Oued Cherf (Guelma), Collo]
– Posterior margin of tergite VIII with minute triangular spines, those on tergite VII needle-shaped; segment 3 of maxillary palp 1.10–1.15× longer than wide at base; gills with 2–3 and 4–5 filaments on lower and upper lamella respectively.... ..... *Habrophlebia ghora* sp. nov. [northeastern Algeria, northwestern Tunisia]
5 Claw with at least 18 teeth ..... *Habrophlebia callensis* sp. nov. [Algeria, El Kala]
– Claw with at most 16 teeth 6
6 Upper lamella of gills with 5–7 filaments ..... *Habrophlebia lauta* McLachlan, 1884 [Europe]
– Upper lamella of gills with 8–10 filaments ..... *Habrophlebia annaba* sp. nov. [Algeria, Mount Edough, Annaba]
7 Apical teeth on claw narrower than the others (e.g. El Alami et al. 2025, fig. 4D); posterior margin of tergite VIII with reduced or needle-shaped spines 8
– Apical teeth on claw of the same width as the others; posterior margin of tergite VIII with generally well developed spines 10
8 Tarsal claw with at most 12 teeth; gills with 2–4 and 3–5 filaments on lower and upper lamella respectively ..... *Habrophlebia abietis* El Alami, Sartori & Vuataz, 2025 [Morocco, Rif]
– Tarsal claw with at least 13 teeth 9
9 Segment 3 of labial palp with 7–9 stout setae on upper face; segment 3 of maxillary palp 1.3–1.4× longer than wide at base; gills with 4–5 and 5–6 filaments on lower and upper lamella respectively ..... *Habrophlebia vaillantorum* Thomas, 1986 [Morocco, High Atlas]
– Segment 3 of labial palp with 4–6 stout setae on upper face; segment 3 of maxillary palp 1.15–1.25× longer than wide at base; gills with 3–4 and 3–7 filaments on lower and upper lamella respectively ..... *Habrophlebia linae* El Alami, Sartori & Vuataz, 2025 [Morocco, Rif]
10 Posterior margin of tergite V with well-developed triangular spines, 2–3× longer than wide (Jacob and Sartori 1984, fig. 21) 11
– Posterior margin of tergite V with needle-shaped spines (Fig. 24E) 13
11 Labrum emargination smooth (Fig. 26A); apex of superlingua of hypopharynx moderately developed (Fig. 26F)..... ..... *Habrophlebia consiglioi* Biancheri, 1959 [Italy, Sardinia]
– Labrum emargination narrow (Fig. 26B); apex of superlingua of hypopharynx well-developed (Fig. 26E)..... 12
12 Anterior margin of pronotum with scattered long setae (Fig. 26D); gills with 2–4 and 3–7 filaments on lower and upper lamella respectively; claw with 14–17 teeth..... ..... *Habrophlebia eldae* Jacob & Sartori, 1984 [southern Europe, in expansion to the north]
– Anterior margin of pronotum with long setae in a regular row (as in Fig. 26C); gills with 3–5 and 7–10 filaments on lower and upper lamella respectively; claw with 15–18 teeth ..... *Habrophlebia dakkii* El Alami, Vuataz & Sartori, 2023 [Morocco, Rif]
13 Stout setae on segment 2 of maxillary palp feathered; third segment of labial palp dorsal surface with 4–7 stout setae; ratio length/width at base ca. 2.0..... *Habrophlebia edough* sp. nov. [Algeria, Mount Edough, Annaba]
– Stout setae on segment 2 of maxillary palp entire; third segment of labial palp dorsal surface with 8–9 stout setae; ratio length/width at base between 1.4 and 1.5 14
14 Posterior margin of tergite VIII with large, triangular spines 2–3× longer than wide; claw with 18–22 denticles; gills with 5–8 and 9–12 filaments on lower and upper lamella respectively..... ..... *Habrophlebia hassainae* Benhadji & Sartori, 2018 [Algeria, Tafna]
– Posterior margin of tergite VIII with small, almost needle-shaped spines; claw with 15–18 denticles; gills with 4–7 and 8–11 filaments on lower and upper lamella respectively..... ..... *Habrophlebia djurdjurensis* Kechemir, Sartori & Lounaci, 2020 [Algeria, Kabylia]

Morphological affinities

The nymphs of four of the five new species described herein possess a striking and rare character: setae on the upper face of hind femora are always entire, not feathered. This character is only shared with *H. fusca* and *H. lauta* (El Alami et al. 2025). Whereas they are truncate in *H. fusca*, the new species have long and pointed setae, and in *H. ghora*, they can be long or short, pointed or rounded. The anterior margin of pronotum always bears numerous stout and long setae, except in *H. ghora* sp. nov. and *H. seybouse* sp. nov., although one or two short setae may be present in the latter. *Habrophlebia callensis* sp. nov. possesses a tarsal claw with numerous teeth (18–21), similar only to that of *H. hassainae*. *Habrophlebia ghora* sp. nov. and *H. seybouse* sp. nov. have few teeth (12–14) and are

only challenged by *H. abietis* (10–12) in the lowest number of teeth on claw. Distal teeth of the new species are normal, and not reduced as in *H. vaillantorum*, *H. abietis* and *H. linae* (El Alami et al. 2025). *Habrophlebia ghora* sp. nov. and *H. seybouse* sp. nov. possess gills with few filaments, 4–6 on upper lamella and 2–4 on lower lamella, somewhat similar to those of *H. abietis* and *H. linae*. Those of *H. callensis* sp. nov. are more similar to those of *H. dakkii* (El Alami et al. 2023) and those of *H. annaba* sp. nov. to those of *H. djurdjurensis* (Kechemir et al. 2020).

Habrophlebia ghora sp. nov. was previously identified as *H. consiglioi* (Zrelli et al. 2011a), mainly based on gills and ornamentation of the egg chorionic structure. Detailed examination of numerous nymphs showed that *H. ghora* sp. nov. differs from *H. consiglioi* by the structure of setae on hind femora (entire in *H. ghora* sp. nov. and feathered in *H. consiglioi*), absence of setae on the anterior margin of the pronotum (see fig. 5 in Belfiore and Gaino 1985, and Fig. 26C for *H. consiglioi*), and spines on posterior margin of tergites VII especially. At the adult stage, *H. ghora* sp. nov. differs mainly from *H. consiglioi* by the absence of a hump at base of first segment of the gonopods, apex of spine on penis lobe not truncate, but pointed, and by the length of the subcostal vein in hindwing.

Habrophlebia ghora sp. nov. and *H. seybouse* sp. nov. are very close morphologically. They share a large number of characters. The nymphs can mainly be differentiated by the ornamentation of tergites VIII and IX. The male imagos of both species can be separated by the length of the subcostal vein in the hindwing.

Finally, *H. edough* sp. nov. occupies a peculiar position. Nymph hind femora bear feathered setae, as well as on the second segment of maxillary palp, whereas all other species treated here have entire setae on hind femora and maxillary palp. Although found in syntopy with *H. annaba* sp. nov., it can be differentiated, besides the two main characters mentioned above, by numerous morphological characters, including: labrum wider (1.75 vs 1.55), numerous thin setae below the mola of the right mandible (17–22 vs 10–11), segment 3 of labial palp much longer than wide at base (1.8–2.0 vs 1.4–1.5), femora of all legs much slender, tergites ornamentation and size and shape of ribs on egg chorion. In Oued Agab, where *H. annaba* sp. nov. and *H. edough* sp. nov. co-occur, they present a seasonal shift, *H. annaba* sp. nov. flying in spring, and *H. edough* sp. nov. in late summer, early autumn.

The nymphal activity period of most studied species extends from January to June, although some, such as *H. edough* sp.nov., persist into late summer (July–September). Swarming behaviour in these species has been documented in mid-May.

Molecular analyses

The COI dataset was >98% complete and contained 35% parsimony-informative sites. COI sequences from *H. ghora* sp. nov. formed a distinct, well-supported clade, sister to that of *H. seybouse* sp. nov. (Fig. 27). These two species together formed a well-supported clade. Likewise, sequences from *H. callensis* sp. nov. and *H. annaba* sp. nov. each formed distinct, well-supported sister clades, which together formed a clade sister to the *H. djurdjurensis* + *H. hassainae* clade. Sequences from *H. edough* sp. nov. also formed a distinct, well-supported clade.

Species delimitation analyses recovered 16 MOTUs using ASAP and mPTP, and 18 using GMYC (Fig. 27). All delimitation methods identified the same five *Habrophlebia* MOTUs, matching the five new species. For the remaining clades, the results were largely congruent, differing only slightly in the delimitation of the *H. fusca*, *H. hassainae*, *H. djurdjurensis*, *H. sp. 1 and H. abietis* + *H. dakkii* + *H. linae* clades.

Pairwise COI p-distances across all sequences ranged from 0.0% to 22.6%. The overall mean p-distance within MOTUs was 0.8% (range: 0.0–2.2%), while the mean p-distance between MOTUs was 14.3% (range: 2.4–20.8%). Maximum within-MOTU p-distances ranged from 0.0% (*H. vaillantorum*, *H. abietis*) to 5.8% (*H. fusca*). Minimum between-MOTU p-distances ranged from 0.9% (*H. sp. 1–H. abietis* + *H. dakkii* + *H. linae*) to 20.5% (*H. sp. 5–H. edough* sp. nov.). Considering only the five newly described species, the overall mean p-distance within MOTUs was 0.4% (range: 0.1–0.9%), while the mean p-distance between MOTUs was 15.6% (range: 4.6–19.7%). Maximum within-MOTU p-distances ranged from 0.2% (*H. edough* sp. nov.) to 1.7% (*H. ghora* sp. nov.), and minimum between-MOTU p-distances ranged from 4.3% (*H. callensis* sp. nov.–*H. annaba* sp. nov) to 19.4% (*H. annaba* sp. nov–*H. edough* sp. nov.).

Discussion

With fourteen endemic *Habrophlebia* species, the Maghreb represents a hotspot of freshwater biodiversity and a key centre of radiation for the genus in the western Mediterranean. Algeria harbours the greatest diversity, with ten species (*H. hassainae*, *H. djurdjurensis*, *H. ghora* sp. nov., *H. callensis* sp. nov., *H. seybouse* sp. nov., *H. annaba* sp. nov., *H. edough* sp. nov., and three undescribed taxa from the Djurdjura Mountains). Morocco supports four species (*H. vaillantorum*, *H. dakki*, *H. abietis*, and *H. linae*), whereas Tunisia contains only one, *H. ghora* sp. nov., which it shares with Algeria. While *H. consiglioi*, previously reported from Tunisia, is likely a misidentification (this study), the occurrence of *H. fusca*, earlier cited from the Maghreb, remains doubtful (Thomas 1998). Extensive surveys in the Rif have failed to detect this species (El Alami et al. 2023).

The addition of these five new species enriches the West Palaearctic fauna, particularly within the genus *Habrophlebia*, which now comprises 19 species, including three additional undescribed taxa from the Djurdjura Mountains in the Great Kabylie, north-central Algeria (Labdaoui et al. 2024). European representatives of the genus include *H. antoninoi*, *H. consiglioi*, *H. eldae*, *H. fusca*, and *H. lauta*. In addition to these described species, at least four distinct

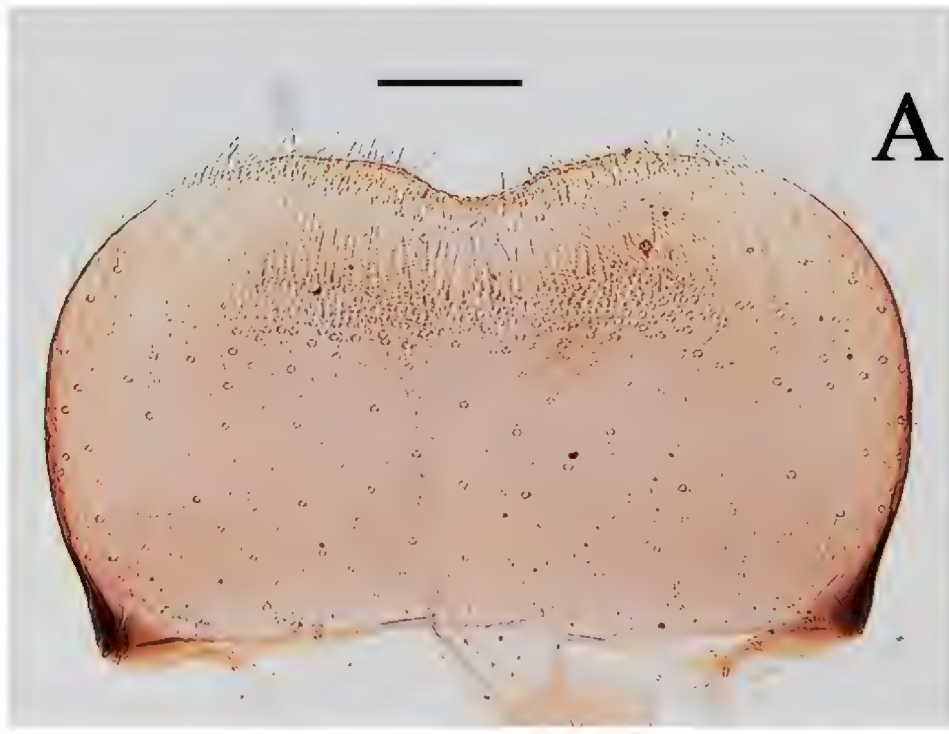

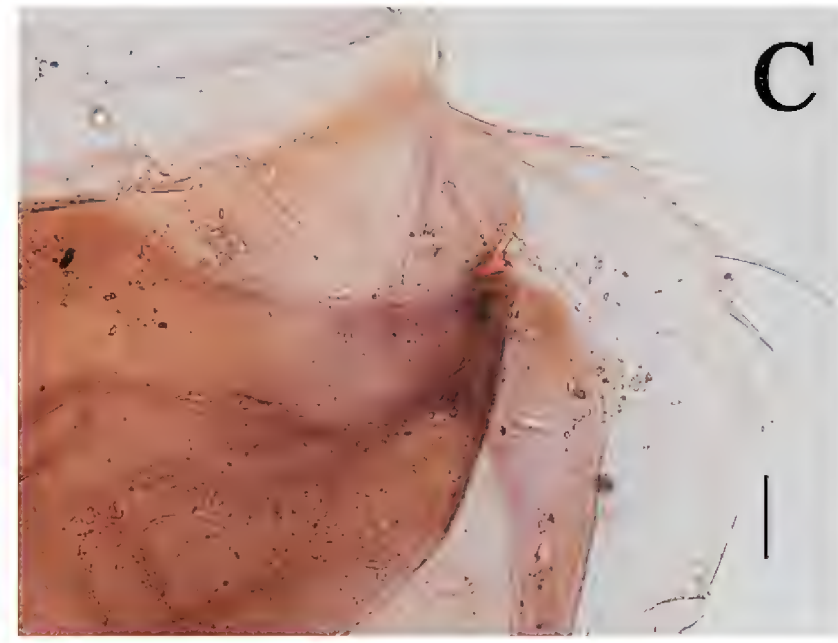

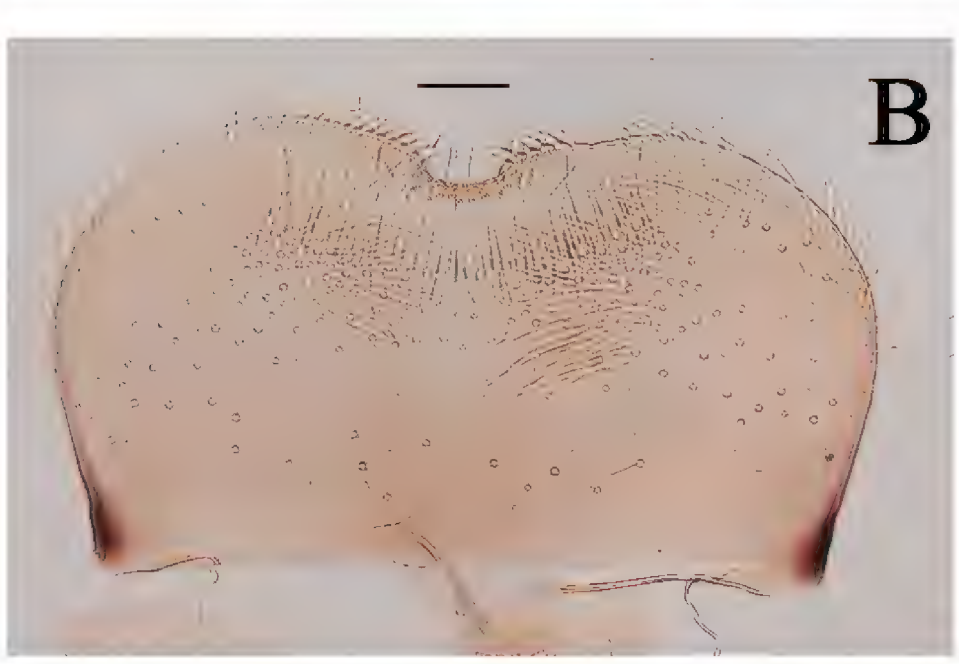

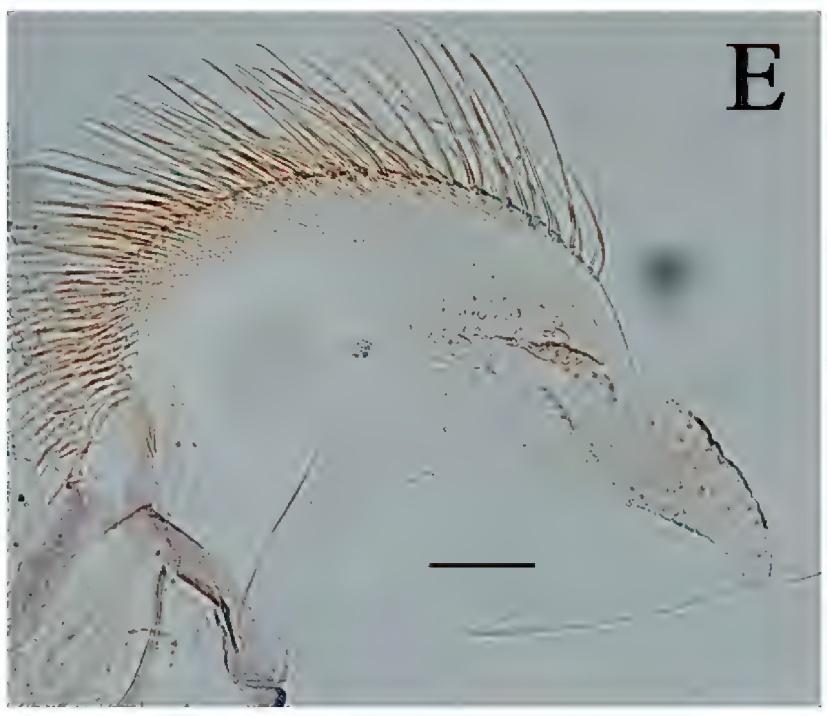

Figure 26. *Habrophlebia* spp. *H. consiglioi* (**A, C, F**) and *H. eldae* (**B, D, E**); labrum (**A, B**); pronotum, right half (**C, D**); hypopharynx, left half (**E, F**). Scale bars: 100 μm (**A**); 50 μm (**B–F**).

genetic Euro-Mediterranean lineages are reported here (Fig. 27). To date, 14 species are known exclusively from the Maghreb, indicating that this region constitutes a major centre of endemism and a potential focus of diversification for the genus. Each Maghrebian *Habrophlebia* species appears to be geographically restricted: *H. annaba* sp. nov. and *H. edough* sp. nov. occur in the Edough Mountains; *H. callensis* sp. nov. in the El Kala northern hills; *H. ghora* sp. nov. in the Kroumiria Mountains spanning Algeria and Tunisia; *H. seybouse* sp. nov. in the Seybouse

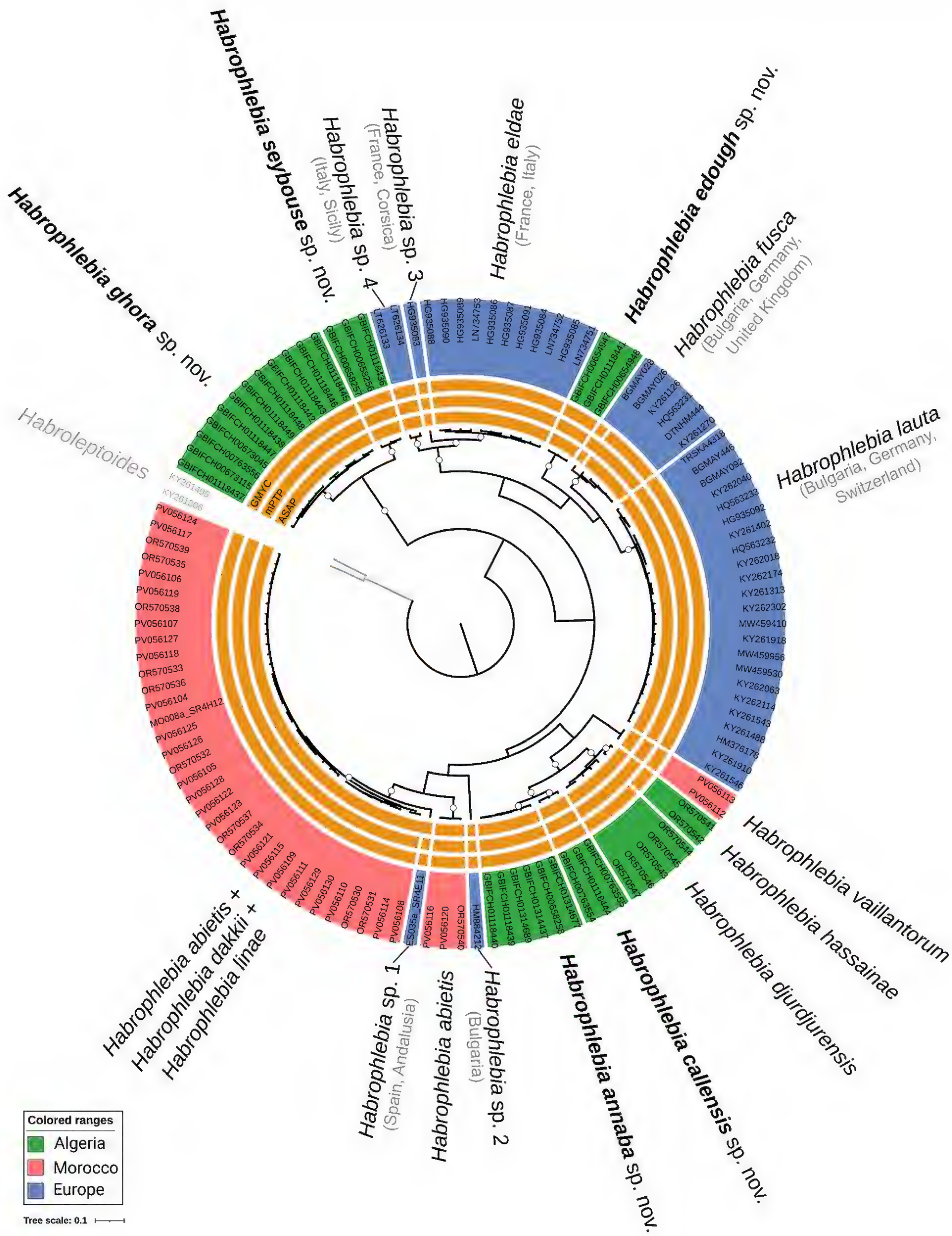

Figure 27. Bayesian (BEAST) maximum clade credibility COI tree of *Habrophlebia* in the West Palearctic. Branch tips labelled with GBIF codes indicate newly sequenced specimens; all other codes correspond to sequences from El Alami et al. (2025). Outer color ranges represent CO1 clades, delimited either following El Alami et al. (2025) or by morphological characters for the five newly described species (green: Algeria; red: Morocco; blue: Europe). Species names (where available) are placed adjacent to their respective clades, with the newly described species highlighted in bold. The three inner brown rings indicate MOTUs inferred from the ASAP, mPTP, and GMYC delimitation methods. Circles on branches denote Bayesian posterior probabilities > 0.9. Outgroup branches are shown in grey.

and Collo regions; *H. hassainae* in north-western Algeria (Benhadji et al. 2018); *H. djurdjurensis* in the Djurdjura Mountains (Kechemir et al. 2020); *H. vaillantorum* in the High Atlas, southern Morocco (Thomas et al. 1999); *H. dakkii* in northern Morocco (El Alami et al. 2023); and *H. abietis* and *H. linae* in the Rif region, northern Morocco (El Alami et al. 2025).

In contrast to what was observed in the Rif region of Morocco, the Algerian species do not exhibit marked phenotypic heterogeneity, which in the Rif had suggested the occurrence of hybridisation between species pairs (*H. dakkii–H. abietis*, *H. dakkii–H. linae*, *H. abietis–H. linae*). These observations were further supported by the topology of the COI gene tree, in which all three *Habrophlebia* species from the Rif region, together with their morphologically intermediate forms, were grouped within a single clade (El Alami et al. 2025). The concentration of endemism in the Maghreb is not confined to mayflies (Samraoui et al. 2021c; Kaltenbach et al. 2022; Dambri et al. 2022, 2023) but extends to diverse freshwater taxa, including Odonata (Ferreira et al. 2014; Bouhala et al. 2019), caddisflies (Bemmoussat-Dekkak et al. 2021; Samraoui et al. 2024), stoneflies (Yasri-Cheboubi et al. 2013, 2016), amphipods (Ayati et al. 2019), and crabs (Rouabhi et al. 2025). It also encompasses vertebrates such as the Maghreb bleak *Tropidophoxinellus callensis* (Guichenot, 1850), the ribbed newt *Pleurodeles nebulosus* (Guichenot, 1850), and the tree frog *Hyla carthaginiensis* Dufresnes et al., 2019.

In northeastern Algeria, wetlands function as refuges for Afrotropical relicts (Samraoui et al. 1993) and as key wintering and breeding sites for waterbirds (Samraoui and Samraoui 2008), highlighting the region's global significance for freshwater biodiversity. The pronounced endemism of Maghrebian biota, shaped by complex topography and long-term climatic fluctuations, has produced a characteristic checkerboard distribution (Husemann et al. 2014; Benslama et al. 2010). Interactions between orography, geodynamics, and climate have further promoted microendemism and local radiations through habitat fragmentation and limited dispersal (Veith et al. 2004; Neubauer et al. 2015).

Most *Habrophlebia* species in the Maghreb exhibit highly restricted ranges and can be regarded as true microendemics. They are typically associated with headwater streams at elevations of 200–900 m, usually characterised by moderate current velocity. The remarkable diversity of the genus in this region is likely linked to its narrow ecological tolerance (stenoecy) and limited dispersal capacity relative to other mayfly lineages (Peredo Arce et al. 2021). Adult mayflies generally live only a few hours to days and possess weak flight capacity, restricting their movements primarily to local or catchment scales, although occasional long-distance dispersal events have been documented (Monaghan et al. 2005; Vuataz et al. 2013; Rutschmann et al. 2014). These dispersal limitations enhance the potential for genetic and phenotypic divergence, particularly in fragmented habitats where geographic isolation fosters allopatric speciation within montane refugia (Hewitt 2004). Consequently, *Habrophlebia* species may serve as reliable bioindicators of relict mountain streams that have remained largely unaffected by human disturbance (Samraoui et al. 2021b). Their persistence in such isolated habitats points to long-term ecological stability and underscores the importance of montane refugia in sustaining freshwater biodiversity across the Maghreb.

During the Quaternary glacial periods, the Maghreb served as an important, though long overlooked, refugium for Western Palaearctic biota, with the narrow straits of Gibraltar and Sicily acting as key biogeographical corridors between North Africa and Europe (Husemann et al. 2014). Evidence from diverse taxa, including colubrid snakes (Carranza et al. 2006), freshwater turtles (Fritz et al. 2006), and nymphalid butterflies (Habel et al. 2011, 2017), indicates the presence of two or more glacial refugia within the region. Quaternary glacial and interglacial oscillations likely drove pronounced east to west divergence and regional disjunctions, notably across Kabylie, the Aures, and the Rif, shaping the phylogeographical structure of Maghrebian biota (Beddek et al. 2018; Dufresnes et al. 2019; Machado et al. 2021).

Earlier, during the Miocene, alternating marine transgressions and tectonic reorganisation of the Tell and Rif belts, including the development of Numidian Flysch basins and uplift of massifs such as Edough, fragmented freshwater habitats and isolated upland streams (Caby et al. 2001; Thomas et al. 2010; Ben Khalifa et al. 2019). Superimposed Pleistocene humidity and aridity cycles (Gasse and van Campo 1994; Zielhofer et al. 2004) further modified connectivity, alternately promoting dispersal and secondary contact before reinstating isolation, a process recognised as a major driver of diversification in North African freshwater biotas (Habel et al. 2008).

Marine incursions may have been particularly influential in shaping the biota of the Edough Mountains, which rise above the Seybouse and Guerbes Senhadja plains and the Fetzara marsh. The massif is a recognised hotspot of Mediterranean North African plant endemism (Véla and Benhouhou 2007), supporting numerous endemic vascular plants (Hamel et al. 2013), the threatened ribbed newt *Pleurodeles poireti* (Carranza and Wade 2004; Veith et al. 2004; Samraoui et al. 2012), several endemic caddisflies (Samraoui et al. 2024), the springtail genus *Edoughnura* (Deharveng et al. 2007), and several locally restricted Collembola species (Brahim-Bounab et al. 2020).

The Messinian Salinity Crisis, approximately 5.97 to 5.33 million years ago, was marked by the near-complete desiccation of the Mediterranean followed by rapid refilling (Duggen et al. 2003; Rouchy and Caruso 2006; Roveri et al. 2014). The temporary emergence of terrestrial corridors during this period may have enabled range expansions from North Africa to southern Europe (Carranza et al. 2006; Habel et al. 2010; Gattolliat et al. 2015). However, biogeographical links between the Maghreb and southern Europe remain poorly understood.

The distribution of *Habrophlebia* species is consistent with the Maghrebian east–west divide, which separates Algerian and Moroccan lineages across several taxa, including the odonates *Gomphus lucasi* and *G. simillimus*, mayflies of the genus *Centroptilum* (Kaltenbach et al. 2022) and *Rhithrogena* (Zrelli et al. 2011b; Samraoui et al. 2021c; El Alami et al. 2022b), and ribbed newts of the genus *Pleurodeles* (Veith et al. 2004). The concentration of *Habrophlebia* diversity in the Maghreb supports the hypothesis that European taxa may have originated from Maghrebian ancestors dispersing northwards across the Strait of Sicily. Alternatively, a reverse colonisation scenario is plausible, with an ancestral lineage entering the Maghreb from Europe and subsequently diversifying in isolation. Such contrasting biogeographical patterns, involving dispersal and in situ diversification, are well documented in both island and continental systems, exemplified by the adaptive radiation of Darwin's finches in the Galápagos (Grant and Grant 2008). Comparable processes have been reported in New Guinea, where Miocene and Pliocene orogeny triggered extensive arthropod diversification through habitat fragmentation and ecological opportunity (Toussaint et al. 2014).

By analogy, the complex topography and climatic oscillations of the Maghreb, combined with intermittent connectivity across the Mediterranean during low sea-level stands, may have facilitated alternating phases of isolation and gene flow, ultimately promoting the diversification of *Habrophlebia* across this region. In this scenario, the Strait of Sicily, much like the Strait of Gibraltar, would have acted as a biogeographic corridor between North Africa and Europe, with glacial periods and associated sea-level fluctuations providing repeated opportunities for faunal exchange (Husemann et al. 2014).

Within Algeria, an east–west disjunction is suggested by the clade *H. djurdjurensis* and *H. hassainae* geographically isolated from their sister clade, comprising *H. callensis* sp. nov. and *H. annaba* sp. nov. This pattern may reflect broader biogeographic structuring across the Maghreb, where recurrent Pleistocene climatic oscillations, marine transgressions, and habitat discontinuities promoted population isolation and lineage divergence. In this context, the Edough, Numidian (Mount Ghora and Kroumiria), and Kabylie massifs appear to have acted as important refugial zones in eastern Algeria, while the Rif and Middle Atlas fulfilled a similar role in the west, together generating a recurrent east–west phylogeographic break across multiple taxa.

Not all *Habrophlebia* species exhibit restricted ranges. *H. ghora* sp. nov. and *H. seybouse* sp. nov. both display relatively wide distributions, similar to other recently described Maghrebian taxa that also occupy broad areas. For example, *H. djurdjurensis* in Algeria is widespread in streams of the Djurdjura Mountains (Kechemir et al. 2020; Labdaoui et al. 2024), and *H. dakkii* in northern Morocco, although endemic to the Rif Mountains, is distributed across much of this range (El Alami et al. 2025). Such cases indicate that dispersal is possible when environmental and geographical conditions are favourable. Factors that may promote wider distributions include the presence of continuous or closely spaced headwater networks, riparian corridors that maintain ecological connectivity, and regional hydrological stability, which reduces the likelihood of local extinctions (Bilton et al. 2001; Finn et al. 2011; Sarremejane et al. 2021). These examples suggest that, despite generally limited dispersal capabilities, certain *Habrophlebia* species can expand beyond isolated refugia when the landscape offers suitable pathways and habitat continuity.

In the Collo–Seybouse Highlands and Mount Ghora (Kroumiria) sector, which is inhabited by two closely related species (*H. seybouse* sp. nov. and *H. ghora* sp. nov.), potential dispersal pathways include the Oued Seybouse corridor and the intervening hill ranges, such as the Monts of Nechmaya, which may intermittently connect headwater systems. The continuity of such routes is likely influenced by historical climate oscillations, with wetter periods enhancing riparian connectivity and drier phases promoting isolation. This pathway also appears to have been utilised by another, as yet undescribed, mayfly species, *Ecdyonurus* sp. C (Hezil et al. 2025), suggesting that it may function as a recurrent conduit for faunal exchange across the region. Similarly, the close relationship between *H. annaba* sp. nov. and *H. callensis* sp. nov. may be attributed to the extensive wetland complex located between Mount Edough and northern El Kala, which is likely to have provided both ecological connectivity and dispersal pathways that subsequently facilitated speciation.

In addition to their underappreciated biogeographical significance, which provides valuable insights into how past climatic oscillations have shaped regional and extra-regional biota (Carrington et al. 2001), North African wetlands deliver essential ecosystem services (Boulton et al. 2016). Yet, they are increasingly threatened by escalating anthropogenic pressures, placing a substantial proportion of Maghrebian freshwater species at risk of extinction (García et al. 2010; Benslimane et al. 2019). A major obstacle to effective conservation is the limited public and institutional recognition of the fundamental role that biodiversity plays in maintaining ecological integrity and supporting human well-being (Aouadi et al. 2022; Samraoui et al. 2025). Bridging this awareness gap is critical for promoting sustainable management and ensuring the long-term resilience of these ecosystems.

Acknowledgements

We are grateful to M. El Alami, R. Godunko, and J.-L. Gattolliat for their valuable comments and suggestions. We sincerely thank Farrah Samraoui for her constant support and assistance throughout the project. We also thank Sonia Zrelli (Bizerte, Tunisia) for providing access to material, and Céline Stoffel (MZL) for her invaluable help with molecular laboratory work. Scanning electron microscopy was carried out at the Electron Microscopy Facility of the University of Lausanne, with the kind assistance of Antonio Mucciolo.

References

Aouadi A, Samraoui F, Talbi A, Souiki L, Samraoui B (2022) Socio-demographic correlates of biodiversity perception: The need for environmental education. Journal of Contemporary Trends and Issues in Education 1: 19–51. https://doi.org/10.55628/jctie.v2i1.15

Ayati K, Hadjab R, Khammar H, Dhaaouadi S, Piscart C, Mahmoudi E (2019) Origin, diversity, and distribution of freshwater epigean amphipods in Maghreb. Annales de Limnologie– International Journal of Limnology 55: 13. https://doi.org/10.1051/limn/2019012

Beddek M, Zenboudji-Beddek S, Geniez P, Fathalla R, Sourouille P, Arnal V, Dellaoui B, Koudache F, Telailia S, Peyre O, Crochet P-A (2018) Comparative phylogeography of amphibians and reptiles in Algeria suggests common causes for the east–west phylogeographic breaks in the Maghreb. PLoS ONE 13(8): e0201218. https://doi.org/10.1371/journal.pone.0201218

Belfiore C, Gaino E (1985) Le specie italiane del genere *Habrophlebia* Eaton, 1881 (Ephemeroptera, Leptophlebiidae). Bollettino dell'Associazione Romana di Entomologia 39: 11–18.

Bemmoussat-Dekkak S, Abdellaoui-Hassaine K, Sartori M, Morse JC, Zamora-Muñoz C (2021) Larval taxonomy and distribution of genus *Hydropsyche* (Trichoptera: Hydropsychidae) in northwestern Algeria. Zootaxa 4915(4): 481–505. https://doi.org/10.11646/zootaxa.4915.4.2

Benhadji N, Abdellaoui Hassaine KA, Sartori M (2018) *Habrophlebia hassainae*, a new mayfly species (Ephemeroptera: Leptophlebidae) from North Africa. Zootaxa 4403(3): 557–569. https://doi.org/10.11646/zootaxa.4403.3.8

Benhadji N, Abdellaoui Hassaine KA, Gattolliat JL, Sartori M (2019) Thirty years after: An update to the mayflies composition in the Tafna basin (Algeria). Zoosymposia 16: 22–35. https://www.mapress.com/zs/article/view/zoosymposia.16.1.6

Ben Hassine J, Escoriza D (2017) Amphibians of Algeria: New data on the occurrence and natural history. Herpetological Bulletin 142: 6–18.

Ben Khalifa K, Zaïbi C, Bonnin J, Carbonel P, Zouari K, Mnif T, Kamoun F (2019) Holocene environmental changes in the Hachichina wetland (Gulf of Gabes, Tunisia) evidenced by foraminifera and ostracoda, geochemical proxies and sedimentological analyses. Rivista Italiana di Paleontologia e Stratigrafia 125(2): 517–549. https://doi.org/10.13130/2039-4942/11958

Benslama M, Andrieu-Ponel V, Guiter F, Reille M, de Beaulieu J-L, Migliore J (2010) Nouvelles contributions à l'histoire tardiglaciaire et holocène de la végétation en Algérie : analyses polliniques de deux profils sédimentaires du complexe humide d'El-Kala. Comptes Rendus Biologies 333(10–11): 744–754. https://doi.org/10.1016/j.crvi.2010.08.002

Benslimane N, Chakri K, Haiahem D, Guelmami A, Samraoui F, Samraoui B (2019) Anthropogenic stressors are driving a steep decline of hemipteran diversity in dune ponds in north-eastern Algeria. Journal of Insect Conservation 23(3): 475–488. https://doi.org/10.1007/s10841-019-00133-1

Biancheri E (1959) Note sugli Efemerotteri italiani. IX. Descrizione di una nuova specie della Sardegna: *Habrophlebia consiglioi* sp. n. Bollettino della Società Entomologica Italiana 89(3–4): 35–38.

Bilton DT, Freeland JR, Okamura B (2001) Dispersal in freshwater invertebrates. Annual Review of Ecology and Systematics 32: 159–181. https://doi.org/10.1146/annurev.ecolsys.32.081501.114016

Bouhala Z, Khemissa C, Márquez-Rodríguez J, Ferreras-Romero M, Samraoui F, Samraoui B (2019) Ecological correlates of odonate assemblages of a Mediterranean stream, Wadi Cherf, northeastern Algeria: Implications for conservation. International Journal of Odonatology 22(3–4): 181–197. https://doi.org/10.1080/13887890.2019.1688199

Boulton AJ, Ekebom J, Gíslason GM (2016) Integrating ecosystem services into conservation strategies for freshwater and marine habitats: a review. Aquatic Conservation: Marine and Freshwater Ecosystems 26: 963–985. https://doi.org/10.1002/aqc.2703

Brahim-Bounab H, Bendjaballah M, Hamra-Kroua S, Lachi N, Bedos A, Deharveng L (2020) Checklist of the springtails (Hexapoda: Collembola) of the Edough massif, northeastern Algeria. Zootaxa 4853(1): 51–78. https://doi.org/10.11646/zootaxa.4853.1.3

Caby R, Hammor D, Cheilletz A (2001) Metamorphic evolution, partial melting and Miocene exhumation of lower crust in the Edough metamorphic core complex, West Mediterranean orogen, eastern Algeria. Tectonophysics 342(3–4): 239–273. https://doi.org/10.1016/S0040-1951(01)00166-4

Carranza S, Arnold EN, Pleguezuelos JM (2006) Phylogeny, biogeography, and evolution of two Mediterranean snakes, *Malpolon monspessulanus* and *Hemorrhois hippocrepis* (Squamata, Colubridae), using mtDNA sequences. Molecular phylogenetics and evolution 40(2): 532–546. https://doi.org/10.1016/j.ympev.2006.03.028

Carranza S, Wade E (2004) Taxonomic revision of Algero-Tunisian *Pleurodeles* (Caudata: Salamandridae) using molecular and morphological data. Revalidation of the taxon *Pleurodeles nebulosus* (Guichenot, 1850). Zootaxa 488(1): 1–24. https://doi.org/10.11646/zootaxa.488.1.1

Chesters D (2013) collapsetypes.pl. computer software. http://sourceforge.net/projects/collapsetypes/

Carrington D, Gallimore R, Kutzbach J (2001) Climate sensitivity to wetlands and wetland vegetation in mid-Holocene North Africa. Climate Dynamics 17: 151–157. https://doi.org/10.1007/s003820000099

Dambri BM, Benhadji N, Vuataz L, Sartori M (2022) *Ecdyonurus aurasius* sp. nov. (Insecta, Ephemeroptera, Heptageniidae, Ecdyonuriinae), a new micro-endemic mayfly species from Aurès Mountains (north-eastern Algeria). Zookeys 1121: 17–37. https://doi.org/10.3897/zookeys.1121.89613

Dambri B, Godunko RJ, Benhadji N (2023) Baetidae (Insecta: Ephemeroptera) of Aurès Mountains (Algeria): A new species of the *Baetis alpinus* species group, with notes on *Baetis* Leach, 1815. Insects 14(1): 899. https://doi.org/10.3390/insects14110899

Darriba D, Taboada GL, Doallo R, Posada D (2012) jModelTest 2: more models, new heuristics and parallel computing. Nature methods 9(8): 772–772. https://doi.org/10.1038/nmeth.2109

Deharveng L, Hamra-Kroua S, Bedos A (2007) *Edoughnura rara* n. gen., n. sp., an enigmatic genus of Neanurinae Collembola from the Edough Massif (Algeria). Zootaxa 1652: 57–61. https://doi.org/10.1016/j.ympev.2019.02.009

Dufresnes C, Beddek M, Skorinov DV, Fumagalli L, Perrin N, Crochet PA, Litvinchuk SN (2019) Diversification and speciation in tree frogs from the Maghreb (*Hyla meridionalis sensu lato*), with description of a new African endemic. Molecular phylogenetics and evolution 134: 291–299. https://doi.org/10.1016/j.ympev.2019.02.009

Duggen S, Hoernle K, van den Bogaard P, Rüpke L, Morgan JP (2003) Deep roots of the Messinian salinity crisis, Nature 422: 602–606. https://doi.org/10.1038/nature01553

Eaton AE (1899) List of Ephemeridae hitherto observed in Algeria with localities. Entomology Monthly Magazine 35: 4–5.

El Alami M, Benlasri M, Sartori M, Vuataz L, Ghamizi M (2022a) A new species of the genus *Prosopistoma* Latreille, 1833 (Ephemeroptera, Prosopistomatidae) from Morocco. ZooKeys 1117: 203–218. https://doi.org/10.3897/zookeys.1117.83539

El Alami M, El Yaagoubi S, Gattolliat J-L, Sartori M, Dakki M (2022b) Diversity and Distribution of Mayflies from Morocco (Ephemeroptera, Insecta). Diversity 14(6): 498. https://doi.org/10.3390/d14060498

El Alami M, Vuataz L, El Yaagoubi S, Sartori M (2023) Another new species of the genus *Habrophlebia* Eaton, 1881 (Ephemeroptera, Leptophlebiidae) from the Maghreb. ZooKeys 1186: 47–70. https://doi.org/10.3897/zookeys.1186.112796

El Alami M, Vuataz L, El Yaagoubi S, Sartori M (2025) Integrative taxonomy of the genus *Habrophlebia* Eaton, 1881 in Morocco (Ephemeroptera, Leptophlebiidae): new species, redescriptions, and morphological-mitochondrial discrepancies. Zootaxa 5642(5): 401–426. https://doi.org/10.11646/zootaxa.5642.5.1

Ezard T, Fujisawa T, Barraclough TG (2021) SPLITS: SPecies' Limits by Threshold Statistics. R-package version 1.0-20/r56. https://r-forge.r-project.org/projects/splits/

Ferreira S, Velo-Antón G, Brochard C, Vieira C, Alves PC, Thompson DJ, Watts PC, Brito JC (2014) A critically endangered new dragonfly species from Morocco: *Onychogomphus boudoti* sp. nov. (Odonata: Gomphidae). Zootaxa 3856(3): 349–365. https://doi.org/10.11646/zootaxa.3856.3.3

Finn DS, Bonada N, Múrria C, Hughes JM (2011) Small but mighty: headwaters are vital to stream network biodiversity at two levels of organization. Journal of the North American Benthological Society 30(4): 963–980. https://doi.org/10.1899/11-012.1

Fujisawa T, Barraclough TG (2013) Delimiting species using single-locus data and the Generalized Mixed Yule Coalescent approach: a revised method and evaluation on simulated data sets. Systematic Biology 62(5): 707–724. https://doi.org/10.1093/sysbio/syt033

Fritz U, Barata M, Busack SD, Fritsch G, Castilho R (2006) Impact of mountain chains, sea straits and peripheral populations on genetic and taxonomic structure of a freshwater turtle, *Mauremys leprosa* (Reptilia, Testudines, Geoemydidae). Zoologica Scripta 35: 97–108. https://doi.org/10.1111/j.1463-6409.2005.00218.x

García N, Cuttelod A, Abdul Malak D [Eds] (2010) The status and distribution of freshwater biodiversity in northern Africa. IUCN, Gland, Switzerland.

Gasse F, Van Campo E (1994) Abrupt post-glacial climate events in West Asia and North Africa monsoon domains. Earth and Planetary Science Letters 126(4): 435–456. https://doi.org/10.1016/0012-821X(94)90123-6

Gattolliat J-L, Cavallo E, Vuataz L, Sartori M (2015) DNA barcoding of Corsican mayflies (*Ephemeroptera*) with implications for biogeography, systematics and biodiversity. Arthropod Systematics & Phylogeny 73(1): 3–18. https://doi.org/10.3897/asp.73.e31813

Grant PR, Grant BR (2008) How and why species multiply: The radiation of Darwin's finches. Princeton University Press. https://doi.org/10.1515/9781400837946

Habel JC, Rödder D, Scalercio S, Meyer M, Schmitt T (2010) Strong genetic cohesiveness between Italy and North Africa in four butterfly species. Biological Journal of the Linnean Society 99(4): 818–830. https://doi.org/10.1111/j.1095-8312.2010.01394.x

Habel JC, Schmitt T, Meyer M, Müller P (2008) Africa goes Europe: The complete phylogeography of the Marbled White butterfly species complex (*Melanargia galathea*, *M. lachesis*). Organisms Diversity & Evolution 8(2): 121–129. https://doi.org/10.1016/j.ode.2007.04.002

Habel JC, Rödder D, Lens L, Schmitt T (2011) From Africa to Europe and back: refugia and range shifts cause high genetic differentiation in the European Marbled White butterfly *Melanargia galathea*. BMC Evolutionary Biology 11: 215. https://doi.org/10.1186/1471-2148-11-215

Habel JC, Vila R, Vodă R, Husemann M, Schmitt T, Dapporto L (2017) Differentiation in the marbled white butterfly species complex driven by multiple evolutionary forces. Journal of Biogeography 44(2): 433–445. https://doi.org/10.1111/jbi.12868

Hamel T, Seridi R, de Bélair G, Slimani A, Babali B (2013) Flore vasculaire rare et endémique de la péninsule de l'Edough (Nord-Est algérien). Synthèse: Revue des Sciences et de la Technologie 26: 65–74.

Hebert PDN, Ratnasingham S, de Waard JR (2003) Barcoding animal life: Cytochrome *c* oxidase subunit 1 divergences among closely related species. Proceedings of the Royal Society B: Biological Sciences 270: 96–99. https://doi.org/10.1098/rsbl.2003.0025

Hewitt GM (2004) Genetic consequences of climatic oscillations in the Quaternary. Philosophical transactions of the Royal Society of London. Series B, Biological sciences 359(1442): 183–195. https://doi.org/10.1098/rstb.2003.1388

Hezil W, Samraoui F, Satour A, Taferghoust M, Boucenna H, Vuataz L, Gattolliat J-L, Sartori M, Samraoui B (2025) Updated checklist of mayflies from northeastern Algeria with biogeographical and ecological insights (Insecta, Ephemeroptera). Alpine Entomology 9: 37–49. https://doi.org/10.3897/alpento.9.156544

Hurvich CM, Tsai CL (1989) Regression and time series model selection in small samples. Biometrika 76(2): 297–307. https://doi.org/10.1093/biomet/76.2.297

Husemann M, Schmitt T, Zachos FE, Ulrich W, Habel JC (2014) Palaearctic biogeography revisited: evidence for the existence of a North African refugium for Western Palaearctic biota. Journal of Biogeography 41(1): 81–94. https://doi.org/10.1111/jbi.12180

Jacob U, Sartori M (1984) Die europäischen Arten der Gattung *Habrophlebia* Eaton (Ephemeroptera, Leptophlebiidae). Entomologische Abhandlungen Staatliches Museum für Tierkunde Dresden 48(5): 45–52.

Kapli P, Lutteropp S, Zhang J, Kobert K, Pavlidis P, Stamatakis A, Flouri T (2017) Multi-rate Poisson tree processes for single-locus species delimitation under maximum likelihood and Markov chain Monte Carlo. Bioinformatics 33(11): 1630–1638. https://doi.org/10.1093/bioinformatics/btx025

Kaltenbach T, Vuataz L, Samraoui B, El Yaagoubi S, El Alami M, Gattolliat J-L (2022) New species of *Centroptilum* Eaton, 1869 from North Africa (Ephemeroptera, Baetidae). Zookeys 1131: 71–97. https://doi.org/10.3897/zookeys.1131.91017

Katoh K, Rozewicki J, Yamada KD (2019) MAFFT online service: multiple sequence alignment, interactive sequence choice and visualization. Briefings in bioinformatics 20(4): 1160–1166. https://doi.org/10.1093/bib/bbx108

Kechemir LH, Sartori M, Lounaci A (2020) An unexpected new species of *Habrophlebia* from Algeria (Ephemeroptera, Leptophlebiidae). ZooKeys 953: 31–47. https://doi.org/10.3897/zookeys.953.51244

Korbaa M, Ferreras-Romero M, Bejaoui M, Boumaiza M (2014) Two species of Odonata newly recorded from Tunisia. African Entomology 22(2): 291–296. https://doi.org/10.4001/003.022.0212

Kumar S, Stecher G, Li M, Knyaz C, Tamura K (2018) MEGA X: molecular evolutionary genetics analysis across computing plat-

forms. Molecular Biology and Evolution 35(6): 1547. https://doi.org/10.1093/molbev/msy096

Labdaoui S, Samraoui F, Vuataz L, Gattolliat J-L, Sartori M, Samraoui B (2024) Stream sentinels: Mayfly diversity, land use, and conservation in Algeria's Djurdjura Mountains. Aquatic Conservation: Marine and Freshwater Ecosystems 34(12): e70025. https://doi.org/10.1002/aqc.70025

Letunic I, Bork P (2024) Interactive Tree of Life (iTOL) v6: recent updates to the phylogenetic tree display and annotation tool. Nucleic Acids Resources 52(W1): W78–W82. https://doi.org/10.1093/nar/gkae268

Lestage JA (1925) Ephéméroptères, Plécoptères et Trichoptères recueillis en Algérie par M.H. Gauthier et liste des espèces connues actuellement de l'Afrique du Nord. Bulletin de la Société d'Histoire Naturelle d'Afrique du Nord 16: 8–18.

Machado L, Harris DJ, Salvi D (2021) Biogeographic and demographic history of the Mediterranean snakes *Malpolon monspessulanus* and *Hemorrhois hippocrepis* across the Strait of Gibraltar. BMC Ecology and Evolution 21: 210. https://doi.org/10.1186/s12862-021-01941-3

Miller M, Pfeiffer WT, Schwartz T (2010) Creating the CIPRES Science Gateway for Inference of Large Phylogenetic Trees. Proceedings of the Gateway Computing Environments Workshop, New Orleans, 2010, 1–8. https://doi.org/10.1109/GCE.2010.5676129

Monaghan MT, Gattolliat JL, Sartori M, Elouard JM, James H, Derleth P, Glaizot O, de Moor F, Vogler AP (2005) Trans-oceanic and endemic origins of the small minnow mayflies (Ephemeroptera, Baetidae) of Madagascar. Proceedings of the Royal Society B: Biological Sciences 272: 1829–1836. https://doi.org/10.1098/rspb.2005.3139

Myers N, Mittermeier RA, Mittermeier CG, da Fonseca GAB, Kent J (2000) Biodiversity hotspots for conservation priorities. Nature 403: 853–858. https://doi.org/10.1038/35002501

Neubauer TA, Harzhauser M, Georgopoulou E, Kroh A, Mandic O (2015) Tectonics, climate, and the rise and demise of continental aquatic species richness hotspots. Proceedings of the National Academy of Sciences of the United States of America 112(37): 11478–11483. https://doi.org/10.1073/pnas.1503992112

Paradis E, Schliep K (2019) ape 5.0: an environment for modern phylogenetics and evolutionary analyses in R. Bioinformatics 35: 526–528. https://doi.org/10.1093/bioinformatics/bty633

Peredo Arce A, Hörren T, Schletterer M, Kail J (2021) How far can EPTs fly? A comparison of empirical flying distances of riverine invertebrates and existing dispersal metrics. Ecological Indicators 125:107465. https://doi.org/10.1016/j.ecolind.2021.107465

Peters WL, Edmunds Jr GF (1970) Revision of the generic classification of the Eastern Hemisphere Leptophlebiidae (Ephemeroptera). Pacific Insects 12(1): 157–240.

Pons J, Barraclough TG, Gomez-Zurita J, Cardoso A, Daniel PD, Hazell S, Kamoun S, William DS, Vogler AP (2006) Sequence-Based Species Delimitation for the DNA Taxonomy of Undescribed Insects. Systematic Biology 55: 595–609. https://doi.org/10.1080/10635150600852011

Puillandre N, Brouillet S, Achaz G (2020) ASAP: assemble species by automatic partitioning. Molecular Ecology Resources 21(2): 609–620. https://doi.org/10.1111/1755-0998.13281

R Core Team (2025) R: A language and environment for statistical computing. R Foundation for Statistical Computing, Vienna, Austria. https://www.r-project.org/

Rambaut A, Drummond AJ, Xie D, Baele G, Suchard MA (2018) Posterior summarization in Bayesian phylogenetics using Tracer 1.7. Systematic biology 67(5): 901–904. https://doi.org/10.1093/sysbio/syy032

Rouabhi N, Bouchelouche D, Vecchioni L, Mabrouki Y, Taybi FA, Marrone F, Faraone FP (2025) The Maghreb as a hotspot of diversity for the freshwater crab genus *Potamon* (Decapoda, Potamidae). Diversity 17(8): 562. https://doi.org/10.3390/d17080562

Rouchy JM, Caruso A (2006) The Messinian salinity crisis in the Mediterranean basin: A reassessment of the data and an integrated scenario, Sedimentary Geology 188–189: 35–67. https://doi.org/10.1016/j.sedgeo.2006.02.005

Roveri M, Lugli S, Manzi V, Schreiber BC, Gennari R (2014) The Messinian Salinity Crisis: Open problems and possible implications for Mediterranean outflow. Marine Geology 352: 25–58. https://doi.org/10.1016/j.margeo.2014.02.002

Rutschmann S, Gattolliat JL, Hughes SJ, Baez M, Sartori M, Monaghan MT (2014) Evolution and island endemism of morphologically cryptic *Baetis* and *Cloeon* species (Ephemeroptera, Baetidae) on the Canary Islands and Madeira. Freshwater Biology 59: 2516–2527. https://doi.org/10.1111/fwb.12450

Srivathsan A, Meier R (2012) On the inappropriate use of Kimura-2-parameter (K2P) divergences in the DNA-barcoding literature. Cladistics 28(2): 190–194. https://doi.org/10.1111/j.1096-0031.2011.00370.x

Samraoui B, Alfarhan AH (2015) Odonata in streams on Mount Edough, Algeria, and in Kroumiria, Tunisia. African Entomology, 23(1): 172–179. https://doi.org/10.4001/003.023.0129

Samraoui B, Benyacoub S, Mecibah S, Dumont HJ (1993) Afrotropical libellulids in the lake district of El Kala, NE Algeria, with a rediscovery of *Urothemis e. edwardsi* (Selys) and *Acisoma panorpoides ascalaphoides* (Rambur) (Anisoptera: Libellulidae). Odonatologica 22(3): 365–372.

Samraoui B, Bouhala Z, Chakri K, Márquez-Rodríguez J, Ferreras-Romero M, El-Serehy HA, Samraoui F, Sartori M, Gattolliat J-L (2021a) Environmental determinants of mayfly assemblages in the Seybouse River, north-eastern Algeria (Insecta: Ephemeroptera). Biologia 76(8): 2277–2289. https://doi.org/10.1007/s11756-021-00726-9

Samraoui B, Márquez-Rodríguez J, Ferreras-Romero M, El-Serehy HA, Samraoui F, Sartori M, Gattolliat J-L (2021b) Biogeography, ecology, and conservation of mayfly communities of relict mountain streams, north-eastern Algeria. Aquatic Conservation: Marine and Freshwater Ecosystems 31(12): 3357–3369. https://doi.org/10.1002/aqc.3719

Samraoui B, Samraoui F (2008) An ornithological survey of Algerian wetlands: Important Bird Areas, Ramsar sites and threatened species. Wildfowl 58: 71–96.

Samraoui B, Samraoui F, Benslimane N, Alfarhan A, Al-Rasheid KAS (2012) A precipitous decline of the Algerian newt *Pleurodeles poiretti* Gervais, 1835 and other changes in the status of amphibians of Numidia, north-eastern Algeria. Revue d'Écologie (Terre & Vie) 67: 71–81. https://doi.org/10.3406/revec.2012.1621

Samraoui B, Segers H, Maas S, Baribwegure D, Dumont HJ (1998) Rotifera, Cladocera, Copepoda, and Ostracoda from coastal wetlands in northeast Algeria. Hydrobiologia 386: 183–193. https://doi.org/10.1023/A:1003538730152

Samraoui B, Samraoui F, Oláh J (2024) Trichoptera of northeastern Algeria: New species, noteworthy records, and a review of the genus *Hydropsyche* (Hydropsychidae). Opuscula Zoologica 55: 59–96. https://doi.org./10.18348/opzool.2024.3.59

Samraoui B, Vuataz L, Sartori M, Gattolliat J-L, Al-Misned FA, El-Serehy HA, Samraoui F (2021c) Taxonomy, distribution and life

cycle of the Maghrebian endemic *Rhithrogena sartorii* (Ephemeroptera: Heptageniidae) in Algeria. Diversity 13(11): 547. https://doi.org/10.3390/d13110547

Samraoui F, Nahli C, Snani S, Nedjah R, Aouadi A, Rouibi Y, Satour A, Samraoui B (2025) Perceptions of ecosystem services and conservation: The role of gender and education in northeastern Algeria. Land 14(7): 1454. https://doi.org/10.3390/land14071454

Sarremejane R, Stubbington R, England J, Sefton CEM, Eastman M, Parry S, Ruhi A (2021) Drought effects on invertebrate metapopulation dynamics and quasi-extinction risk in an intermittent river network. Global Change Biology 27(17): 4024–4039. https://doi.org/10.1111/gcb.15720

Sartori M, Brittain JE (2015) Chapter 34. Order Ephemeroptera. In: Thorp J, Rogers DC (Eds) Thorp and Covich's freshwater invertebrates. Vol. 1 Ecology and general biology. Academic Press, New York, 873–891. https://doi.org/10.1016/B978-0-12-385026-3.00034-6

Sartori M, Gattolliat J-L (2023) Chapter 9. Order Ephemeroptera. In: Maasri A, Thorp J (Eds) Identification and Ecology of freshwater Arthropods in the Mediterranean Basin. Elsevier, Amsterdam, 283–309. https://doi.org/10.1016/B978-0-12-821844-0.00011-9

Soldán T, Godunko RJ, Thomas AGB (2005) *Baetis chelif* n. sp., a new mayfly from Algeria with notes on *B. sinespinosus* Soldán & Thomas, 1983, n. stat. (Ephemeroptera: Baetidae). Genus 16: 155–165.

Stecher G, Tamura K, Kumar S (2020) Molecular evolutionary genetics analysis (MEGA) for macOS. Molecular Biology and Evolution 37(4): 1237–1239. https://doi.org/10.1093/molbev/msz312

Suchard MA, Lemey P, Baele G, Ayres DL, Drummond AJ, Rambaut A (2018) Bayesian phylogenetic and phylodynamic data integration using BEAST 1.10. Virus Evolution 4(1): vey016. https://doi.org/10.1093/ve/vey016

Talavera G, Dincă V, Vila R (2013) Factors affecting species delimitations with the GMYC model: insights from a butterfly survey. Methods in Ecology and Evolution 4(12): 1101–1110. https://doi.org/10.1111/2041-210X.12107

Thomas AGB (1998) A provisional checklist of the mayflies of North Africa (Ephemeroptera). Bulletin de la Société d'Histoire Naturelle de Toulouse 134: 13–20.

Thomas A, Gaino E, Marie V (1999) Complementary description of *Habrophlebia vaillantorum* Thomas, 1986, in comparison with *H. fusca* (Curtis, 1984) (Ephemeroptera, Leptophlebiidae). Ephemera 1: 9–21.

Thomas D, Bodin S, Redfern J, Irving D (2010) A reinterpretation of the Numidian Flysch in Algeria and Tunisia, and its implications for the Oligo–Miocene evolution of the Maghrebian margin of North Africa. Earth-Science Reviews 104(1–3): 1–20. https://doi.org/10.1016/j.earscirev.2010.03.001

Toussaint EFA, Hall R, Monaghan MT, Sagata K, Ibalim S, Shaverdo HV, Vogler AP, Pons J, Balke M (2014) The towering orogeny of New Guinea as a trigger for arthropod megadiversity. Nature Communications 5: 4001. https://doi.org/10.1038/ncomms5001

Veith M, Mayer C, Samraoui B, Donaire-Barroso D, Bogaerts S (2004) From Europe to Africa and vice versa: Evidence for multiple intercontinental dispersal in ribbed salamanders (Genus *Pleurodeles*). Journal of Biogeography 31(1): 159–171. https://doi.org/10.1111/j.1365-2699.2004.00957.x

Véla E, Benhouhou S (2007) Évaluation d'un nouveau point chaud de biodiversité végétale dans le Bassin méditerranéen (Afrique du Nord). Comptes Rendus Biologies 330(8): 589–605. https://doi.org/10.1016/j.crvi.2007.04.006

Vences M, Miralles A, Brouillet S, Ducasse J, Fedosov A, Kharchev V, Kumari S, Patmanidis S, Puillandre N, Scherz MD, Kostadinov I, Renner SS (2021) iTaxoTools 0.1: Kickstarting a specimen-based software toolkit for taxonomists. Megataxa 6: 77–92. https://doi.org/10.11646/megataxa.6.2.1

Vuataz L, Sartori M, Wagner A, Monaghan MT (2011) Toward a DNA taxonomy of Alpine *Rhithrogena* (Ephemeroptera: Heptageniidae) using a mixed Yule-coalescent analysis of mitochondrial and nuclear DNA. PLoS ONE 6(5): e19728. https://doi.org/10.1371/journal.pone.0019728

Vuataz L, Sartori M, Gattolliat J-L, Monaghan MT (2013) Endemism and diversification in freshwater insects of Madagascar revealed by coalescent and phylogenetic analysis of museum and field collections. Molecular Phylogenetics and Evolution 66(3): 979–991. https://doi.org/10.1016/j.ympev.2012.12.003

Waterhouse AM, Procter JB, Martin DMA, Clamp M, Barton GJ (2009) Jalview Version 2 – a multiple sequence alignment editor and analysis workbench. Bioinformatics 25: 1189–1191. https://doi.org/10.1093/bioinformatics/btp033

Wickham H (2011) The split-apply-combine strategy for data analysis. Journal of Statistical Software 40(1): 1–29. https://doi.org/10.18637/jss.v040.i01

Yasri-Cheboubi N, Vinçon G, Lounaci A (2013) A review of the Algerian Leuctridae with the description of *L. dhyae* sp. N., from Central Algeria (Plecoptera: Leuctridae). Mitteilungen der Schweizerischen Entomologischen Gesellschaft 86: 175–188.

Yasri-Cheboubi N, Vinçon G, Lounaci A (2016) The Nemouridae from Algeria (Insecta: Plecoptera). Zoosystema 38(3): 295–308. https://doi.org/10.5252/z2016n3a1

Zielhofer C, Faust D, Linstädter J, Maher H, Makhzani S (2004) Centennial-scale Late Pleistocene to mid-Holocene environmental change along the Medjerda Valley, northern Tunisia. Quaternary International 175–176: 125–139. https://doi.org/10.1016/j.quaint.2007.05.012

Zrelli S, Boumaiza M, Bejaoui M, Gattolliat J-L, Sartori M (2011a) New reports of mayflies (Insecta: Ephemeroptera) from Tunisia. Revue Suisse de Zoologie 118 (1): 18.

Zrelli S, Sartori M, Bejaoui M, Boumaiza M (2011b) *Rhithrogena sartorii*, a new mayfly species (Ephemeroptera: Heptageniidae) from North Africa. Zootaxa 3139(1): 63–68. https://doi.org/10.11646/zootaxa.3139.1.4